Drag Reduction with the Aid of Air Bubbles and Additives

by

Pouria Baghaei

A thesis
presented to the University of Waterloo
in fulfillment of the
thesis requirement for the degree of
Master of Applied Science
in
Chemical Engineering

Waterloo, Ontario, Canada, 2009

I hereby declare that I am the sole author of this thesis. This is a true copy of the thesis, including any required final revisions, as accepted by my examiners.

I understand that my thesis may be made electronically available to the public.

Signature:_____

Abstract

The effect of additives on friction loss in upward turbulent flow was investigated in this experimental study. Additives such as air bubbles, frother and polymer were added to water flow to study their influence on the friction factor.

In order to perform this research an experimental set-up was designed and developed. The test sections of the set-up consisted of three vertical pipes of different diameters. The set-up was equipped with three pressure transducers, a magnetic flowmeter, gas spargers and a gas rotameter.

The first phase of the experimental program involved calibration of the various devices and pipelines test-sections. The single-phase pressure loss data obtained from the pipelines exhibited good agreement with the standard equations. The second phase of the experimental program dealt with the effect of air bubbles and additives (frother and polymer) on drag reduction in turbulent flows.

The experimental results showed that bubbles in the range of 1 mm-3 mm increased the wall shear stress. Therefore, no drag-reduction effect was observed. On the contrary, a significant increase in friction factor was observed at low Reynolds numbers as a result of larger bubble sizes and lower turbulence intensities. The friction factor at low Reynolds numbers could be decreased by decreasing the bubble size by addition of frother to the flow system.

The combination of polymer and air bubbles showed a drag reduction of up to 60%. It is also evident from the experiment results that the addition of polymer to bubbly flow system leads to fully homogeneous mixture.

Acknowledgements

I would like to thank my supervisor, Professor Rajinder Pal, for his guidance and support during this study. His efforts in thoroughly revising the thesis are also highly appreciated.

I would like also to thank Mr. Habicher and Mr. Vasil for their technical support during design and construction of experimental apparatus.

Special thanks to Natural Sciences and Engineering Research Council of Canada (NSERC) for their financial support of this study.

At the end, I would like to thank my family for their patience and moral support.

Table of Contents

APPENDICES

List of Figures

List of Tables

Chapter 1

Introduction and Objectives

1.1 Overview

The purpose of this chapter is to clarify the main concepts of this research and point out the objectives of this work.

A brief introduction about drag reduction and its importance in industry is given in section 1.2 to show the necessity of doing more research about drag reduction methods. Section 1.3 is dedicated to motivation of doing this research and to explain purpose of this research.

Objectives of the thesis are discussed in section 1.4 with some explanation about how to reach these objectives.

An outline of the thesis is presented in section 1.5 to give readers comprehensive idea about the procedure of this thesis.

1.2 Introduction

The importance of drag reduction in many engineering fields, such as oil production and fluids transportation, has made it a subject of extensive research in the past years (Astarita (1965), Banijamali et al. (1974), etc.). Drag reduction is a remarkable ability of certain additives to reduce the frictional resistant in turbulent flow. Some benefits of reducing drag in the pipelines are decrease in pumping costs, decrease in capital cost by selecting smaller pipe size, increase in flow rate in pipes, and in the indirect way, increase in pump operating lifetime by operating at lower speed. Some industrial data shows that by aid of drag reduction in the fluid transportation system, pumping pressure can be reduced by 80% at the same flow rate or at the same pumping pressure flow rate can be increased by 30% to 40%. This reduction is caused by adding some drag reducing agents (DRA) to the flow system. Polymers, Air bubbles, and frothers are some examples of DRAs with different advantages and disadvantages in practice.

One of the most important facts about polymeric drag reduction is that it occurs only in turbulent flow and at low concentration of polymer in the system. A drag reduction of up to 70% has been observed (Toms (1948), Wells and Spangler (1967), etc.). However, drag reduction decreases with flow time because of degradation of polymer chain in pipelines. This is the undesirable effect of polymeric drag reduction.

Another method of drag reduction is the injection of gas bubbles to the liquid boundary layer. The injection of gas results in the formation of microbubbles that cause drag reduction. Studies show that the drag reduction by this method is due to a combination of density reduction and turbulence modification (Lu et al. (2005)).

Frothers, which are a class of surfactants, can also lead to drag reduction in several applications, for example by reducing pressure drop in the flow of gas/liquid systems. They reduce the bubble size in flow. However, frothers are not as effective as other DRA (such as polymers) in single-phase flows.

Although the importance of drag reduction has persuaded many researchers to carry out investigations of different DRAs and their effects in several applications, more work needs to be done in the area.

1.3 Motivation

Several studies have been carried out on reducing the friction factor in flow system using different drag reducing agents. However, there are a few investigations carried out on the effects of combining two or more DRAs.

The purpose of this research was to study the effects of single (bubbles, frother, and polymer) and combined additives (bubbles and polymer) on drag reduction in vertical pipelines.

1.4 Objectives

The objectives of this study are listed below:

1. Investigate the effect of air bubbles on drag reduction in the vertical pipelines
2. Study the effect of frother on drag reduction in bubbly flow
3. Study the effect of polymer on drag reduction in vertical single-phase flow
4. Study the effect of combined bubbles and polymer on drag reduction

In order to achieve these objectives following steps are required:

1. Design and build an experimental set-up complete with the essential measuring instruments to implement the experimental program
2. Calibrate the apparatus to achieve reliable experimental data
3. Collect experimental data by implementing series of experiments
4. Analyze experimental data

1.5 Outline of the Thesis

Chapter 2 gives the background information about single-phase and two-phase flows.

Chapter 3 discusses the literature about two methods of drag reduction: microbubble drag reduction and drag reduction by aid of additives (frother and polymer).

The experimental apparatus has been explained in chapter 4. Detailed information about the apparatus layout, calibration of instruments, and analytical procedures are provided in this chapter.

The effects of single and mixed additives on drag reduction are discussed in chapter 5. The discussion is divided in two categories, namely single-phase flow and two-phase flow.

The conclusions of this experimental work are summarized in chapter 6. Recommendations for further investigation are also presented in this chapter.

Chapter 2

Background

2.1 Overview

The theoretical background related to this thesis is provided in this chapter to familiarize readers with the basic concepts.

Section 2.2.1 gives the theoretical background about single-phase flow and provides the basic information about friction factor.

The two-phase flow concepts and the information about flow regimes, bubble sizes, and fluid properties are discussed in section 2.2.2.

2.2 Background

Prior to the discussion of drag reduction by aid of micro bubbles and additives, it is necessary to cover the theoretical background concerning single-phase flow and two-phase flow.

2.2.1 Single-Phase Flow

The flow of only one material, gas or liquid, in a pipeline refers to single-phase flow. One of the most investigated aspects of single-phase flow is friction factor. A number of empirical and analytical equations are proposed for friction factor in laminar and turbulent flows.

Nikuradse (1932) introduced an empirical equation for friction factor in fully turbulent flows based on his experimental data:

$$\frac{1}{\sqrt{f}} = 2.28 - 1.738\frac{\epsilon}{D} \tag{2.1}$$

where f is the friction factor, ϵ is pipe roughness and D is pipe diameter.

Colebrook (1938) proposed another empirical equation for turbulent flow region:

$$\frac{1}{\sqrt{f}} = -1.738\ln\left(\frac{\epsilon/D}{3.7} + \frac{1.2615}{Re\sqrt{f}}\right) \tag{2.2}$$

where Re is the Reynolds number.

Another empirical friction factor equation was introduced by Blasius (1913) which is valid for smooth pipes in turbulent flow region up to the Reynolds number of 100,000:

$$f = \frac{0.079}{Re^{0.25}} \tag{2.3}$$

Friction factor in the laminar region can be obtained analytically and is given by Hagen-Poiseuille equation:

$$f = \frac{16}{Re} \tag{2.4}$$

2.2.2 Two-Phase Flow

Two phase flow refers to the system containing the mixture of two immiscible phases, for example air-water system, or water-oil system. Some of the important areas in this subject are flow patterns, fluid properties, prediction of bubble size and pressure drop.

2.2.2.1 Flow Patterns

The term "flow pattern" or "flow regime" is used to refer to the geometrical configurations of each phase in contact with other phase. There are different flow regimes associated with two-phase flow, depending on the fluid properties, flow rate of phases and the pipe dimensions. In general the flow patterns can be categorized as either disperse flows or separated flows. Dispersed flows are flows where one phase (dispersed phase) is fully distributed into the other continuous phase. In separated flows, both phases are continuous phases and are separated by interface.

In addition to this general classification, flow patterns are described by different names. The flow regimes introduced by Aziz et al. (1972) for vertical flow are described below (see Fig.2.1).

1. Bubbly flow

Bubbly flow regime is a flow regime where the dispersed phase (say gas) is uniformly distributed through the continuous phase in the pipe; this flow is approximately homogeneous flow.

2. Slug flow

Upon increasing the gas flow rate, the number of bubbles and hence coalescence of bubbles increases resulting in larger bubble sizes. This phenomenon produces non-homogeneous flow with slippage between the two phases.

3. Transition flow

By increasing the amount of gas flow in slug flow regime, the bubbles undergo break-up and produce unsteady transitional flow (see Fig.2.1).

4. Annular-mist flow

In this type of flow, the continuous phase is changed from liquid phase to the gas phase. The liquid droplets flow along with the gas phase.

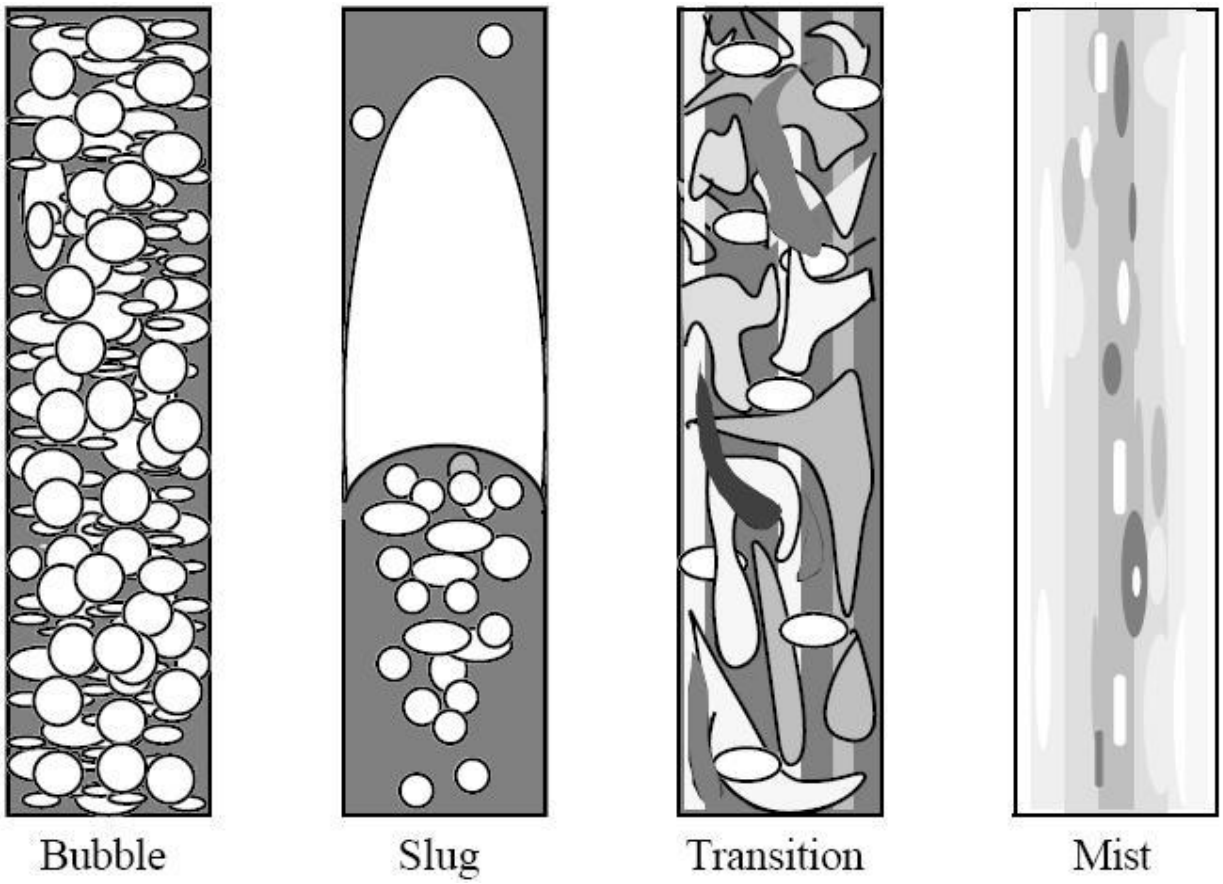

Figure 2.1 Flow regimes of Aziz, Govier and Fograsi (1972)

2.2.2.2 Prediction of Flow Patterns

Determination of flow pattern is a crucial step in predicting two-phase flow properties and pressure drop. Numerous experimental studies have been done by researchers in this area, for instance Beggs and Brill (1973), Orkiszewski (1967), Aziz, Govier, and Fogarasi (1972), etc., predicted flow patterns by aid of mathematical calculations. In this thesis, Aziz et at. (1972) method is selected to predict two-phase flow pattern. Flow patterns by the Aziz et al. method are identified by two variables:

$$N_X = V_{sg}\left(\frac{\rho_G}{0.0764}\right)^{1/3}\left(\frac{72\rho_L}{62.4\sigma_L}\right)^{1/4} \tag{2.5}$$

$$N_Y = V_{sl}\left(\frac{72\rho_L}{62.4\sigma_L}\right)^{1/4} \tag{2.6}$$

where ρ_G is gas density $\left(\frac{lb}{ft^3}\right)$, ρ_L is liquid density $\left(\frac{lb}{ft^3}\right)$, V_{SL} is liquid superficial velocity $\left(\frac{ft}{s}\right)$, V_{SG} is gas superficial velocity $\left(\frac{ft}{s}\right)$, and σ_L is liquid surface tension $\left(\frac{dyne}{cm}\right)$.

These variables show the location on the flow pattern diagram (see Fig. 2.2) while the boundaries of regimes are given by:

$$B_{12} = 0.51\,(100N_Y)^{0.172} \tag{2.7}$$

$$B_{23} = 8.6 + 3.8N_Y \tag{2.8}$$

$$B_{34} = 70(100N_Y)^{-0.152} \tag{2.9}$$

By use of these boundary and location variables, flow regimes can be identified as follows:

Bubbly Flow: $N_X < B_{12}$ (2.10)

Slug Flow: $B_{12} \leq N_X \leq B_{23}$ (2.11)

Transition Flow: $B_{23} \leq N_X \leq B_{34}\ ;\ N_Y < 4$ (2.12)

Annular-Mist: $B_{34} \leq N_X$ (2.13)

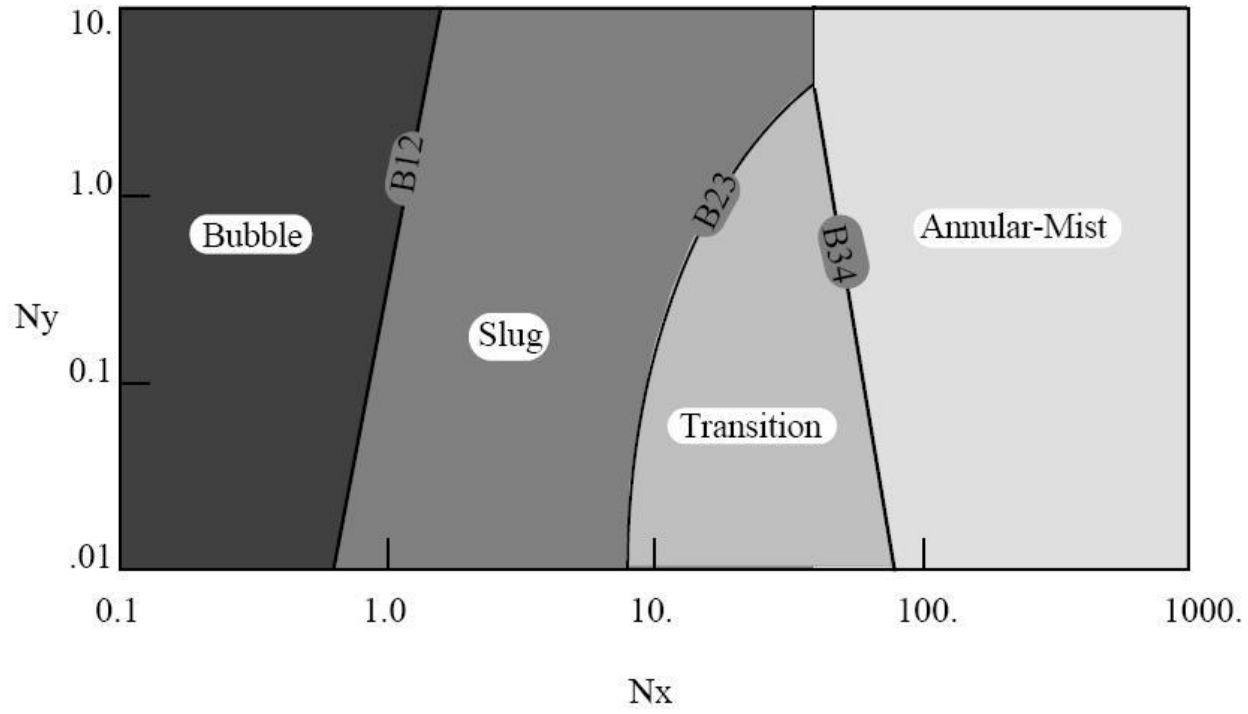

Figure 2.2 Flow Pattern diagram for Aziz, Govier and Fogarasi method

2.2.2.3 Prediction of Bubble Size in Two-Phase Flow

Bubble size in two-phase flow is an important parameter. The effect of bubble size on wall shear stress, density of mixture, and flow pattern is important. This has persuaded scientists to work on the prediction of bubble size in two-phase flow.

Hibiki and Ishii (2002) introduced an empirical equation to predict the Sauter mean diameter of bubbles in vertical flows. They proposed that the non-dimensional Sauter mean diameter is related to the non-dimensional energy dissipation rate and non-dimensional Laplace length by the following equations:

$$\widetilde{D}_{sm} = 1.99\,\tilde{L}_0^{-0.335}\,\tilde{\varepsilon}^{-0.0796} = 1.99\tilde{L}_0^{-0.335}\,\widetilde{Re}^{-0.239} \tag{2.14}$$

The parameters in this empirical equation are given as follows:

$$\tilde{L}_0 = \frac{L_0}{D_H} \tag{2.15}$$

$$L_0 = \sqrt{\frac{\sigma_l}{g\Delta\rho}} \tag{2.16}$$

$$\tilde{\varepsilon} = L_0^4\left(\frac{\varepsilon}{v_f^3}\right) \tag{2.17}$$

$$\varepsilon = gV_{sg}exp\left(5.839E-4Re_f\right) + \frac{j}{\rho_{tp}}\left(-\frac{dp}{dz}\right)_F\left(1-\exp\left(5.839E-4Re_f\right)\right) \tag{2.18}$$

$$\widetilde{Re} = \frac{\varepsilon^{1/3}L_0^{4/3}}{v_f} \tag{2.19}$$

$$\widetilde{D}_{sm} = \frac{D_{sm}}{L_0} \tag{2.20}$$

where L_0 is the Laplace length, $\tilde{L}_0$ is the non-dimensional Laplace length, ε is the energy dissipation rate per unit mass, $\tilde{\varepsilon}$ is the non-dimensional energy dissipation rate per unit mass, j is the mixture volumetric flux, V_{sg} is the superficial gas velocity, v_f is the kinematic viscosity of liquid, σ_l is the surface tension, $\Delta\rho$ is the density difference, ρ_{tp} is the density of mixture, D_{sm} is the Sauter mean diameter of bubbles, D_H is the hydraulic equivalent diameter of flow channel, Re_f is the liquid Reynolds number, and $\left(-\frac{dp}{dz}\right)_F$ is the pressure loss per unit length due to friction.

Hibiki and Ishii (2002) reported that this empirical equation predicts the Sauter mean diameter in fully developed bubbly flow with ±22% relative deviation.

2.2.2.4 Two-Phase Flow Properties

Some of the important parameters that should be calculated in order to model and analyze two-phase flow are velocity, density, hold-up, void fraction and transport properties (for instance, viscosity). Theoretical models have been developed to estimate these parameters for two-phase flow system with and without slip between phases. In this work, only the models assuming no slip between phases are studied and presented here.

In the no- slip or homogeneous flow model, the two phases move at the same velocity and the mixture is treated as a pseudo homogeneous fluid that obeys the equations of single phase flow with average values of different properties. Before discussing the homogeneous flow model there are some general two phase flow terms and definitions that should be introduced:

Gas and liquid flow rates: $$Q_g = \frac{\dot{M}_g}{\rho_g}, Q_l = \frac{\dot{M}_l}{\rho_l} \quad (2.21)$$

Total volumetric flow rate: $$Q_{tp} = Q_g + Q_l \quad (2.22)$$

Total mass flow rate: $$\dot{M}_{tp} = \dot{M}_l + \dot{M}_g \quad (2.23)$$

Mass flux : $$G_l = \frac{\dot{M}_l}{A}, G_g = \frac{\dot{M}_g}{A} \quad (2.24)$$

Total mass flux: $$G_{tp} = G_l + G_g \quad (2.25)$$

Superficial velocity: $$V_{sg} = \frac{Q_g}{A}, V_{sl} = \frac{Q_l}{A} \quad (2.26)$$

Void fraction: $$\alpha = \frac{A_g}{A} \quad (2.27)$$

Volumetric flow fraction: $$\beta = \frac{Q_g}{Q_{tp}} \quad (2.28)$$

Quality: $$X = \frac{\dot{M}_g}{\dot{M}_{tp}} \quad (2.29)$$

where $\dot{M}_l$ is the liquid mass flow rate (kg/s), $\dot{M}_g$ is the gas mass flow rate (kg/s), A is the total cross-sectional flow area (m^2), A_l is the cross-sectional flow area occupied by the liquid phase (m^2), A_g is the cross-sectional flow area occupied by the gas phase (m^2), ρ_l is the density of liquid phase (kg/m^3), and ρ_g is the density of gas phase (kg/m^3).

By assuming that both phases move at the same velocity (no-slip flow) i.e. α=β, homogenous flow model can be used to estimate the essential parameters of two-phase flow.

The two-phase mixture density based on the gas phase volumetric flow fraction is given by:

$$\rho_{tp} = \beta\rho_g + (1-\beta)\rho_l \quad (2.30)$$

The two-phase mixture density based on the quality is as follows:

$$\rho_{tp} = \frac{1}{\left(\frac{X}{\rho_g} + \frac{(1-X)}{\rho_l}\right)} \quad (2.31)$$

The homogenous flow velocity is calculated by:

$$\bar{V}_{tp} = G_{tp}\left(\frac{X}{\rho_g} + \frac{(1-X)}{\rho_l}\right) \quad (2.32)$$

The last parameter that needs to be defined in homogeneous flow model is the dynamic viscosity. There are at least three ways to estimate the average viscosity as described below:

Method 1:

$$\mu_{tp} = \mu_l(1-\beta)(1+2.5\beta) + \mu_g\beta \tag{2.33}$$

Method 2:

$$\mu_{tp} = \frac{1}{\left(\frac{X}{\mu_g} + \frac{(1-X)}{\mu_l}\right)} \tag{2.34}$$

Method 3:

$$\mu_{tp} = X\mu_g + (1-X)\mu_l \tag{2.35}$$

The two-phase flow is treated as single-phase flow with average properties. Consequently, Reynolds number for homogeneous flow can be defined as follows:

$$Re = \frac{\rho_{tp}\bar{V}_{tp}D}{\mu_{tp}} \tag{2.36}$$

To analyze the data obtained in microbubble drag reduction experiments, equations 2.30, 2.32, 2.33 and 2.36 are used.

Chapter 3

Literature Review

3.1 Overview

This chapter is dedicated to the literature review about different aspects of this study.

Section 3.3.1 presents the literature review about microbubble drag reduction and its mechanism.

The effects of frother on drag reduction and the related mechanisms are presented in section 3.3.2.

The literature on polymeric drag reduction, polymer degradation, and the mechanism of polymer drag reduction is also discussed.

3.2 Brief Historical Review of Drag Reduction

Reducing drag force in different applications has been an attractive research field since Blatch (1906) first observed drag reduction in the flow of paper pulps. The importance of saving energy and minimizing its costs for industries has led to a significant amount of research on drag reduction by aid of chemical additives and in some cases by aid of air bubbles.

Drag reduction phenomenon by aid of chemical additives was discovered by Toms (1948) who observed that by the addition of a few ppm of polymethylmethacrylate to turbulent pipe flow of monochlorobenzene, the pressure drop decreased significantly in comparison to the pure solvent. Some years later Dodge and Metzner (1959) observed the same behavior for solutions of sodium carboxymethylcellulose and water. In 1964, the possibility of reducing energy loss through use of chemical additives in fluid transportation was demonstrated by Savins. In 1972, this demonstration and previous studies led to the use of polymer as a drag reducing agent in Trans-Alaska-pipeline - the first industrial project where polymer was used as a drag reducing agent. Although chemical additives were a great discovery in the field of drag reduction, they are not the only method to induce drag reduction in liquid flows.

Another method that produces drag reduction in flow systems is the injection of microbubbles. Some applications of microbubble drag reduction (MDR) method are related to oil production, naval industries, and flotation. The MDR effect was first observed and investigated by McCormick and Bhattacharyya in 1973. By implementation of experimental work on a fully submerged hull in a towing tank, they demonstrated that frictional resistance can be reduced by aid of microbubble injection around the hull. Madavan et al. (1984) later showed that frictional resistance can be reduced up to 80% by aid of injection of microbubbles to the turbulent boundary layer of system. After successful experiments of Madavan et al. (1984), many studies were conducted on microbubble drag reduction by Merkle et al. (1986), Tokunaga (1986), Takahashi et al. (1997), Kodama et al. (1999), etc. Guet et al. (2003) demonstrated that by injection of small bubbles to vertical water flow, the pressure gradient can be decreased compared to pure water flow.

Although many studies have been done on drag reduction phenomenon involving chemical additives and microbubbles, more work needs to be done in this area. In particular, the combination of different drag reduction methods needs to be explored.

3.3 Literature Review

Drag reduction is a subject of intensive research because of potential energy and cost savings. Industrial and laboratory investigations in this field have led to the development of different drag reduction methods. Microbubble drag reduction and drag reduction by aid of additives such as polymer are the most well-known among different methods of drag reduction.

This experimental work investigates combination of microbubble drag reduction and additive drag reduction.

3.3.1 Microbubble Drag Reduction

Based on experimental work and numerical modeling, Skudarnov and Lin (2006) illustrated that injection of microbubbles to turbulent flow near a flat plate causes drag reduction. They pointed out that the density ratio (ratio of density of gas to density of water) plays an important role in microbubble drag reduction. As a result, the injection of gas does not have a significant effect on drag reduction at small gas flow rates. At high gas injection rates, drag reduction becomes significant.

Another numerical work on the effect of density ratio on microbubble drag reduction was conducted by Xu et al. (2002). They observed that the effect of density changes is more significant in laminar flows than in turbulent flows. They showed that the effect of density on microbubble drag reduction in laminar flow is around 10%, while in turbulent flow it is 6%.

Madavan et al. (1985) implemented a numerical investigation of the effects of density and viscosity changes on microbubble drag reduction. They found out that microbubbles affect the local density and viscosity resulting in skin drag reduction. Moreover they proposed that bubbles change the turbulent energy by interacting with the buffer layer.

Other important parameters that have attracted a lot of attention in microbubble drag reduction are bubble size and void fraction. Guin et al. (1996) proposed that near wall void fraction is an important parameter for drag reduction on plates. They showed that the effect of near-wall void fraction on drag reduction is more important than the effect of averaged void fraction. By increasing the near-wall void fraction, drag reduction increases.

The effect of bubble size on drag reduction was investigated by Merkle et al. (1985). They found that bubble size decreases when the flow velocity is increased and increases when the air flow rate is increased.

Sanders et al. (2006) investigated the effects of bubble size on turbulent water flow. They suggested that drag reduction is influenced by gas flow rate and static pressure. However, they did not see any significant effects of bubble size on drag reduction in the tested range of bubble sizes.

Lu et al. (2005) studied the effects of bubble on drag force in bubbly channel flow by using numerical simulation. They reported that the near-wall microbubbles influence drag force on the wall. They showed numerically that more deformable bubbles tend to reduce drag force on the wall by decreasing the streamwise vorticity.

Another numerical work has been conducted by Ferrante and Elghobashi (2004). In agreement with Lu et al. (2005), they claimed that the addition of air bubbles to the flow system results in drag reduction due to the displacement of vortical structure away from the wall.

Bubble size distribution has been investigated by Afacan et al. (2004). In their experimental work, they studied the effects of nozzle diameter, pipe length, and gas flow rate on the bubble sizes and their distribution. Like Sanders et al. (2006), they found that the most dominant parameter that affects the bubble size and its distribution is the gas flow rate.

Zaruba et al. (2007) showed that small bubbles tend to migrate towards the pipe wall and larger bubbles tend to migrate towards the center of the pipe. These movements have a significant impact on the near-wall and averaged void fractions.

Although the reduction of frictional resistance on flat plates by aid of microbubbles has been reported by many researchers, the effect of microbubbles in pipeline flow is not clear.

In vertical pipeline flow, Descamps et al. (2008) found that microbubbles increase the wall shear stress and hence the drag force on the wall. They also showed that small bubbles tend to increase drag force more than large bubbles. However, due to the density effect of microbubbles injection, the pressure drop in upward two phase flow decreased in comparison with single phase flows.

3.3.1.1 Mechanism of Microbubble Drag reduction

The exact mechanism as to how microbubbles affect drag force is not well understood. The theoretical studies carried out so far are not sufficient to explain all aspects of the mechanism. However, it is believed that drag reduction by microbubbles is produced by combination of density reduction and turbulence modification.

Turbulence modification is one of the hypotheses that is claimed to explain the effect of bubbles on drag force. Meng and Uhlman (1998) proposed that bubble splitting is the mechanism that affects turbulence intensity in microbubble-laden turbulent boundary layer. Kanai and Miyata (2001) suggested that microbubbles decrease turbulent energy by reducing spanwise vorticity formation near the wall. In agreement with Kanai and Miyata (2001), Ferrante and Elghobashi (2004) showed numerically that microbubbles displace turbulent vortical structure away from the wall.

Another parameter that influences drag force is density reduction. Legner (1984) suggested that density effect is the dominant source of drag reduction. Moreover, Skudarnov and Lin (2006) have demonstrated that density change has a significant effect on the velocity profile and turbulent kinetic energy which may be the reason for reducing the drag force.

Although the mechanism of microbubble drag reduction is still not clear, many parameters, such as bubble deformation, void fraction, turbulent modification, and density change, seem to have a significant effect on drag.

3.3.2 Frother Effects

Frothers are a class of surfactants. However, they do not have a direct influence on drag force. They impact drag force by altering the bubble sizes and changing the two-phase flow pattern.

Frother structure is a combination of hydrophobic and hydrophilic parts. The hydrophobic part consists of hydrocarbon chain and the hydrophilic part can be a group such as –OH, as in alcohols, or alkoxy as in polyglycols. At the air-water interface the hydrophobic group will get attached to bubble side and the hydrophilic group will remain on the water side. Figures 3.1 and 3.2 give chemical formulae of some frothers.

Figure 3.1 Polyglycol Ethers formula

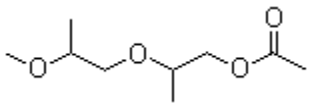

Figure 3.2 Dipropylene Glycol Methyl Ether structure

Nesset et al. (2006) investigated the impact of frothers on bubble size distribution. They observed that the bubble size distribution changes from bi-modal in pure water to uni-modal in the presence of frother in the system.

Another investigation about the effect of frother on bubble size was conducted by Grau and Laskowski (2006). They found that the Sauter mean diameter decreases significantly in presence of frother. They also introduced the critical coalescence concentration (CCC) which is the concentration of frother where bubble reaches its minimum size.

Nesset et al. (2007) illustrated the dependency of bubble size on frother concentration by testing 5 different types of frother. They found that all five types of frothers decreased the Sauter mean bubble diameter to a minimum size upon increasing the frother concentration. They also showed that different types of frothers exhibit the same trend of bubble size reduction. Figure 3.3 shows their Sauter mean diameter data as a function of normalized frother concentration C/CCC95, where CCC95 is the concentration of frother which gives 95% reduction in Sauter mean diameter.

The shape and velocity of bubble are also affected by the frother. Clift et al. (2005) proposed that bubbles in pure water are deformed due to the change of pressure around the rising bubble. However, by adding a few ppm of frother to the system, bubbles tend to be spherical even in the presence of pressure gradient. They also found that bubbles travel faster in pure water than in the presence of frother in the system.

Malysa et al. (2005) also reported that by adsorption of frother at the bubble surface, the bubble rise velocity decreases significantly. They found that by adding a few ppm of terpineol to water, the bubble terminal velocity decreases by more than 40%.

Cooper et al. (2004) reported that frother not only controls the bubble size, but also affects the creation size of bubbles. They showed that by extrapolation of the graph of bubble Sauter mean diameter versus gas velocity, the initial diameter of the bubbles produced are around 0.5 mm.

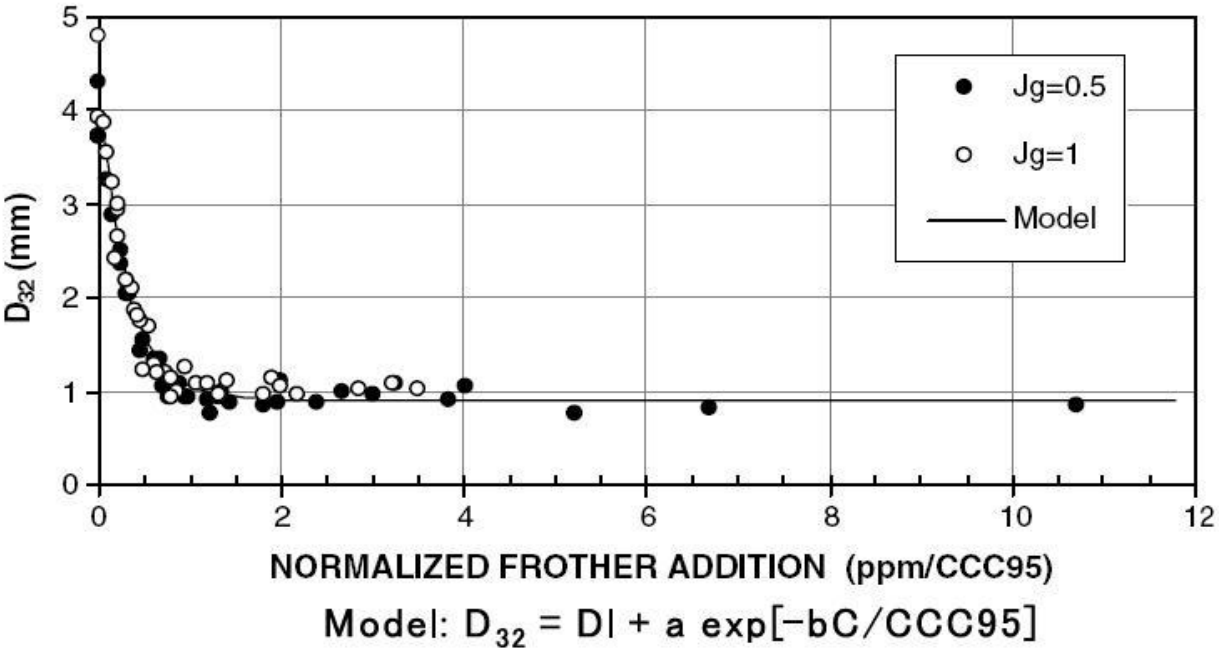

Figure 3.3 Same impact of 5 different types of frother on bubble Sauter mean diameter presented by Nesset et al. (2007)

3.3.2.1 Mechanism of Frother Effects

Reduction in surface tension and coalescence prevention are two mechanisms that are believed to be responsible for the effects of frother on bubble size and shape.

- Reduction of Surface Tension

Surface tension is the force acting on the surface of a liquid, tending to minimize the area of the surface. It is believed that the frother decreases the surface energy (tension) and as a result more surface area can be created. This phenomenon leads to the creation of more fine bubbles with smaller diameters. Although reduction of surface tension is a plausible reason for production of smaller bubbles, many experimental studies show that it is not the only reason for the effect of frother on bubble diameter.

Sweet et al. (1997) demonstrated that by adding MIBC (frother) to the system, the bubble size decreased without a significant change in the surface tension. Moreover, Finch et al. (2008)

reported that a decrease in bubble size occurred with the addition of salt to the system even though the surface tension was found to increase.

- Coalescence Prevention

Another theory to explain the effect of frother on bubble dimensions is "coalescence prevention". The hydrophobic group of the frother prefers to stay on the gas side of bubble. On the other hand, the hydrophilic group of the frother bonds and interacts with the molecules of water (see Fig. 3.4). Consequently, the frother acts as an inter-layer that prevents coalescence of bubbles (see Fig. 3.5).

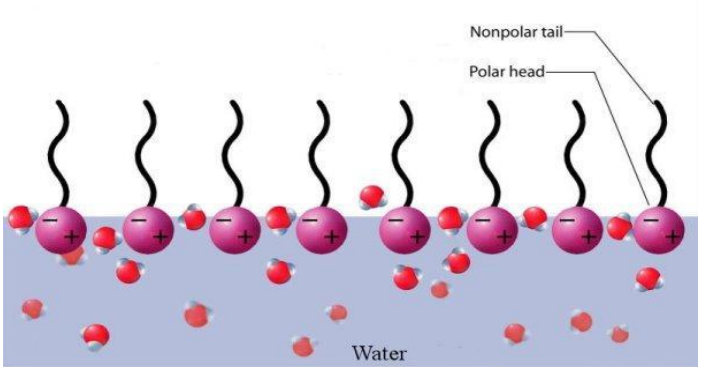

Figure 3.4 Frother molecules on a surface of water and air (adapted from random Google search)

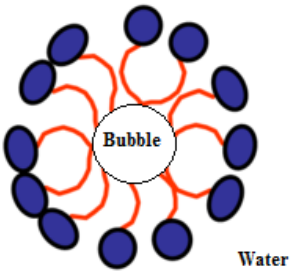

Figure 3.5 Frother molecules around a bubble in water (adapted from random Google search)

3.3.3 Polymeric Drag Reduction

Drag reduction by aid of polymers is considered to be the most effective method of reducing drag. Among the synthetic and organic polymers, synthetic ones give better drag reduction. Polymer structural parameters, such as molecular weight and chain length, are important parameters determining the effectiveness of polymer. It has been shown through many experiments that polymers with higher molecular weight give better drag reduction (see Fig. 3.6). Figure 3.7 shows different polymer structures. An ideal polymeric flow enhancer (drag reducer) should have a long, linear chain without any branching. As shown in Figure 3.8, the degree of drag reduction increases with the increase in chain length (degree of polymerization P_w). In our work, polyacrylamide with good solubility in water was selected for drag reduction experiments.

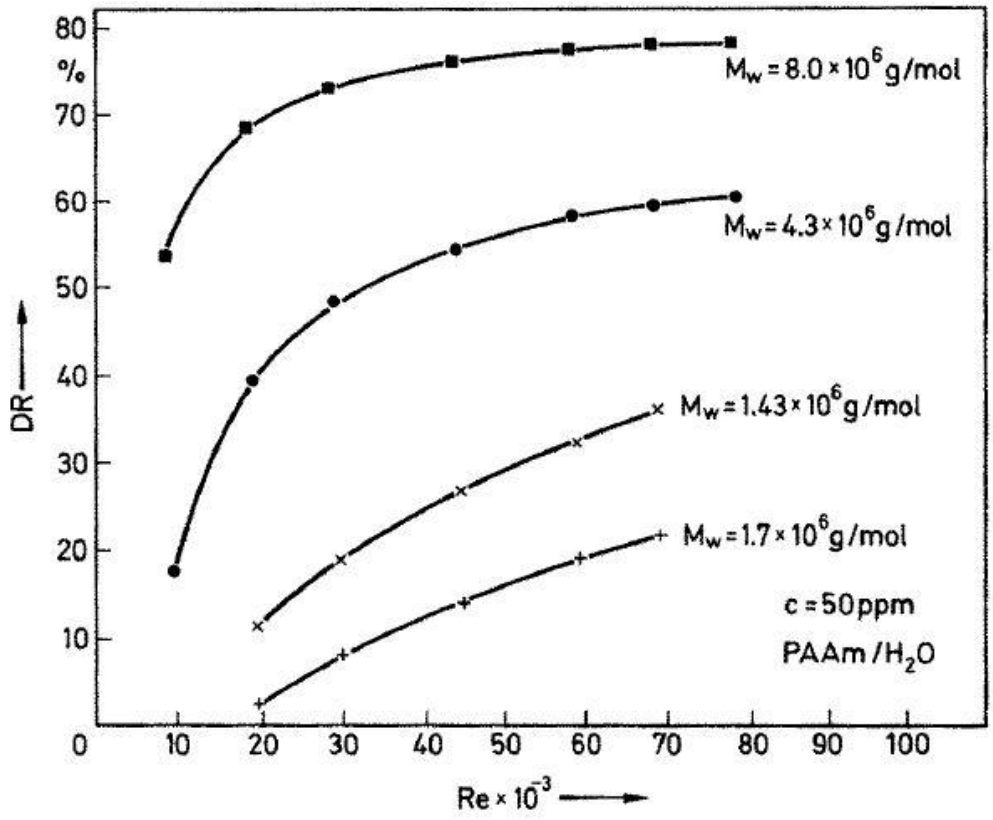

Figure 3.6 Effect of Polymer molecular weight on drag reduction (adapted from Gampert, Wagner 1985)

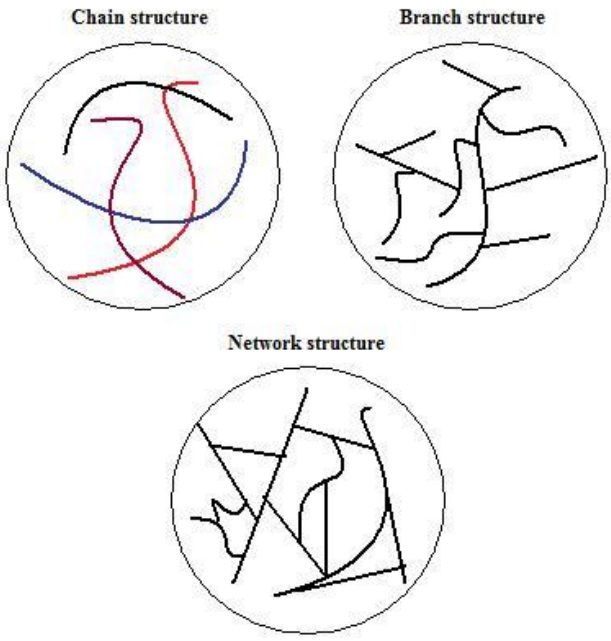

Figure 3.7 Polymer structures

Concentration: c = 30 ppm				
PAAm	B1	M3	40/1	37/05
P_w	15500	55000	115000	142000
M_w (g/mol)	$1.1 \cdot 10^6$	$3.9 \cdot 10^6$	$8.2 \cdot 10^6$	$10.1 \cdot 10^6$
DR_{max} (%)	17	40	72	73
RE	48000	25000	26000	26000
Concentration: c = 98 ppm				
DR_{max} (%)	32	60	77	78
Re	47000	41000	52000	64000

Figure 3.8 Effect of polymer chain length (degree of polymerization) on drag reduction (adapted from Kotter et al. 1989)

Drag reduction by aid of polymer was first observed by Toms in 1948. He found that the addition of a small amount of monochlorobenzene (polymer) to flow reduced the pressure drop. Since then several studies have been done on polymeric drag reduction to find out the influence of polymer on the flow structure.

Wells and Spangler (1967) injected polymer solution to the center of pipe (turbulent core) to investigate the effect of polymer on turbulent flow. They found that the injected polymer does not show any local drag reduction effect until the polymer reaches the wall region.

McComb and Rabie (1982) also performed injection experiments with two types of injection techniques, namely, core injection and wall region injection. They showed that when polymer is injected at the center of the pipe, local drag reduction increases with the increase in the distance from the injection point due to diffusion of polymer to the wall region. For injection in the pipe wall region they observed that the drag reduction increases with the distance from the injection point and it happens faster than the injection at the center of the pipe.

The effect of polymer concentration was investigated by Bewersdorff (1982). He found that higher polymer concentration gives better drag reduction. He also showed that by increasing polymer concentration; the onset point of drag reduction is not clearly observed; the onset point is clearly distinguishable at low polymer concentration.

Hershey and Zakin (1967) studied the onset point of drag reduction in low and high concentration ranges of polymer. He categorized polymeric solution into two groups: dilute drag-reducing solution which exhibits an onset point for drag reduction (breaking point between laminar and turbulent regimes is observed) and concentrated drag-reducing solution which does not exhibit a clear starting point for drag reduction, i.e. no breaking point between laminar and turbulent regimes is observed.

The effect of polymer molecular properties on drag reduction has been investigated by many researchers. Hoyt and Fabula (1964) conducted experiments with different types of natural and synthetic polymers. Their experiments suggested that polymers with linear structure give better drag reduction than the branched polymers. They also showed that polymers with high molecular weight have better drag reduction effect than the polymers with low molecular weight. They

claimed that polymers with molecular weight less than 100,000 are not effective drag reducing additive.

Banijamali et al. (1974) studied the influence of the degree of polymerization on polymer drag reduction effectiveness. They found that by increasing the degree of polymerization of linear polymer, the drag reduction effect increases.

3.3.3.1 Mechanism of Polymeric Drag Reduction

Polymers have been used as drag reducing additives for a long time; however, there is still no comprehensive agreement on the mechanism of friction reduction caused by polymers. A number of mechanisms have been proposed as listed below.

- Wall Effect- Shear Thinning

Shear thinning wall layer idea was suggested by Toms as a possible mechanism. According to this mechanism, a very low viscosity layer is formed near the wall that causes reduction in frictional resistance. However, this mechanism is in contrast with the experimental work of Walsh (1967) who showed that even in shear-thickening solutions, considerable drag reduction occurs.

- Adsorption Effect

The next mechanism of drag reduction by aid of polymer was introduced by EI'perin et al. (1967). They proposed that adsorption of a polymer layer on the pipe wall causes slip of flow on the wall; it also dampens turbulence fluctuations, and prevents the formation of vortices at the wall. However, Little (1967) showed that the adsorption of polymer layer could be due to the release of trapped polymer in the pressure measuring static tubes. Moreover, Gyr and Mueller (1974) found that the adsorbed polymer on the wall does not have any interaction with bulk flow and cannot change the flow properties.

- Normal Stress –Non Isotropic Viscosity

Another possible mechanism of reduction of drag force is the existence of non-isotropic viscosity in the flow. Non- isotropic viscosity is the viscosity that decreases in the direction of flow and increases in other directions resulting in reduced turbulent fluctuations. The changes of viscosity in different directions also produce differences in normal stresses. However, Gadd (1966) reported no relation between reducing drag force and normal stresses in his experiments. Boggs and Tompson (1966) by aid of theoretical calculation showed that frictional drag reduction is a function of one-third the power of the ratio of the elastic forces to the viscous forces and suggested that drag reduction could be because of viscoelastic effects.

- Decrease of Turbulence Production

Decrease of turbulence production is the other probable mechanism. Astarita (1965) believed that turbulence is less dissipative in viscoelastic liquids than in viscous liquids. On the other hand Gadd (1965) introduced reduction of turbulence production, instead of dissipation of turbulence, as a possible mechanism of drag reduction. In agreement with Gadd (1965), Johnson and Barchi (1968) showed that with the addition of polymer to the system, the production of small eddies in developing boundary layer decreases.

- Vortex Stretching

Development of resistance to vortex stretching is another possible mechanism of drag reduction caused by polymeric additives. Rapid decay of eddies, as a consequence of the resistance to stretching, is suggested as a friction reduction mechanism by Gadd (1965). On the other hand, it is proved by Gyr (1968) that this mechanism is only effective in the case of small eddies near the wall.

- Molecular Stretching

Another explanation for polymeric drag reduction is molecular stretching. Tulin (1966) observed that a polymer molecule extends in the shear direction. He proposed that the stretching of a polymer molecule causes reduction in the energy of turbulent eddies and radiates them (eddies)

away by absorbing the released energy. Furthermore, he showed that molecular stretching increases the laminar sublayer thickness.

Similar to Tulin (1966) results, Pfenninger (1967) suggested that the stretching of polymer molecules influences turbulence energy and decreases vorticity. He also pointed out that molecular stretching increases the laminar sublayer thickness by absorption of kinetic energy of the vortices. Consequently the frictional resistance on the wall decreases.

Peterlin (1970) claimed that molecular stretching is due to micro vortices as a mechanical source of elongation of polymer molecule. He proposed that this elongation absorbs energy and dissipate the vortices and as a result of these effects, drag reduction appears in the flow system.

3.3.3.2 Polymer degradation

Polymers are the most effective drag reducing additive agents. However due to the mechanical and chemical degradation of polymer chains, drag reduction decreases with time (see Fig. 3.9). The reasons for the degradation of polymer molecules are not clear yet but it is believed that the break-up of polymer chain occurs due to chemical and mechanical influences.

Ellis et al. (1970) demonstrated that fresh polymer solution shows better drag reduction than the polymer solution stored for several weeks. Another example of chemical degradation of polymer was reported by Kulicke (1986). He suggested that the viscosity of polymer solution changes upon storage of solution in the dark and without shaking (in absence of mechanical impact) due to chemical degradation of polymer.

Mechanical forces can also cause degradation of polymer solutions. Shear stress acting on the polymer molecule, for example in the pump or in the pipeline, has a significant influence on polymer degradation. Buoldin (1988) has suggested that due to mechanical impact on polymer molecule, all the intermolecular coupling points are loosened and results in the separation of polymer chain and hence degradation of polymer molecule.

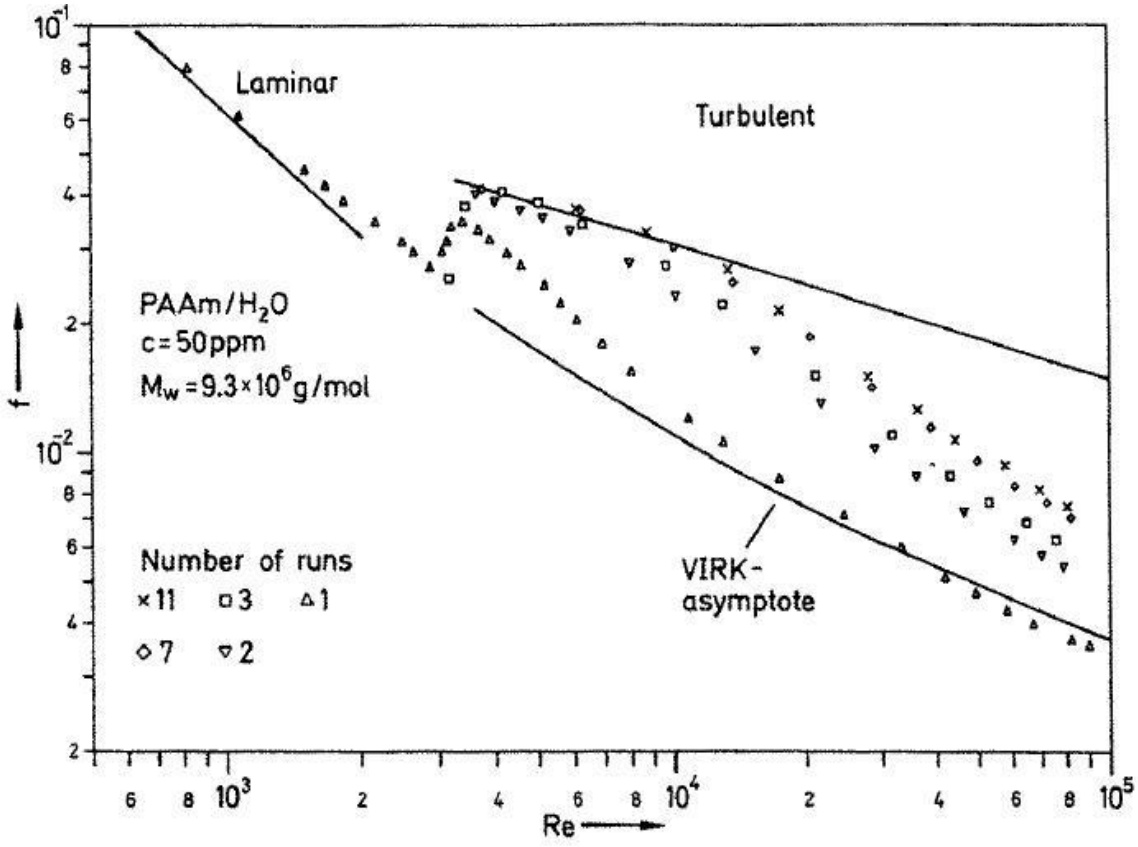

Figure 3.9 Influence of Polymeric degradation on drag reduction (adapted from Gampert and Wagner 1985)

Chapter 4

Experimental Apparatus and Procedures

4.1 Overview

A new experimental apparatus was built for the investigation of effect of additives on drag reduction. The experimental apparatus and related procedures for data acquisition are explained in this chapter.

Information about different components of the apparatus, namely instruments and test sections, is given. The data acquisition procedures and data analysis methods are described in the last section of the chapter.

4.2 Description of the Experimental Layout

To investigate the effects of air bubbles and additives on drag reduction in vertical pipelines a new experimental set-up was designed. The system, shown in Figure 4.1, consists of a magnetic flowmeter to measure the water flow rate, spargers to generate air bubbles and to inject them into the system, pressure transducers to measure the pressure drop in the test sections, and a rotameter to measure the gas flow rate.

The water flows into the system from tank 2 and enters one pipe at a time in the test sections consisting of 3 pipes with different diameters. The flow rate of water is measured by aid of a magnetic flow meter. The temperature of water in the tank is controlled by a temperature controller at 21 °C.

Air from the air supply system is passed through the pressure regulator at a constant air pressure of 22 psig. To measure the amount of injected air into the system, a rotameter is used. The air is injected into the test section through a stainless steel sparger.

The measurement of pressure drop in the test section is done by aid of two pressure transducers (0.5 and 5 psi). The signal from the pressure transducer is sent to the computer interface. By aid of this signal and the transducer calibration curve, the actual pressure drop in the test section is determined.

After flowing through the test section, the air and water mixture enteres tank 1, where the air is separated from water and released to the atmosphere. The level of water in the tank number 1 is controlled by a valve in the drain section of the tank. After separation of air in tank 1, the water is recycled to tank 2.

The signals from the pressure transducers and magnetic flowmeter are analyzed by a computer program (Labveiw). Figures 4.2- 4.7 show different views of the experimental set-up.

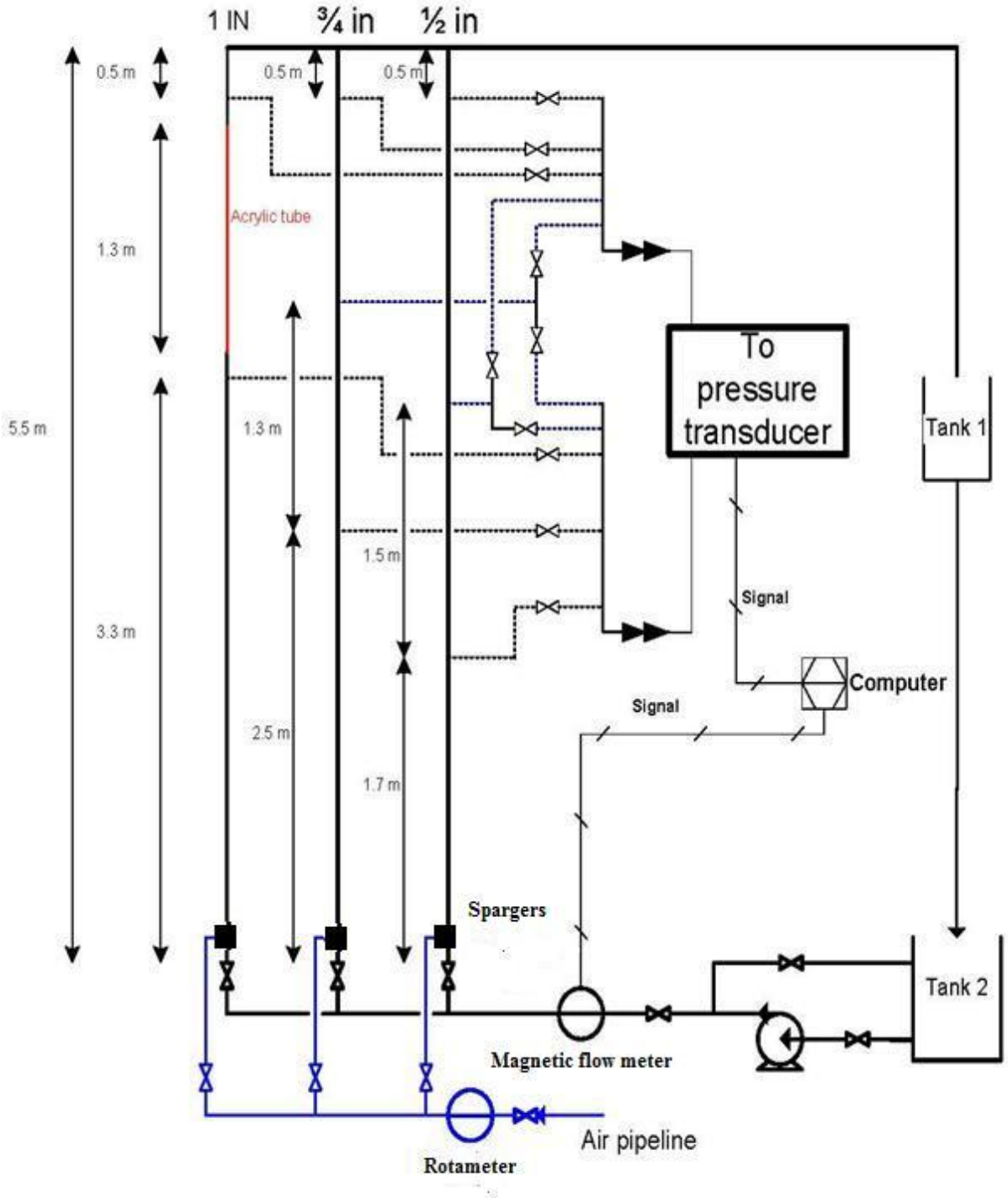

Figure 4.1 Experimental layout

Nominal diameter of test sections (inch)	Internal diameter of test sections (inch)	Entrance length (m)	Total length of test section (m)	Distance between used pressure taps (m)
½”	0.52	1.7	5.5	3.3
¾”	0.73	2.5	5.5	2.5
1”	0.93	3.3	5.5	1.3

Table 4.1 Dimension of test sections

Figure 4.2 View of gas sparger in the test sections

Type of sparger	Nominal size	Pressure range	Filtration range
Porous stainless steel sparger	3/8”	175 psi	50 microns

Table 4.2 specification of sparger

Figure 4.3 View of the test section and pressure transducers tubing

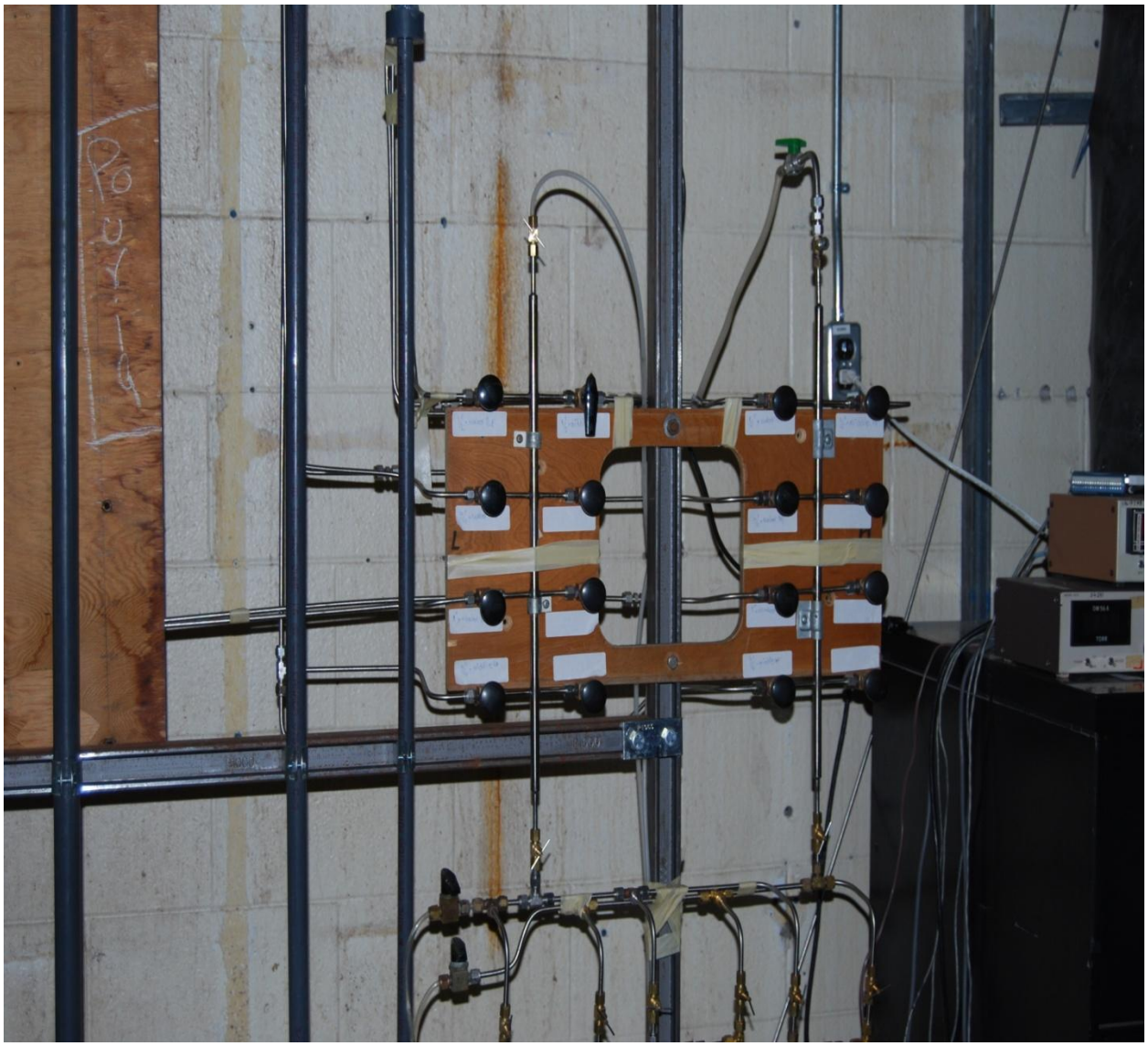

Figure 4.4 View of pressure transducers manifolds and tubing

Figure 4.5 View of storage tank number 2 and its mixer

Figure 4.6 View of the liquid flowmeter and its signal converter

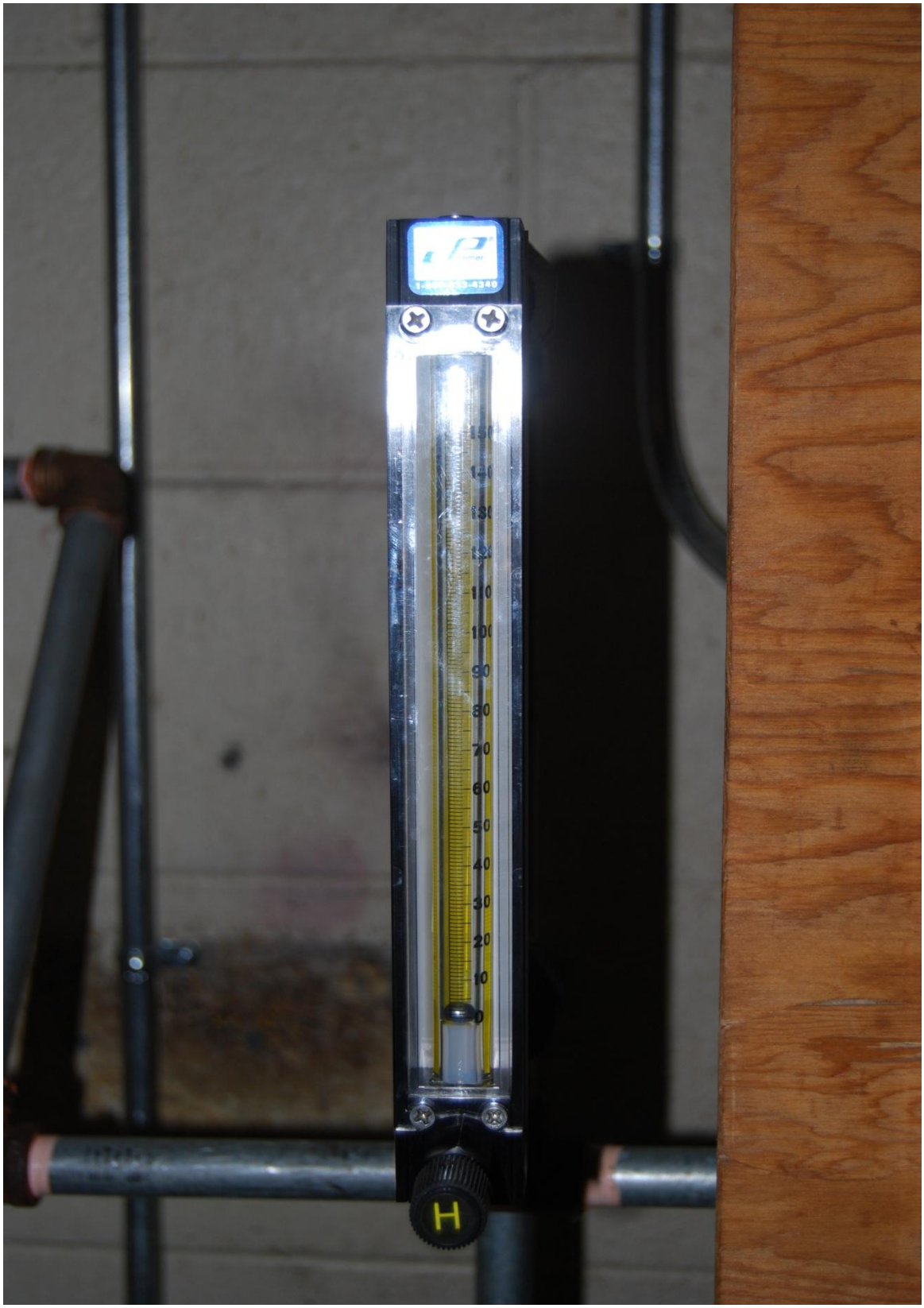

Figure 4.7 View of gas flowmeter

4.2.1 The Air Supply System

The air for this experiment was supplied by the University facility with the maximum pressure of 110 psig. The pressure of air to the system was adjusted and controlled by a pressure regulator that maintained a pressure of 22 psig. The amount of air injected onto the apparatus through the sparger was measured by a rotameter (Fig. 4.7).

4.2.2 The Liquid Supply System

City tap water was used in the experiments. The water was supplied to tank number 2 (see Fig. 4.1). Additives, such as Polyacrylamide and Aerofroth, were added to tank2 and mixed with water by aid of a high duty three blade mixer.

After preparation of solution in tank 2, the liquid was pumped into the system by aid of a 1.5 hp centrifugal pump. The flow rate of the liquid that was pumped to the system was controlled by a ball value on the outlet of the pump and the pump bypass line.

The magnetic flow meter was utilized to measure the flow rate of liquid in the test section.

4.2.3 Description of Instrumentation and Controls

In this section, the operational principles of magnetic flow meter, pressure transducer, and rotameter are discussed.

4.2.3.1 Flow rate Measurement

Two types of flowmeters have been used in this work: rotameter and magnetic flow meter. They are described below.

4.2.3.1.1 The Liquid Flow Measurement

4.2.3.1.1.1 Operational Principle of Magnetic Flowmeter

Magnetic flowmeters are volumetric flow meters with high accuracy, low maintenance design, and no moving part to measure the flow rate. The principle of operation of magnetic flowmeters are based on Faraday's law which states that the voltage induced in any conductor that moves at the right angles to a magnetic field is proportional to the velocity of that conductor (see Fig. 4.8):

$$E \propto V \times B \times D \tag{4.1}$$

where E is the voltage generated in a conductor, V is the velocity of the conductor, B is the magnetic field strength, and D is the length of the conductor.

To measure flow rate with this type of flowmeters, the fluid must be conductive. As the conductive fluid passes through the magnetic flowmeter, the induced voltage develops proportional to the flowrate. Therefore, the magnetic flow meter generates a signal corresponding to the induced voltage and transmits the signal to its signal converter. The transmitted signal is converted to the standard DC voltage, which is directly proportional to the volumetric flowrate.

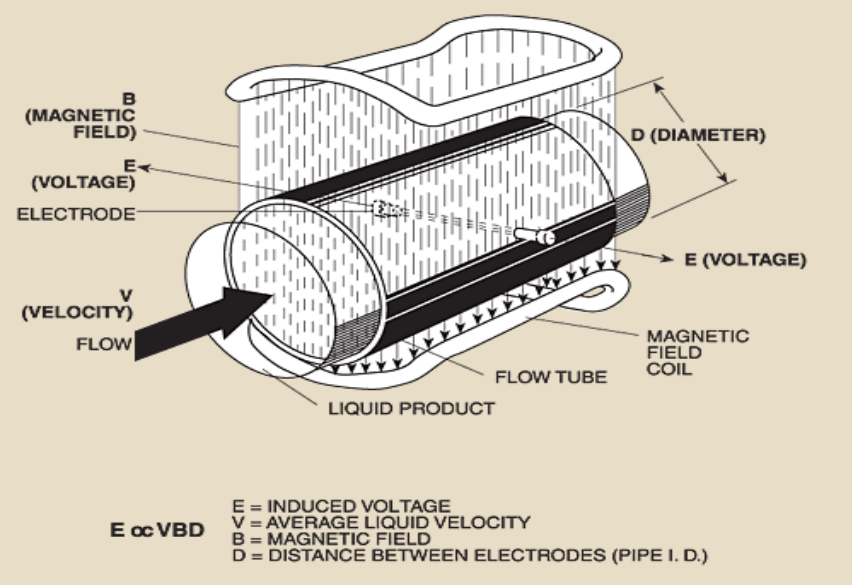

Figure 4.8 Basic operational concepts of magnetic flowmeters (Brooks magnetic flowmeter manual)

4.2.3.1.1.2 Specification of Magnetic Flowmeter used in the Experiments

A Brooks magnetic flowmeter, model 7601-1A1A8AA, with its signal converter, model PMI400, was used to measure the flowrate of liquid in the experiments. The output signal from signal converter was in the range of 0-2V DC. This signal was transmitted to the computer interface which converted the DC voltage to the signal that is recognizable by computer.

4.2.3.1.2 The Gas Flow Measurement

4.2.3.1.2.1 Operational Principles of Rotameters

Rotameters or variable-area flowmeters are the most common type of measuring devices that are used for measuring the gas volumetric flow rate. These meters consist of a vertical (transparent) tapered tube which is narrow at the bottom and wide at the top. A float is present inside the tube. As illustrated below (Fig. 4.9) the float moves up and down depending on the volumetric flowrate of the fluid that passes through the cross-sectional area of tapered tube.

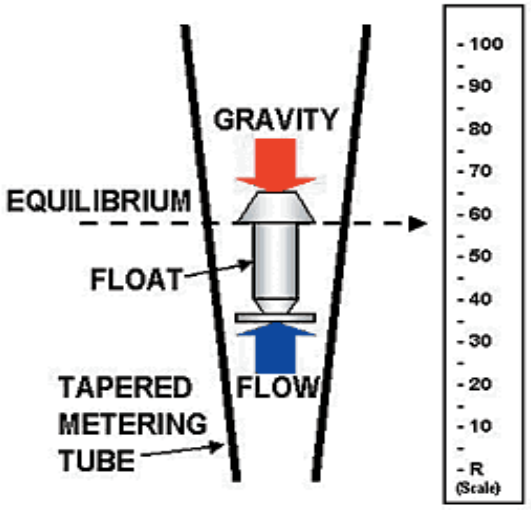

Figure 4.9 Principle of operation of rotameters

The higher the flowrate the larger is the cross-sectional area needed for fluid to flow through the rotameter. Therefore the float is pushed up by increasing the fluid flowrate to reach wider corss-sectional area and the new equilibrium condition. The equilibrium condition is the condition where fluid drag force is balanced by gravity force and buoyancy force. Therefore, the height of the float inside the tube is proportional to the flowrate.

4.2.3.1.2.2 Specification of Rotameter Used in the Experiments

The air flow rate was measured by aid of a Cole-Parmer gas rotameter with 150 mm glass tube and stainless steel float with a density of 8.04 g/ml. The overall flow range of rotameter was 0-17,000 ml/min and the accuracy was ±2% of full scale.

4.2.3.2 Differential Pressure Measurement

Pressure transducers were utilized to measure pressure drop across the test section. Accurate measurement of differential pressure data depends on pressure transducers and impulse tubing system. There are 5 possible sources of error in the measurement of differential pressure in a system:

1. Pressure transducer
2. Leakage in impulse tubing
3. Trapped gas in the impulse tubing
4. Density variation between pressure transducer legs
5. Plugging of impulse tubing

To minimize errors in the measurements, the following steps were taken:

i. Minimized the length of impulse tubes
ii. Checked the valves in the impulse tubing for leakage
iii. Vent the gas out of the impulse tubing
iv. Ensured no gas entered the impulse tubing.
v. Filled the high pressure and low pressure impulse tubing (connected to the pressure transducer) with the same type of fluid

4.2.3.2.1 Principle of Operation of Differential Pressure Transducers

The pressure sensing part of a pressure transducer is a flat diaphragm that separates the high pressure side from the low pressure side and is located between magnetic field producing blocks (see Fig. 4.10). By applying differential pressure to the measuring device, the diaphragm bends and the magnetic flux passing through each side of diaphragm changes, i.e. the magnetic flux decreases on one side of the diaphragm and increases on the other side.

The change in the magnetic flux produces a signal that is proportional to the applied differential pressure. The type of signal varies with the kind of pressure transducer; it can be a DC voltage or a DC current.

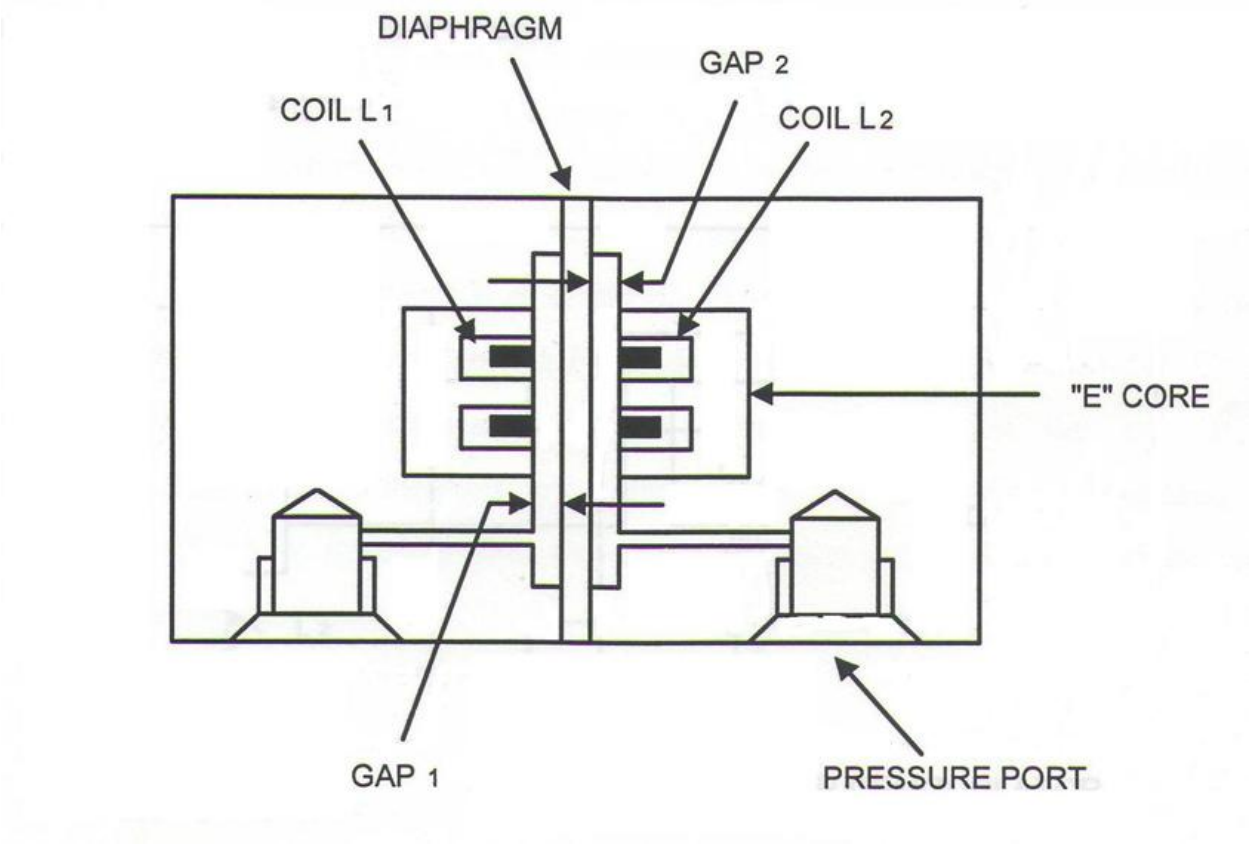

Figure 4.10 Cross-section of pressure transducer

4.2.3.3 The Differential Pressure Transducers Used in the Experiments

Rosemount pressure transducers were utilized in the experiments to measure the pressure drop in the test section (see Fig. 4.11). Two pressure transducers in the range of 0-5 psi and 0-0.5 psi were used. The measurement error was less than 1% of full range. The output signal from the pressure transducer was DC voltage.

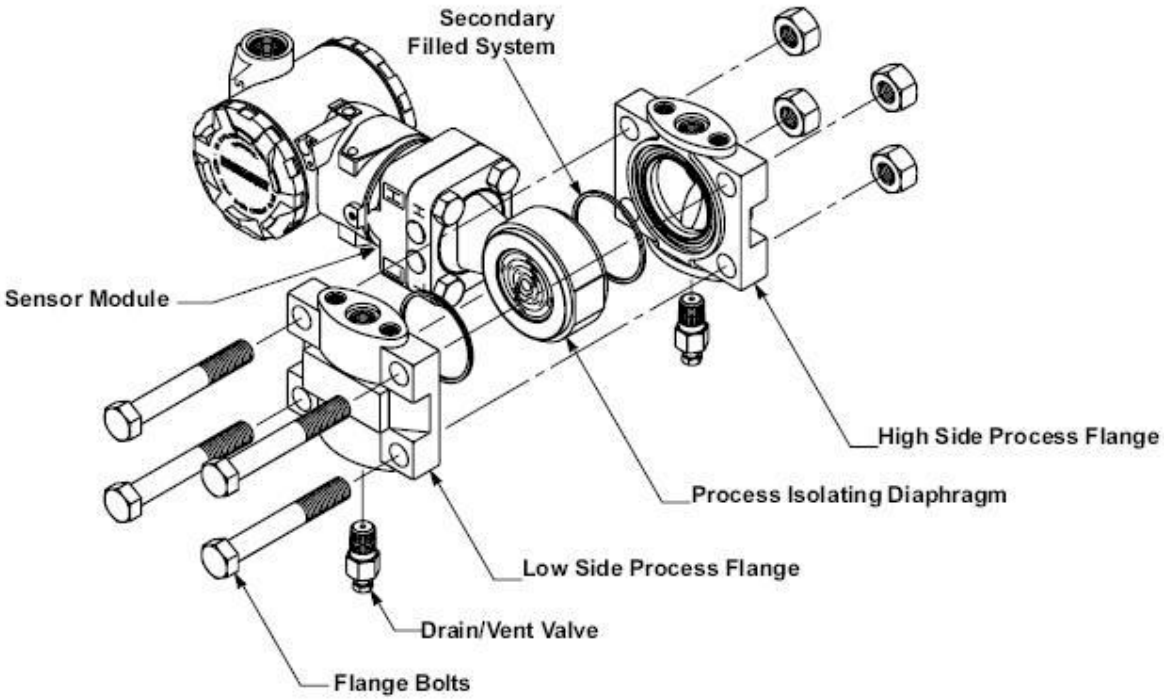

Figure 4.11 Detailed view of Rosemount pressure transducer (Rosemount pressure transducer manual)

4.2.3.4 Temperature Control System

An automatic on and off temperature controller (Fig. 4.12) was used to control the temperature of the liquid in the storage tank (tank 2 of Fig. 4.1). The input to the controller was a signal from a thermocouple installed inside the storage tank. The signal from the thermocouple to the controller was analyzed and compared with the temperature set point. Based on the difference between the controller set point and the thermocouple signal, an appropriate signal was sent to two solenoid valves (see Fig. 4.13) which controlled the flow of cold and hot water through the coil installed inside the storage tank. These processes continued in order to maintain the storage tank temperature at the set point of temperature controller.

Figure 4.12 View of temperature controller

Figure 4.13 View of solenoid valve

4.2.3.5 Computer Interface

To record the voltage signals from pressure transducers and magnetic flowmeter, the voltage signal should be converted to the computer signal. In this work, a USB-based DAQ module with 8 analog channels (see Fig. 4.14 and 4.15) was used. By aid of this interface, the voltages were converted to digital signals recognizable by the computers. The computer signals were interpreted by a computer program, called LabView.

Figure 4.14 USB-based DAQ module with 8 analog channels of 16 bit resolution

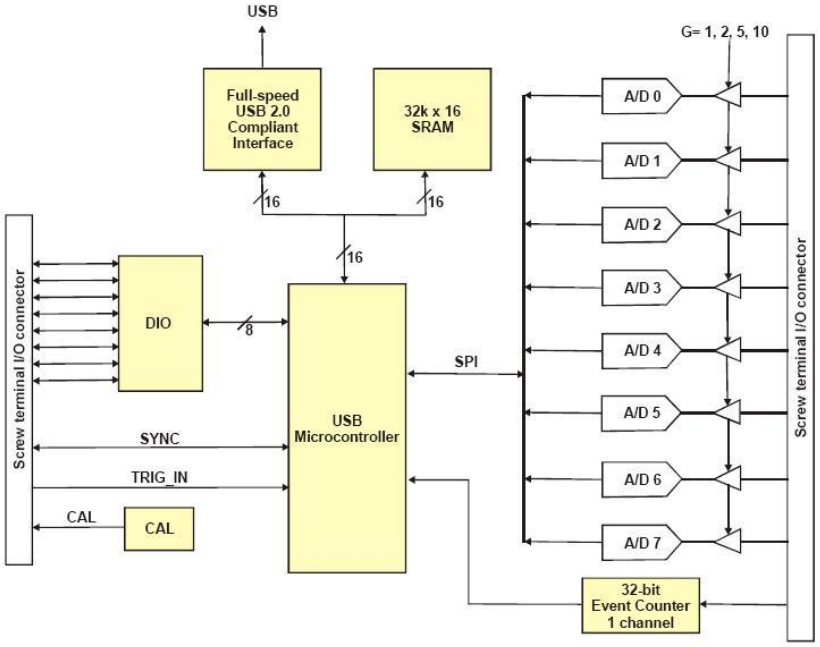

Figure 4.15 USB-based DAQ module with 8 analog channels functional block diagram

4.2.4 The Test Sections

The experimental test sections consisted of three vertical pipes with diameters in the range of ½" to 1". To measure pressure drop in the pipes, pressure taps were built on the pipes (see Fig. 4.16). The hole diameter of the pressure taps and the location of the pressure taps on the pipes are determined as explained in the following sections.

Figure 4.16 View of pressure tap on 1/2" pipe

4.2.4.1 Hole Diameter of Pressure Taps

The hole diameter for pressure taps are determined with the rule of thumb given below:

$$D_h = 0.1 \times D \tag{4.2}$$

where D_H is the hole size (m) and D is the pipe diameter(m).

4.2.4.2 Pressure Tap Locations

The locations of pressure taps in the test section are a very important part of pressure tap design. To have reliable data about pressure drop in pipes, the pressure taps should be located in the fully developed region (Fig. 4.17) and far enough from both ends of the pipe to minimize the entrance effects on the measurements. The entry length can be estimated from:

$$L_e = EL \times D \tag{4.3}$$

For turbulent flow :

$$EL = 0.06 \times (Re) \tag{4.4}$$

For laminar flow:

$$EL = 4.4 \times (Re)^{\frac{1}{6}} \tag{4.5}$$

where L_e is the entry length, Re is the Reynolds number, and D_p is the pipe diameter.

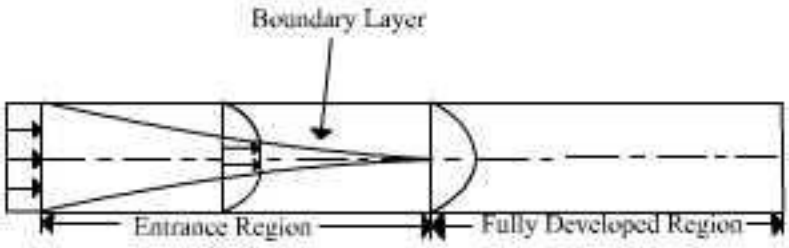

Figure 4.17 Development of flow in a pipe

4.3 Calibration Procedures

Calibration of instruments is a crucial part of the experimental work. In the following sections, calibration procedures for pressure transducers, magnetic flowmeter, and air rotameter are described.

4.3.1 Calibration of Pressure Transducers

The precise measurement of pressure drop in a test section depends on the accuracy of the pressure transducers. Therefore, accurate calibration of pressure transducers is a necessary operation. Calibration of pressure transducers was done by Meriam DP2000I digital Manometer /

pressure calibrator (see Fig. 4.18). The following calibration procedure was followed (see Fig.4.19):

1. The pressure calibrator was connected to its air pump and high pressure side of pressure transducer.
2. The low pressure side of the transducer was open to atmosphere
3. The output from the transducer was connected to a computer interface to display the DC volt signal.
4. The air pressure in the calibration loop was increased by pumping the air to the system
5. The actual value of the pressure was read from the pressure calibrator
6. Several pressures between zero and full scale were applied to the transducer and the corresponding output signals were recorded
7. The values of applied pressures obtained from the calibrator were plotted versus transducer output voltages. The plot showed a linear relationship between applied pressure and output voltage
8. By aid of a linear regression model, a straight line was fitted to the calibration data and regression equations were derived from the applied model. The equations were used to convert the voltage signal from the pressure transducers to the actual pressure drop.

Figure 4.18 Digital manometer/ Pressure calibrator

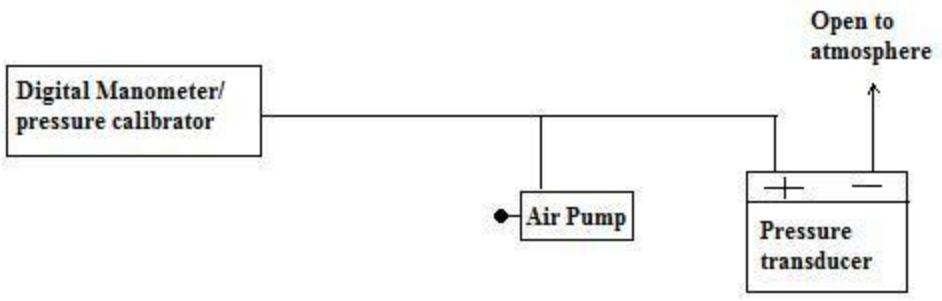

Figure 4.19 Block diagram of pressure transducers' calibration loop

4.3.2 Calibration of the Magnetic Flowmeter

Calibration of the magnetic flowmeter is another important step in the data acquisition procedure. The bucket and stopwatch method was used to calibrate the magnetic flowmeter. The calibration steps are listed below:

1. Water was pumped from storage tank to the flow loop through the magnetic flowmeter
2. The water was passed through the magnetic flowmeter for approximately 10 minutes to reach the steady state condition
3. The water from the flow loop was diverted to the weighting bucket placed on the scale with certain weight. Meanwhile the time that the discharged water took to balance the weight on the scale was recorded
4. The output voltage signal of the magnetic flowmeter was recorded at the same time as weighing was done by the computer program
5. The same procedure was repeated for different flowrates passing through the magnetic flowmeter (within the range of magnetic flowmeter)
6. From mass flowrate and liquid density, the volumetric flowrate was calculated and plotted versus the corresponding magnetic flowmeter voltage signal.
7. A linear relationship was observed between output voltage and volumetric flowrate
8. A straight line was fitted to the calibration data and regression equation was derived from the applied model.

The calibration equation for the magnetic flowmeter was used in the computer program to convert the flowmeter voltage signal to actual volumetric flowrate.

4.3.3 Calibration of the Air Rotameter

To measure the amount of air injected into the test section, an air rotameter was used. The calibration for the rotameter was provided by the manufacturer at the standard condition of 14.7 psia, and 70°F with air as a reference gas. Therefore, no laboratory calibration was needed.

4.3.4 Calibration Results

The data resulting from the calibration of instruments (pressure transducers, magnetic flowmeter, and air rotameter) were plotted as shown in Figures 4.20 to 4.23.

Table 4.3 gives the operational range of the instruments and table 4.4 gives the regression values corresponding to calibrations.

Name of instrument	Unit of measurement	Output	Range
Pressure transducer	Psi	DC voltage	0-5
Pressure transducer	Psi	Dc voltage	0-0.5
Magnetic flowmeter	l/min	Dc voltage	0-180
Rotameter	ml/min	Scale reading	0-17000

Table 4.3 Utilized instruments and their operational range

Name of instrument	Y= AX+B	
	A	B
Magnetic flow meter	112.81	- 45.338
5psi pressure transducer	1.2264	- 1.2648
0.5 psi pressure transducer		
Air rotameter	$y = 0.0002x^3 - 0.0804x^2 + 120.88x - 80.478$	

Table 4.4 Summary of calibration results

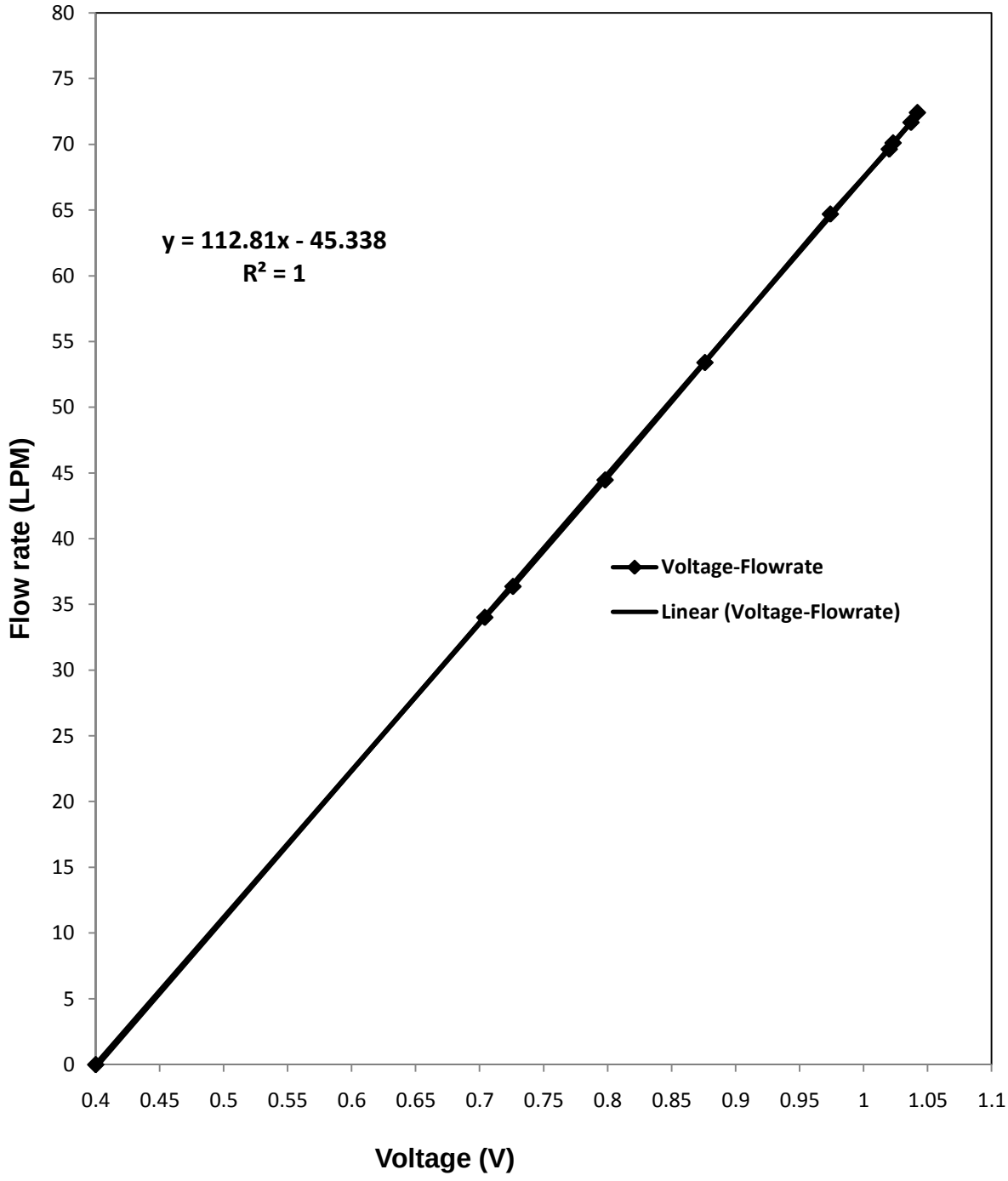

Figure 4.20 Calibration of magnetic flowmeter

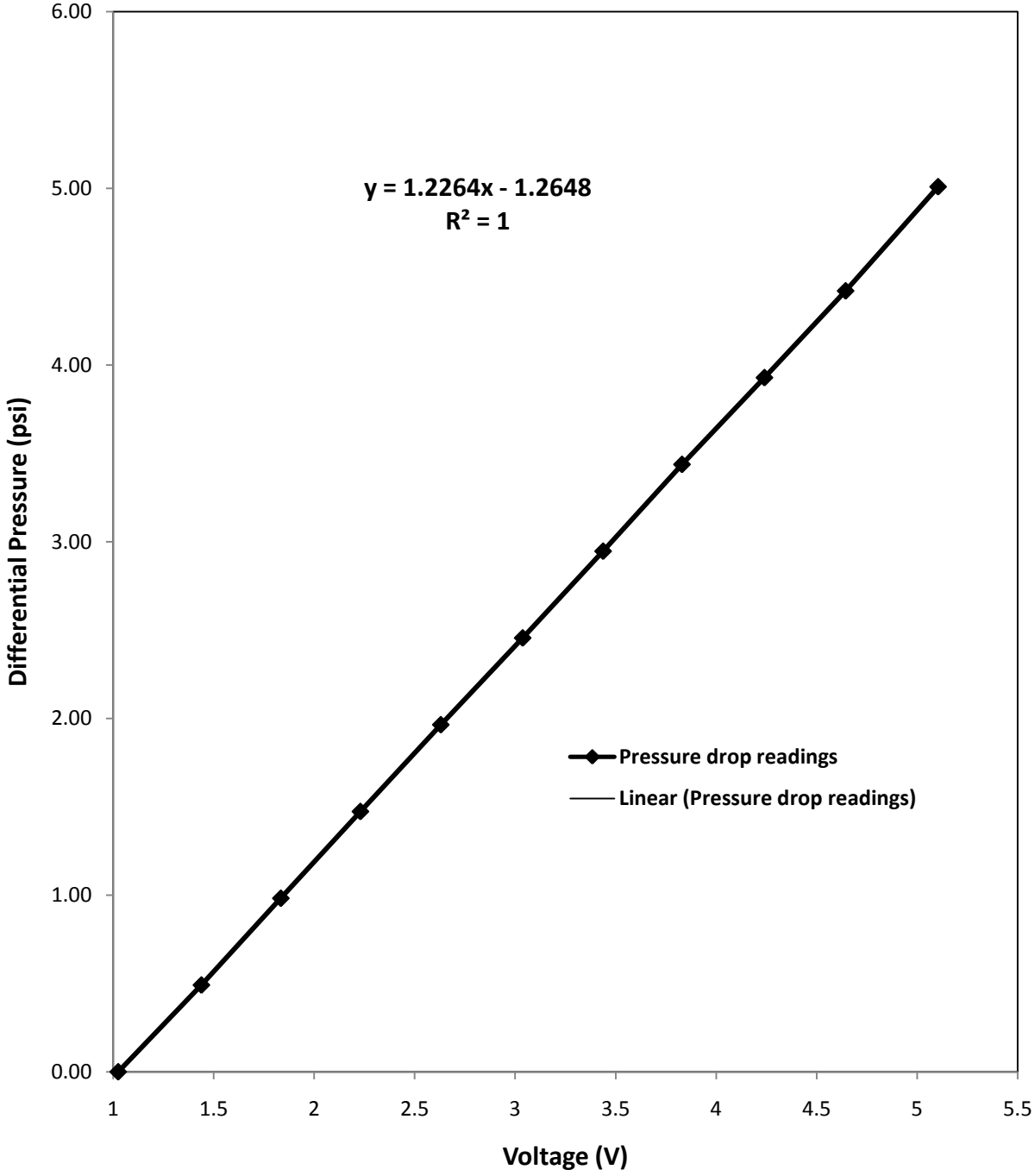

Figure 4.21 Calibration of pressure transducer (5 psi)

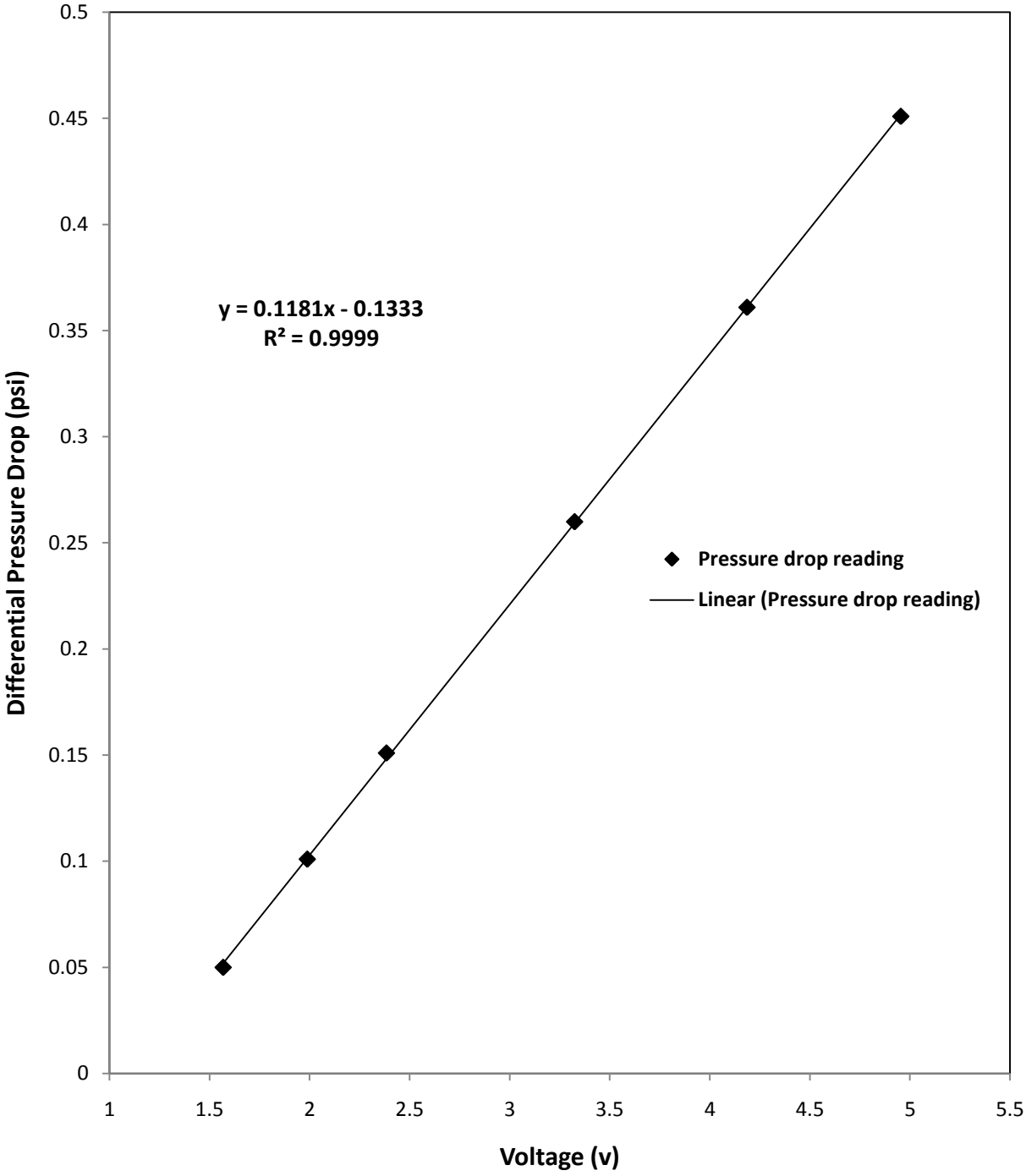

Figure 4.22 Calibration of pressure transducer (0.5psi)

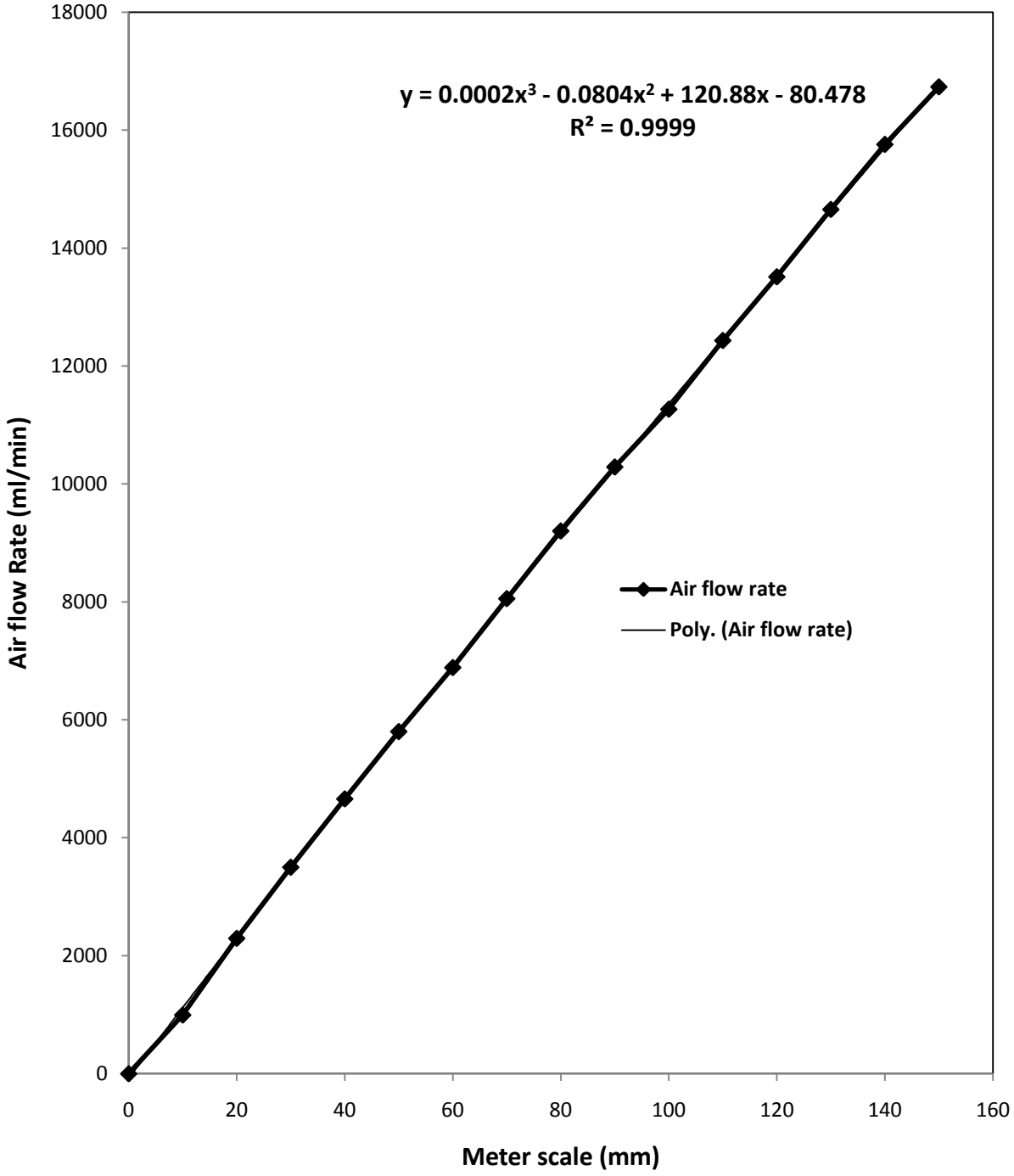

Figure 4.23 Calibration of air rotameter

4.4 Experimental Data Collection Procedures

The data collection procedures are discussed under two separate headings:

1. Single-phase flow and
2. Two-phase flow

4.4.1 Data Collection Procedure for Single-Phase Flow

For single-phase flow, the following procedure was followed to achieve accurate measurement of the experimental data.

1. Prior to start of the experiments, water was purged through the impulse tubing of the pressure transducers. This was essential to remove trapped bubbles from the tubing connected to the pressure transducers.
2. Fluid was pumped from the storage tank to the flow loop while the purging of the impulse tubing was purging still in progress
3. The automatic temperature controller was switched on to control the fluid temperature and keep it constant at 20°C. It took 15 to 20 minutes to reach the steady state temperature.
4. After removing all the trapped air bubbles from the impulse tubing, the purging was stopped to allow the pressure transducers to collect pressure drop data
5. The fluid flow rate was set to some low value by a ball valve located at the outlet of the pump
6. The flow rate was increased gradually in the system. To reach the steady state condition in the test section, flowrate was changed in increments of 10 minutes. The signals from the magnetic flowmeter and the pressure transducers were recorded by the computer at each flowrate
7. Since the pressure drop and fluid flowrate measurements tend to fluctuate, the average values over a period of 30 seconds were recorded by the computer

4.4.2 Data Collection Procedure for Two-Phase Flow

Although the data collection procedure for two-phase flow was essentially the same as that for single-phase system, some additional steps and measurements were necessary as described below:

1. After the system was ready for single-phase flow experiment, the air was introduced into the system through the designated spargers.
2. The air volumetric flowrate was measured at steady state condition with the rotameter. The air pressure and temperature were measured using pressure gauge and temperature gauge installed near the inlet of the rotameter.
3. Different combinations of air and liquid flow rates were tested. The air and liquid flow rates, and the corresponding pressure drops were recorded

The effects of additives such as polymer and frother on single-phase and two-phase flows were determined using these procedures.

4.4.2.1 Correction of Air Flowrate Measurements

Experimental conditions, such as operational temperature and pressure, have significant influence on the operation of rotameter and gas properties. Therefore, the reading from the rotameter needs to be corrected according to the experiment state conditions. Some values have been provided by the rotameter manufacturer for the reading correction that should be applied to the rotameter scale number if the system is not working at the standard conditions for which the rotameter is calibrated.

Specific Gravity Correction Factors																	
	Gas Being Used																
Gas Meter is Calibrated With	Hydrogen	Helium	Methane	Ammonia	Neon	Acetylene	Nitrogen / Carbon Monoxide	Ethylene	Air	Ethane	Oxygen	Hydrogen Sulfide	Argone	Nitrous / Carbon Dioxide	Propane	Butane	Sulfur Dioxide
Hydrogen	1	0.70	0.35	0.34	0.32	0.28	0.27	0.27	0.26	0.26	0.25	0.24	0.22	0.21	0.21	0.18	0.18
Helium	1.41	1	0.50	0.48	0.45	0.38	0.38	0.38	0.37	0.36	0.35	0.34	0.32	0.30	0.30	0.26	0.25
Methane	2.82	2	1	0.97	0.89	0.78	0.76	0.75	0.74	0.73	0.71	0.68	0.63	0.60	0.59	0.52	0.49
Ammonia	2.92	2.06	1.03	1	0.92	0.81	0.78	0.78	0.77	0.75	0.73	0.70	0.66	0.62	0.62	0.54	0.51
Neon	3.17	2.25	1.12	1.08	1	0.88	0.85	0.84	0.83	0.82	0.80	0.76	0.71	0.67	0.67	0.58	0.55
Acetylene	3.62	2.56	1.28	1.24	1.14	1	0.97	0.96	0.95	0.93	0.91	0.87	0.81	0.77	0.76	0.66	0.63
Nitrogen / Carbon Monoxide	3.74	2.64	1.32	1.28	1.18	1.03	1	1	0.98	0.96	0.94	0.90	0.84	0.80	0.79	0.68	0.65
Ethylene	3.74	2.66	1.33	1.26	1.18	1.03	1	1	1.01	0.96	0.94	0.90	0.84	0.80	0.79	0.69	0.66
Air	3.61	2.69	1.35	1.30	1.20	1.04	1.02	1.01	1	0.98	0.95	0.92	0.85	0.81	0.80	0.70	0.66
Ethane	3.90	2.76	1.38	1.33	1.23	1.08	1.04	1.04	1.02	1	0.98	0.94	0.88	0.83	0.82	0.71	0.68
Oxygen	4	2.82	1.41	1.36	1.26	1.10	1.06	1.06	1.05	1.02	1	0.95	0.90	0.85	0.84	0.73	0.70
Hydrogen Sulfide	4.15	2.94	1.47	1.42	1.31	1.15	1.11	1.11	1.09	1.06	1.04	1	0.93	0.88	0.88	0.76	0.72
Argon	4.45	3.15	1.58	1.52	1.40	1.23	1.19	1.18	1.17	1.14	1.12	1.07	1	0.94	0.94	0.82	0.78
Nitrous Oxide / Carbon Dioxide	4.70	3.33	1.67	1.61	1.48	1.30	1.26	1.25	1.24	1.21	1.18	1.13	1.06	1	0.99	0.88	0.82
Propane	4.76	3.36	1.68	1.63	1.50	1.31	1.27	1.26	1.25	1.22	1.19	1.15	1.07	1.01	1	0.87	0.83
Butane	5.46	3.66	1.93	1.67	1.72	1.51	1.46	1.45	1.43	1.40	1.37	1.32	1.22	1.16	1.15	1	0.95
Sulfur Dioxide	5.72	4.05	2.03	1.96	1.81	1.58	1.53	1.52	1.50	1.47	1.43	1.38	1.28	1.22	1.20	1.05	1

Table 4.5 Rotameter correction constants for the change in the specific gravity of gas (Cole-Parmer rotameter manual)

Multiply Reading By	Flowmeter Pressure Correction																				
	Working Pressure of Flowmeter – PSIG																				
Pressure at Which Meter Was Calibrated – PSIG	0	5	10	15	20	25	30	35	40	45	50	60	70	75	80	90	100	110	120	130
0	1	1.15	1.29	1.41	1.53	1.64	1.74	1.84	1.93	2.02	2.1	2.26	2.4	2.47	2.54	2.67	2.8	2.92	3.03	3.14
5	.86	1	1.12	1.23	1.33	1.42	1.51	1.59	1.67	1.74	1.81	1.94	2.07	2.13	2.19	2.31	2.42	2.52	2.62	2.71
10	.77	.89	1	1.1	1.19	1.27	1.35	1.42	1.49	1.56	1.62	1.74	1.85	1.91	1.96	2.06	2.16	2.25	2.33	2.41
15	.7	.81	.91	1	1.08	1.16	1.23	1.3	1.36	1.42	1.48	1.59	1.69	1.74	1.79	1.88	1.97	2.05	2.13	2.21
20	.65	.75	.84	.92	1	1.07	1.14	1.2	1.26	1.31	1.36	1.46	1.56	1.61	1.65	1.74	1.82	1.9	1.97	2.04
25	.61	.7	.78	.86	.93	1	1.06	1.12	1.18	1.23	1.28	1.37	1.46	1.5	1.54	1.62	1.7	1.77	1.84	1.91
30	.57	.66	.74	.81	.88	.94	1	1.05	1.1	1.15	1.2	1.29	1.38	1.42	1.46	1.53	1.6	1.67	1.74	1.8
35	.54	.63	.71	.78	.84	.90	.95	1	1.05	1.1	1.14	1.22	1.3	1.34	1.38	1.46	1.53	1.59	1.65	1.71
40	.52	.6	.67	.74	.8	.85	.9	.95	1	1.04	1.09	1.17	1.25	1.28	1.32	1.39	1.45	1.51	1.57	1.63
45	.5	.57	.64	.71	.76	.81	.86	.91	.96	1	1.04	1.12	1.19	1.23	1.26	1.33	1.39	1.45	1.5	1.56
50	.48	.55	.62	.68	.73	.78	.83	.88	.92	.96	1	1.07	1.15	1.18	1.21	1.28	1.33	1.39	1.44	1.5
60	.44	.51	.57	.63	.68	.73	.77	.82	.86	.89	.93	1	1.06	1.10	1.13	1.19	1.24	1.3	1.35	1.4
75	.4	.47	.52	.58	.62	.67	.71	.75	.78	.82	.85	.91	.97	1	1.03	1.08	1.13	1.18	1.23	1.27
100	.36	.41	.46	.51	.55	.59	.63	.66	.69	.72	.75	.81	.86	.89	.91	.95	1	1.04	1.08	1.12

Table 4.6 Rotameter correction constants for the change in the working pressure of rotameter (Cole-Parmer rotameter manual)

4.5 Procedures for Data Analysis

To draw any useful conclusions from the experimental data, the raw information needs to be analyzed. Data analyses in this work can be divided into two sections:

1. Single-phase flow analysis
2. Two-phase flow analysis

4.5.1 Single-Phase Flow Analysis

To analyze the single-phase flow data, the following parameters need to be calculated:

1. Frictional pressure drop
2. Friction factor

4.5.1.1 Frictional Pressure Drop in Single-Phase Flow

In single phase flow, the density of liquid in the test section is the same as the density of liquid in the impulse tubing of pressure transducers. Therefore, the pressure drop measured through the pressure transducer is equal to the frictional pressure drop.

$$\Delta P_{meas} = \Delta P_{Friction} \tag{4.6}$$

where ΔP_{meas} is the pressure drop measured by the transducers, and $\Delta P_{Friction}$ is the frictional pressure drop.

4.5.1.2 Friction Factor in Single-Phase Flow

Friction factor for single-phase flow in a pipeline can be calculated as:

$$f = \frac{\tau_w}{1/2\,\rho \bar{V}^2} \tag{4.7}$$

where

$$\tau_w = \frac{\Delta P_f\ D}{4L} \tag{4.8}$$

From equations (4.7) and (4.8):

$$f = \frac{\Delta P_f\ D}{2L\ \rho\ \bar{V}^2} \tag{4.9}$$

where τ_w is the wall shear stress, ΔP_f is the frictional pressure drop, $\bar{V}$ is the average velocity, ρ is the fluid density, L is the length of the pipe, D is the pipe diameter, and f is the friction factor.

4.5.2 Two-Phase Flow Analysis

4.5.2.1 Frictional Pressure Drop in Two-Phase Flow

Measurement of frictional pressure drop in vertical two-phase flow system requires some additional consideration. Contrary to single-phase flow, the frictional pressure drop in two-phase flow is not equal to the pressure drop measured by the pressure transducers.

The total pressure drop between two pressure taps in Figure 4.24 is:

$$P_h - P_l = P_h^{'} - P_l^{'} + \rho_{im}\, g l \tag{4.10}$$

Or

$$\Delta P_{total} = \Delta P_{meas} + \rho_{im}\, g l \tag{4.11}$$

The application of Bernoulli equation between two pressure taps gives:

$$\frac{P_h}{\rho_{pipe}} + g z_h = \frac{P_l}{\rho_{pipe}} + g z_l + h_f \tag{4.12}$$

where h_f is given by:

$$h_f = \frac{\Delta P_f}{\rho_{pipe}} \tag{4.13}$$

and $z_l - z_h$ is the distance l between the pressure taps (see Fig. 4.24).

Combination of equations (4.12) and (4.13) gives:

$$\Delta P_f = \Delta P_{meas} + g l(\rho_{im} - \rho_{mixture}) \tag{4.14}$$

The hydrostatic pressure drop between two points is given by:

$$\Delta P_h = \rho_{mixture}\ g l \tag{4.15}$$

where ΔP_{meas} is the pressure drop measured by the pressure transducer, ΔP_f is the frictional pressure drop between two pressure taps, ΔP_{total} is the total pressure drop between two pressure taps, ρ_{im} is the density of liquid inside the impulse tubing, $\rho_{mixture}$ is the density of mixture inside the test section, l is the distance between two pressure taps, and g is the gravity.

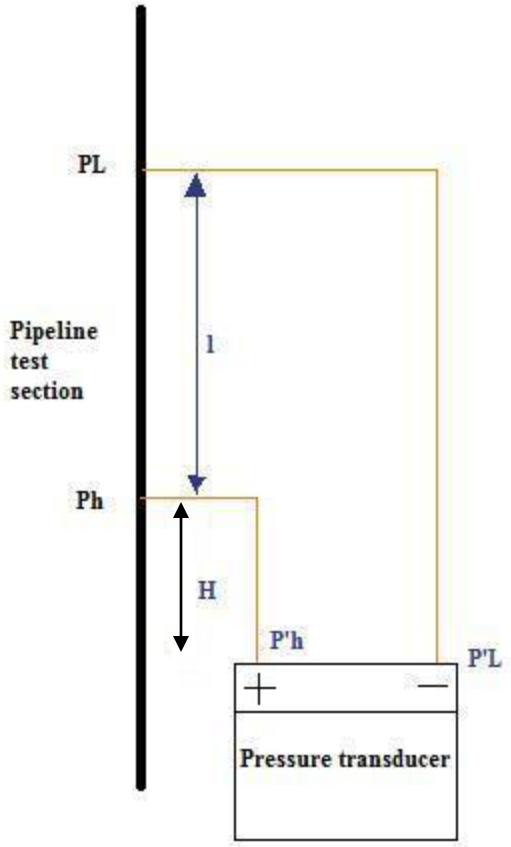

Figure 4.24 Pressure transducer's impulse tubing system

Chapter 5

Results and Discussion

5.1 Overview

The experimental work was conducted in two steps: single-phase experiments and two-phase flow experiments. The effects of additives, namely polyacrylamide polymer, and aerofroth, on drag force in vertical flows were investigated. The results of these investigations are presented and discussed in this chapter.

In section 5.2, the experimental results dealing with single-phase flow of water and polyacrylamide solution are presented. The results for two-phase flow experiments are presented in section 5.3. This section includes prediction of bubble sizes and the effect of frother on two-phase air/water flow.

5.2 Single-Phase Flow Results

The first phase of the experimental work dealt with single-phase flow. Pure water and water-polyacrylamide solution were tested separately and the friction factors in each case were calculated from the corresponding pressure drop measurements. The pressure drops at different liquid flow rates were measured with pressure transducers following the procedures explained in section 4.4.1.

5.2.1 Calibration of the System with Pure Water

The friction factors obtained for pure water flow in ½" and ¾" diameter pipes are plotted in Figure 5.1 and Figure 5.2. The results follow the Blasius equation (Eq(2.3)) reasonably well. A good agreement with the Blasius equation shows that the pipes are smooth and the experimental procedures are adequate.

5.2.2 Effect of Polymer Addition

After calibration of the system with pure water, the effect of polyacrylamide addition on friction factor was studied. The experimental friction factors for 500 ppm water-Polyacrylamide solution are plotted as a function of generalized Reynolds number in Figures 5.3 and 5.4. Note that the generalized Reynolds number is defined as:

$$Re_G = \frac{\rho D^n \bar{V}^{2-n}}{K 8^{n-1} \left[\frac{3n+1}{4n}\right]^n} \tag{5.1}$$

where K and n are power law constants of the polymer solution. For 500 ppm polyacrylamide solution, K=7.14E-3 and n=0.827. The friction factors for the polymeric solution fall well below those predicted by empirical Blasius equation. Although the polymer solution does not give any drag reduction effect in the laminar regime, it shows up to 70% drag reduction in turbulent flow regime.

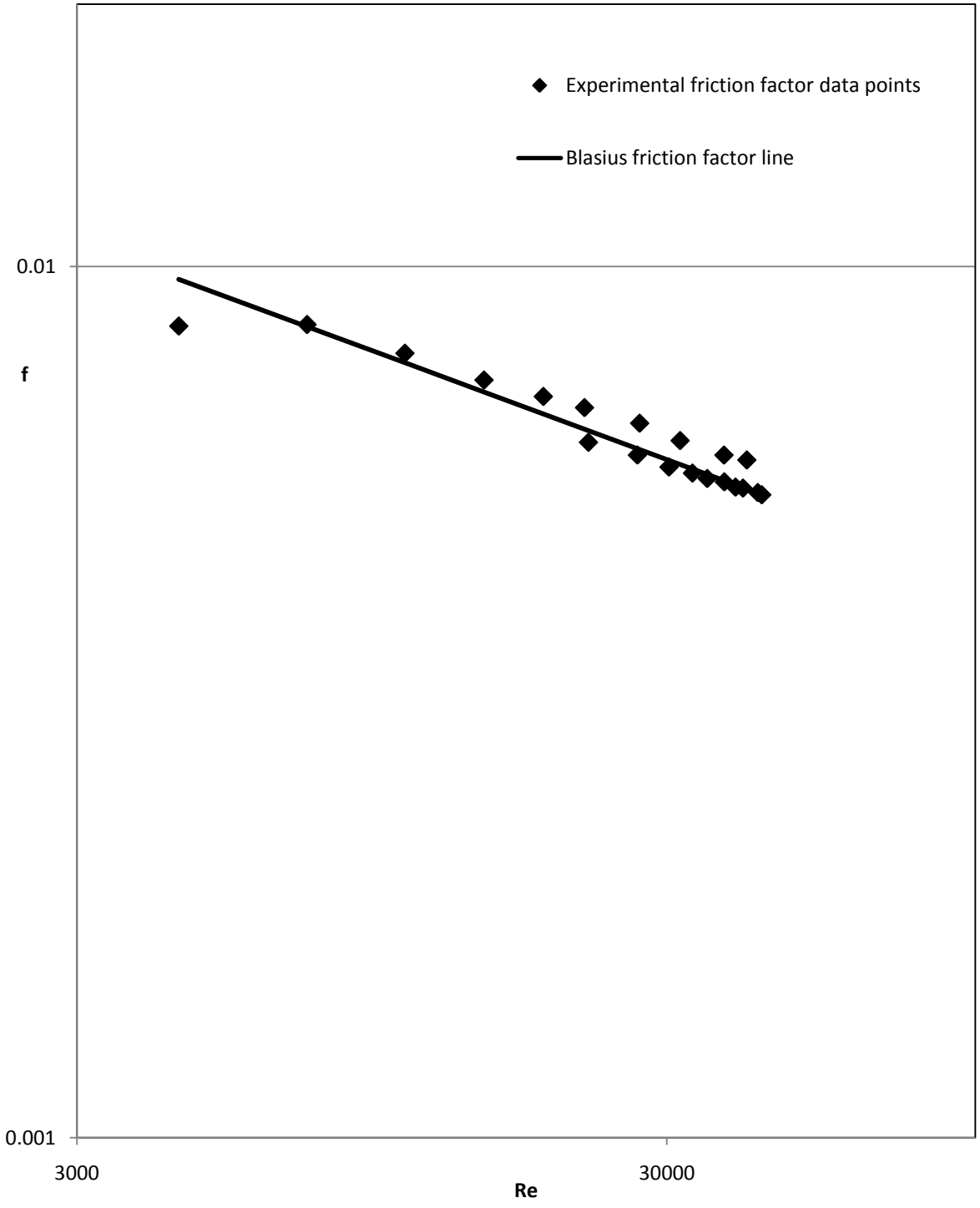

Figure 5.1 Friction factor versus Reynolds number for pure water in ½" pipe

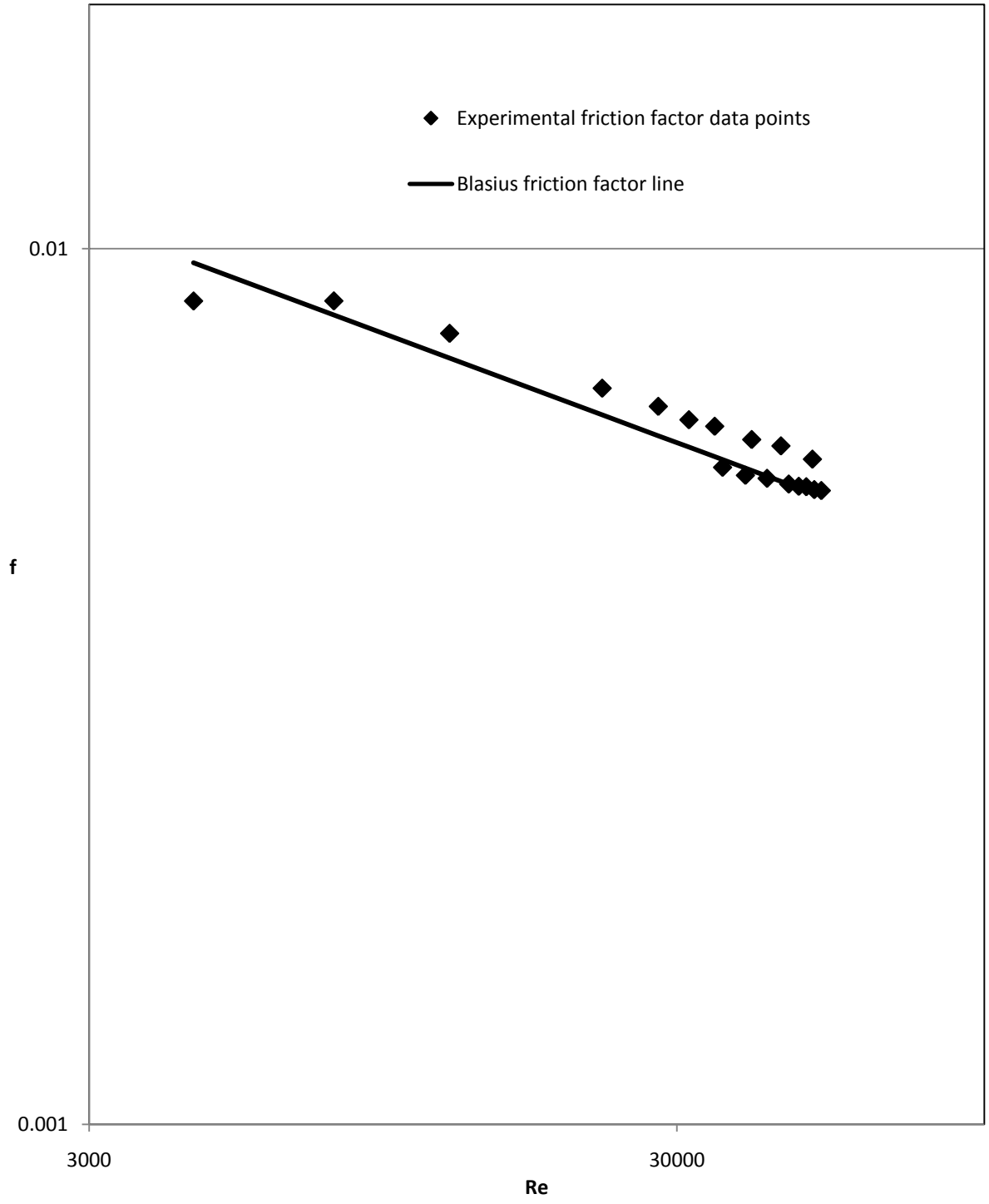

Figure 5.2 Friction factor versus Reynolds number for pure water in ¾" pipe

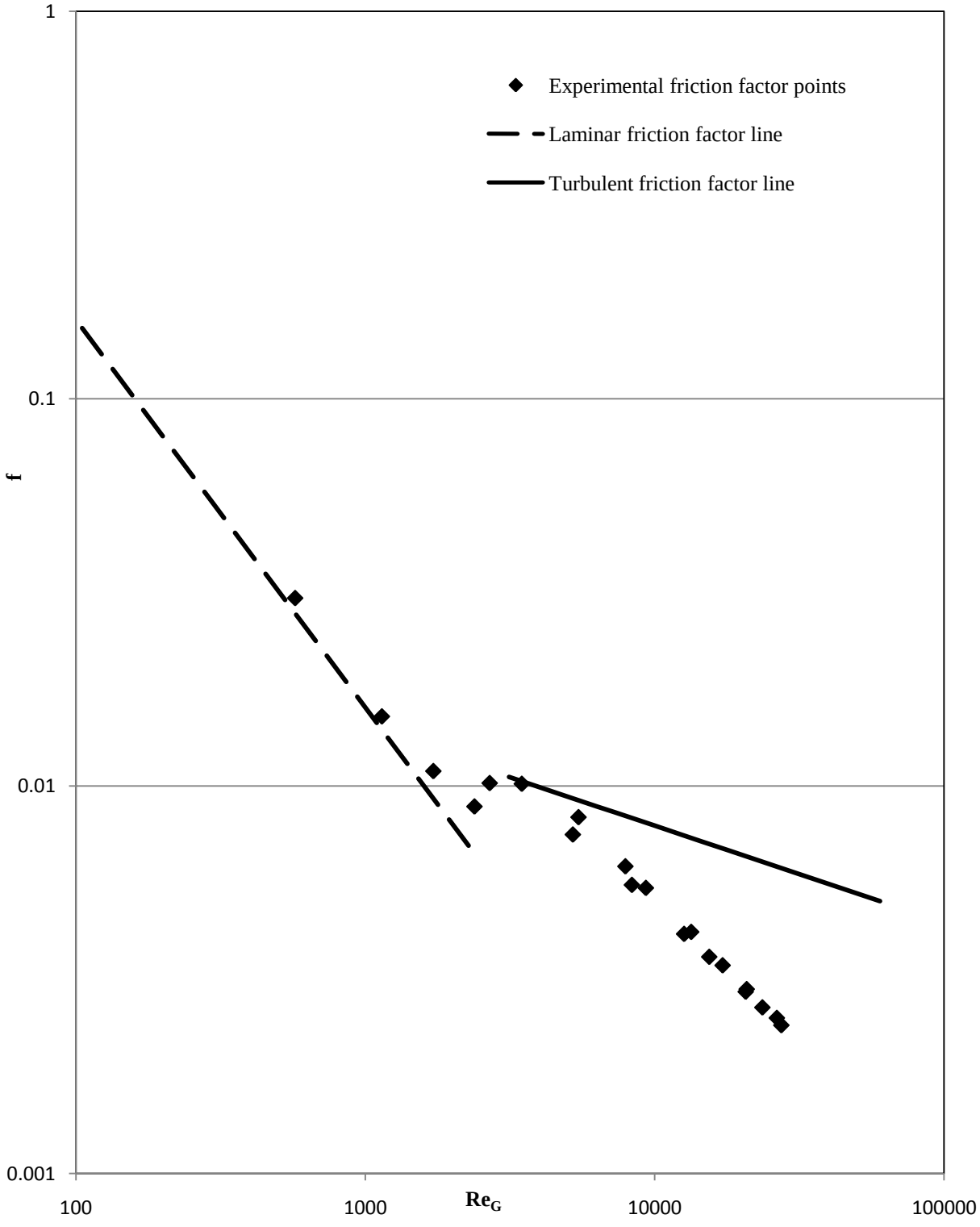

Figure 5.3 Friction factor versus generalized Reynolds number for polymeric solution in ½" pipe

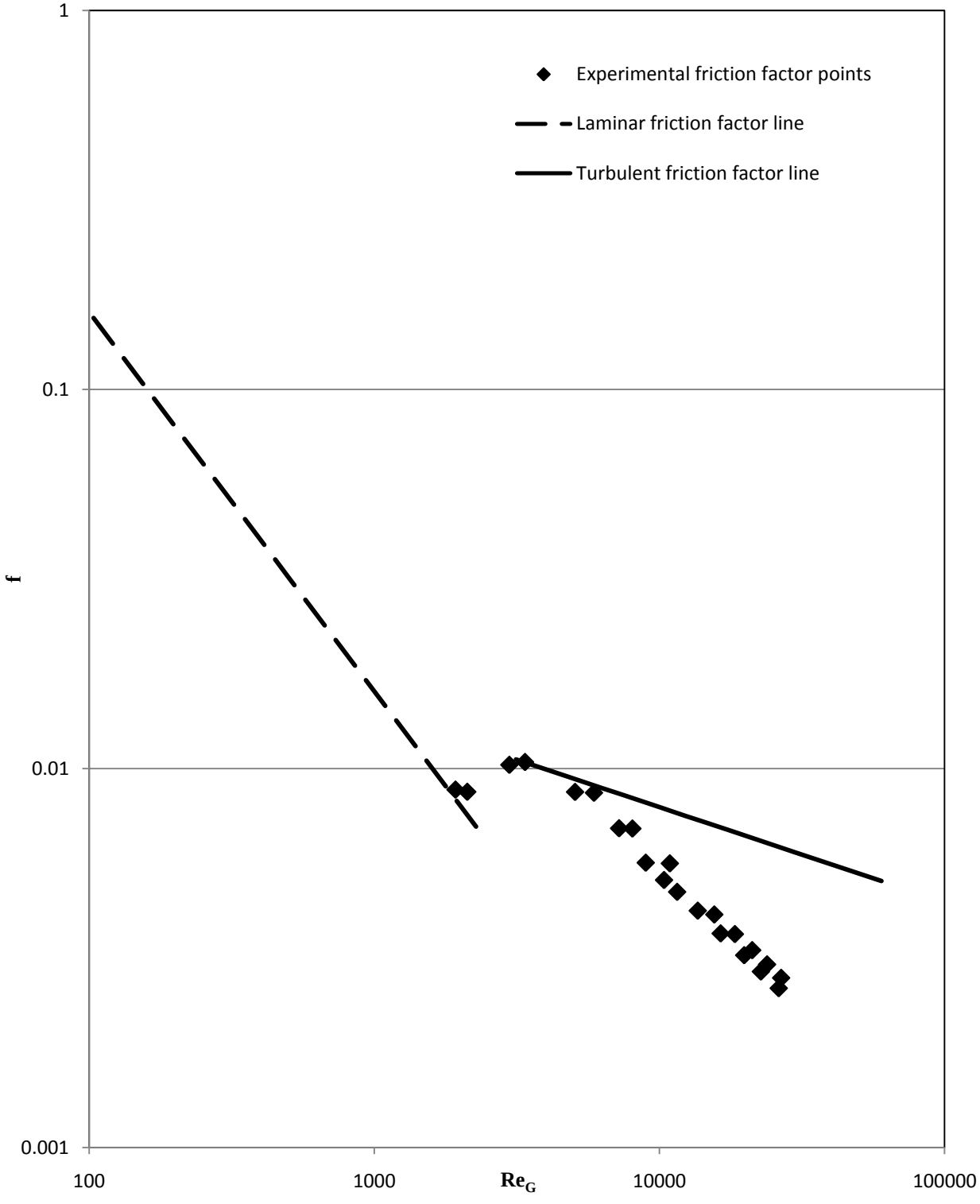

Figure 5.4 Friction factor versus generalized Reynolds number for polymeric solution in ¾" pipe

5.3 Two-Phase Flow Results

The second phase of the experimental program dealt with two-phase flow. Combinations of different materials were tested and their effect on friction was investigated. The experimental work consisted of two parts: effect of air bubbles with and without the presence of frother, and effect of air bubbles with the presence of polymer and frother on friction in vertical pipelines.

5.3.1 Effects of Air Bubbles on Friction

The effect of air bubbles on friction in the pipeline test section was investigated by studying wall shear stress and friction factor. The bubble sizes in the absence of frother were predicted from Habiki et al. (2002) model. The effect of frother on bubble sizes and friction factor were determined.

5.3.1.1 Wall Shear Stress

One of the parameters that has been studied in the experimental work is the wall shear stress. In Figures 5.5 and 5.6, wall shear stress is plotted as a function of gas superficial velocity at constant liquid superficial velocities. The plots demonstrate:

- The wall shear stress increases with the increase in superficial velocity of liquid at constant air superficial velocity
- The wall shear stress increases with the increase in superficial velocity of air at constant liquid superficial velocity

The increase in wall shear stress shows that the drag force increases with the addition of air bubbles to the system. The results of our experiments are in good agreement with some of earlier studies (Descamps et al. (2008), Lu et al. (2005), Magaud et al. (2001), etc).

5.3.1.2 Friction Factor

To have a better understanding of the effect of bubbles, graphs of friction factor versus mixture Reynolds number for different pipe sizes have been plotted in Figures 5.7 and 5.8. The plots show that experimental friction factors are close to the empirical Blasius equation at high mixture Reynolds numbers. The values of the experimental friction factor deviate from the Blasius equation at low mixture Reynolds number.

The observed trends of experimental friction factor and wall shear stress can be explained in terms of bubble sizes and flow properties.

5.3.1.3 Prediction of Bubble Size

The prediction of bubble sizes was done by Hibiki and Ishii (2002) model. The implementation of their model shows that bubble sizes are in the range of 1mm-3mm. Figures 5.9 and 5.10 illustrate that at high Reynolds numbers bubble sizes are smaller than those at low Reynolds numbers. The changes in experimental friction factors from high to low Reynolds numbers can be explained in terms of the changes in the bubble sizes. The high intensity of turbulence and small bubbles allow the two-phase mixture to behave as a pseudo-homogenous fluid that obeys the single-phase flow equations. The deviation of air-water mixture from pseudo-homogenous fluid and Blasius friction factor equation at low Reynolds numbers is due to a decrease in the intensity of turbulence and increase in bubble sizes.

5.3.1.4 Effect of Frother

Frothers are widely used as flotation chemicals. They have a significant effect on the bubble properties. Aerofroth 60 at different concentration was used and tested. Figures 5.11 and 5.12 show the effect of different frother concentrations on the friction factor in pipes. The results indicate that 20 ppm is the critical coalescence concentration of frother where the bubbles reach their minimum size. Addition of more frother to the flow system has little effect on the bubble

diameter. However, the addition of more frother increases the density of the bubbles and the friction factor compared to the frother concentration of 20ppm.

In Figures 5.13 and 5.14, friction factor versus mixture Reynolds number data for air-water flow with and without the presence of 20 ppm frother are plotted. The result shows that the system becomes more homogenous upon the addition of frother. The friction factor data for two-phase flow fall closer to the single-phase line.

5.3.2 Effect of Polymer

The combination of 500 ppm aqueous polymer solution and air bubbles was studied. The experimental results are shown in Figure 5.15. From the plot, it is evident that the polymer solution retains its drag reduction effect even in the presence of bubbles; drag reduction of up to 70 percent is observed at high Reynolds numbers. The interesting part about the combination of polymer solution and air bubbles is that the two-phase mixture behaves more like a homogeneous fluid. The friction factor data for polymer solution-air bubble mixture are close to the friction factor data for polymer solution alone even at low Reynolds numbers.

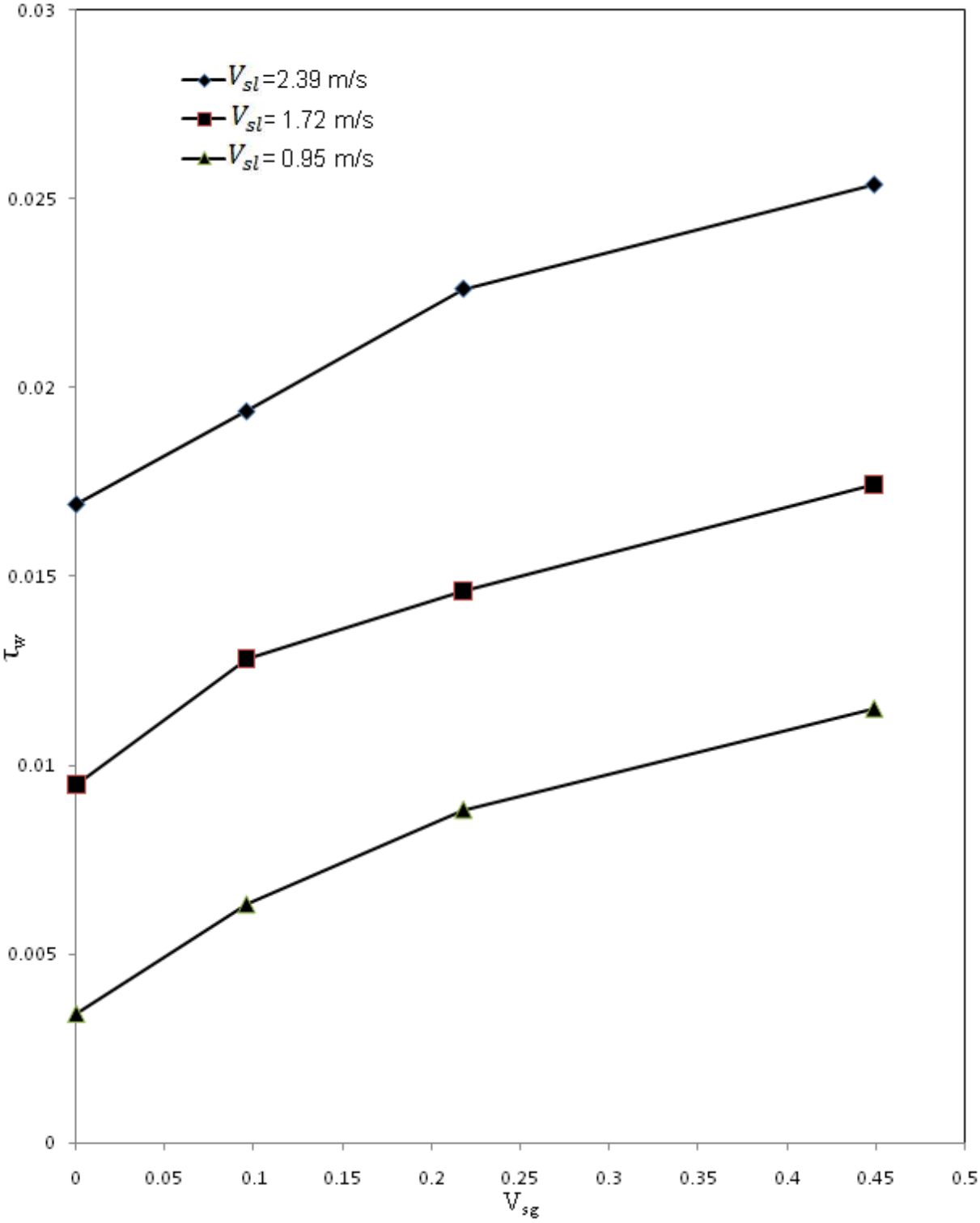

Figure 5.5 Wall shear stress versus air superficial velocity for ½" pipe

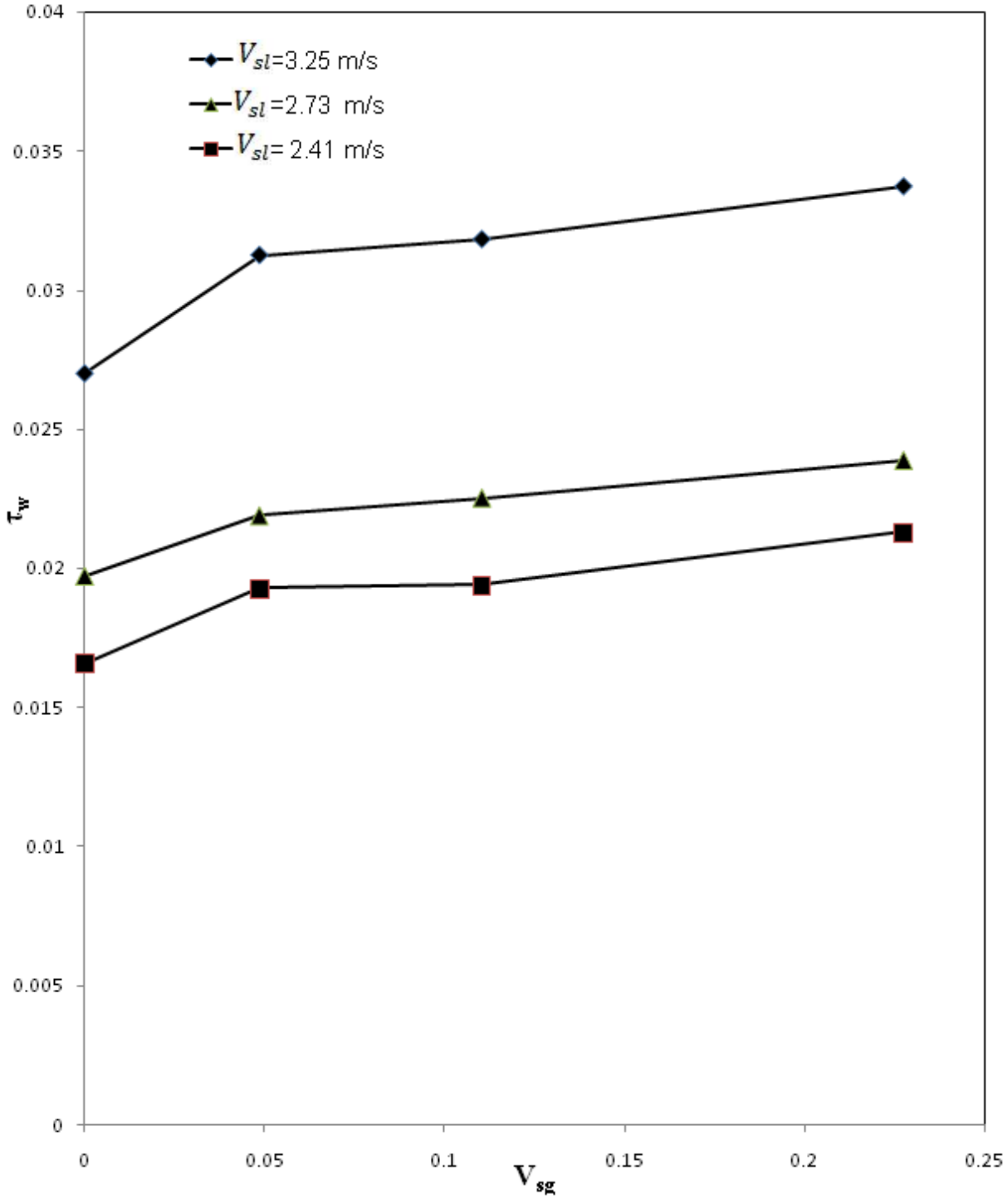

Figure 5.6 Wall shear stress versus air superficial velocity for ¾" pipe

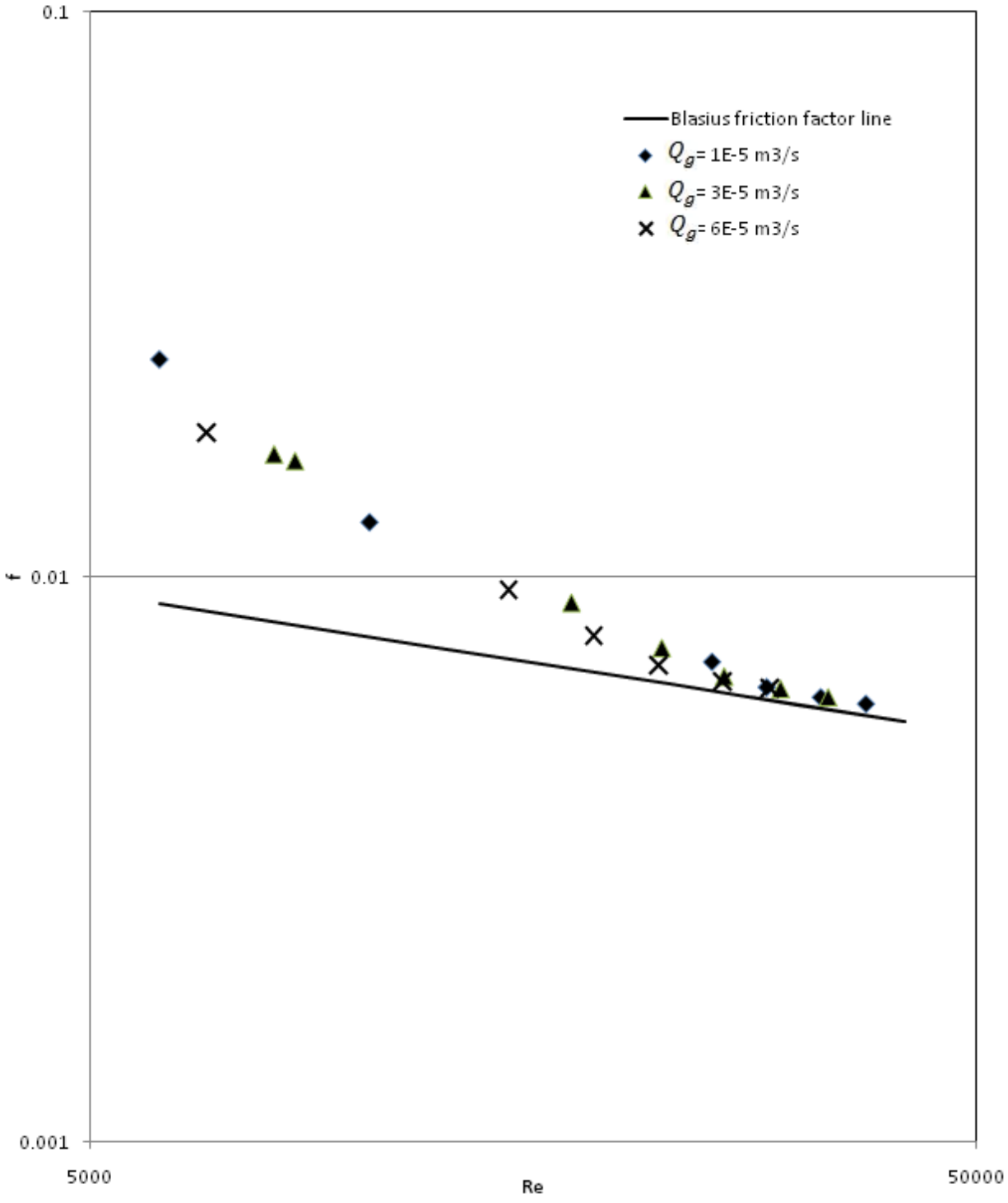

Figure 5.7 Friction factor versus mixture Reynolds number for ½" pipe

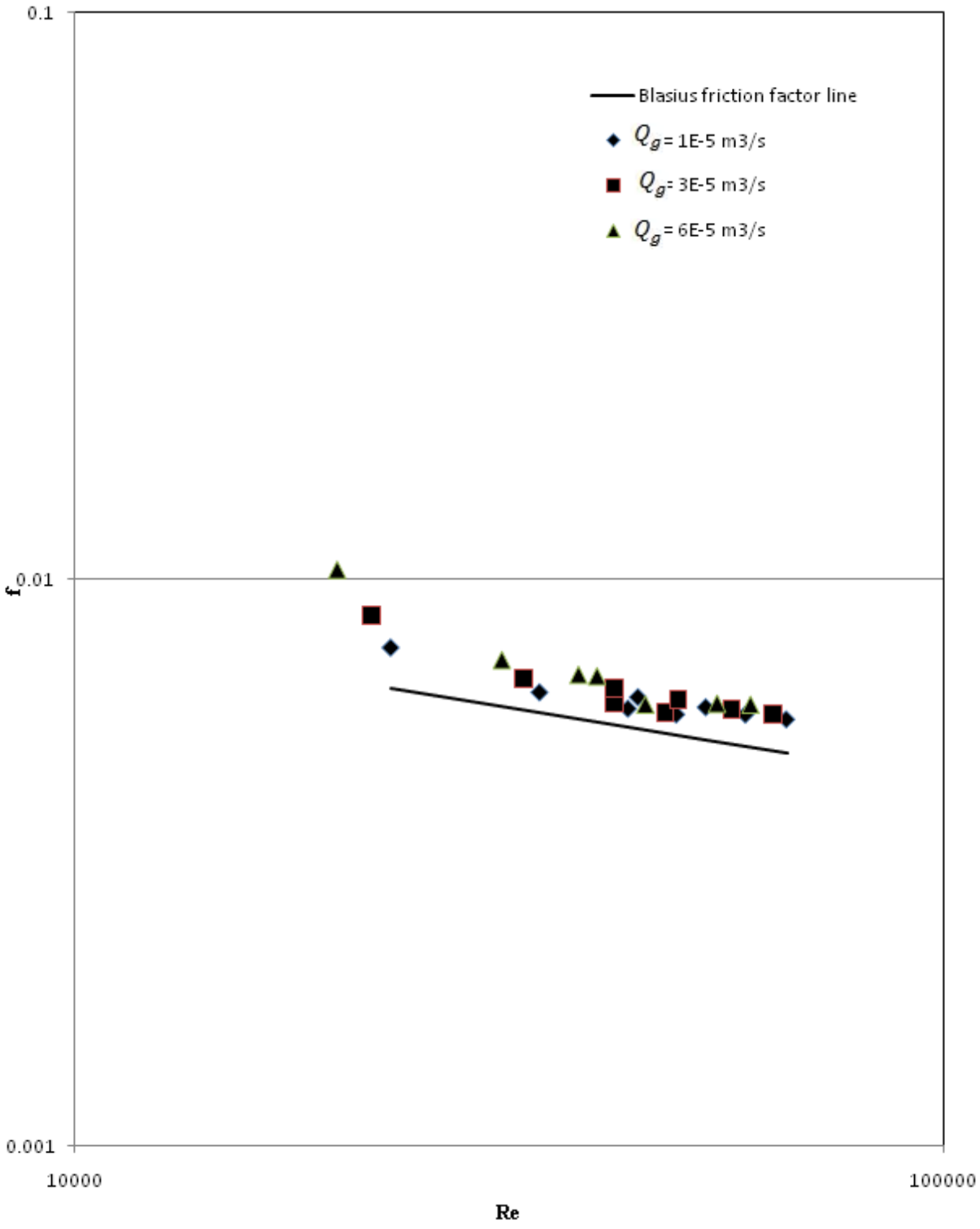

Figure 5.8 Friction factor versus mixture Reynolds number for ¾" pipe

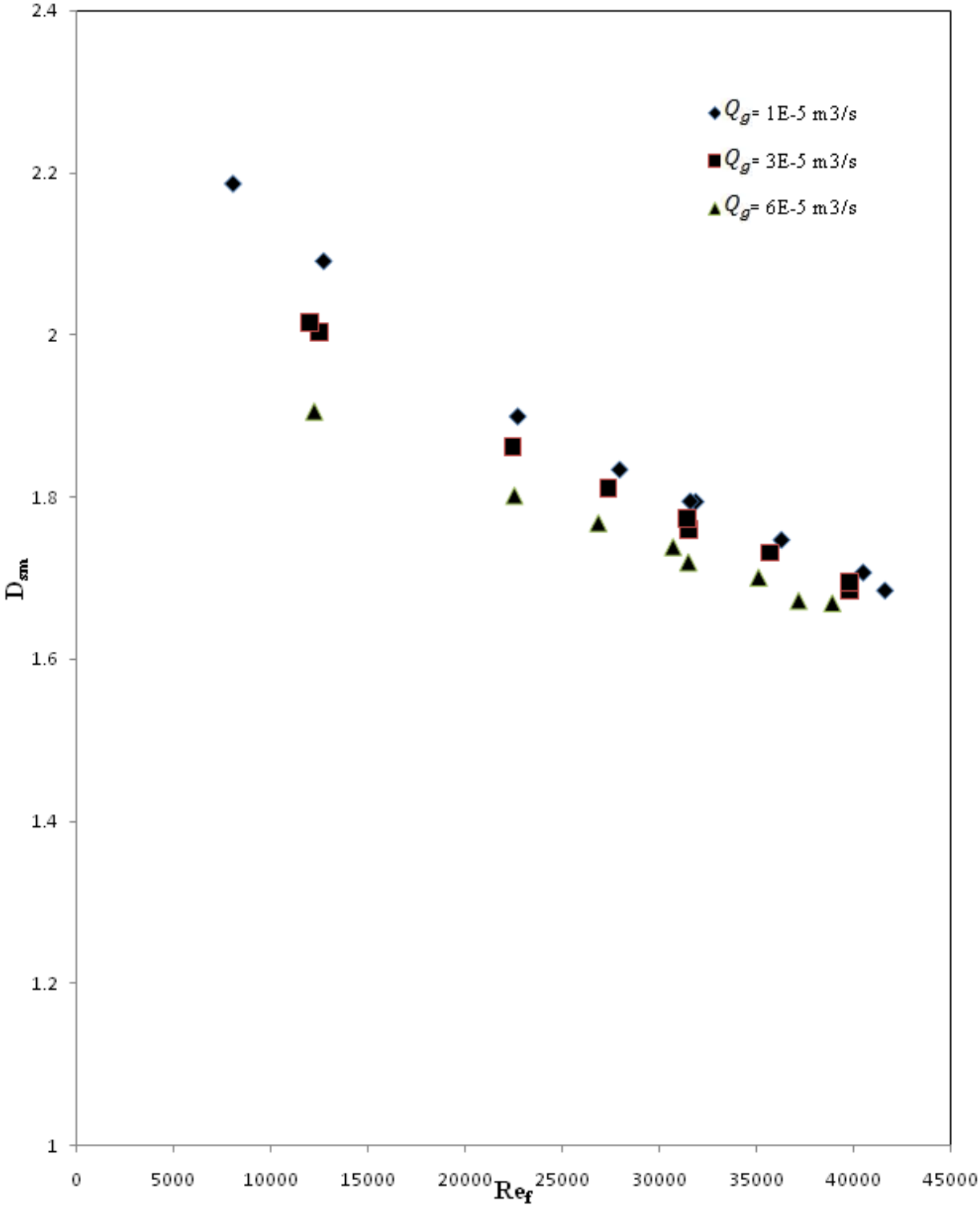

Figure 5.9 Predicted Sauter mean bubble diameters versus liquid Reynolds number for ½" pipe

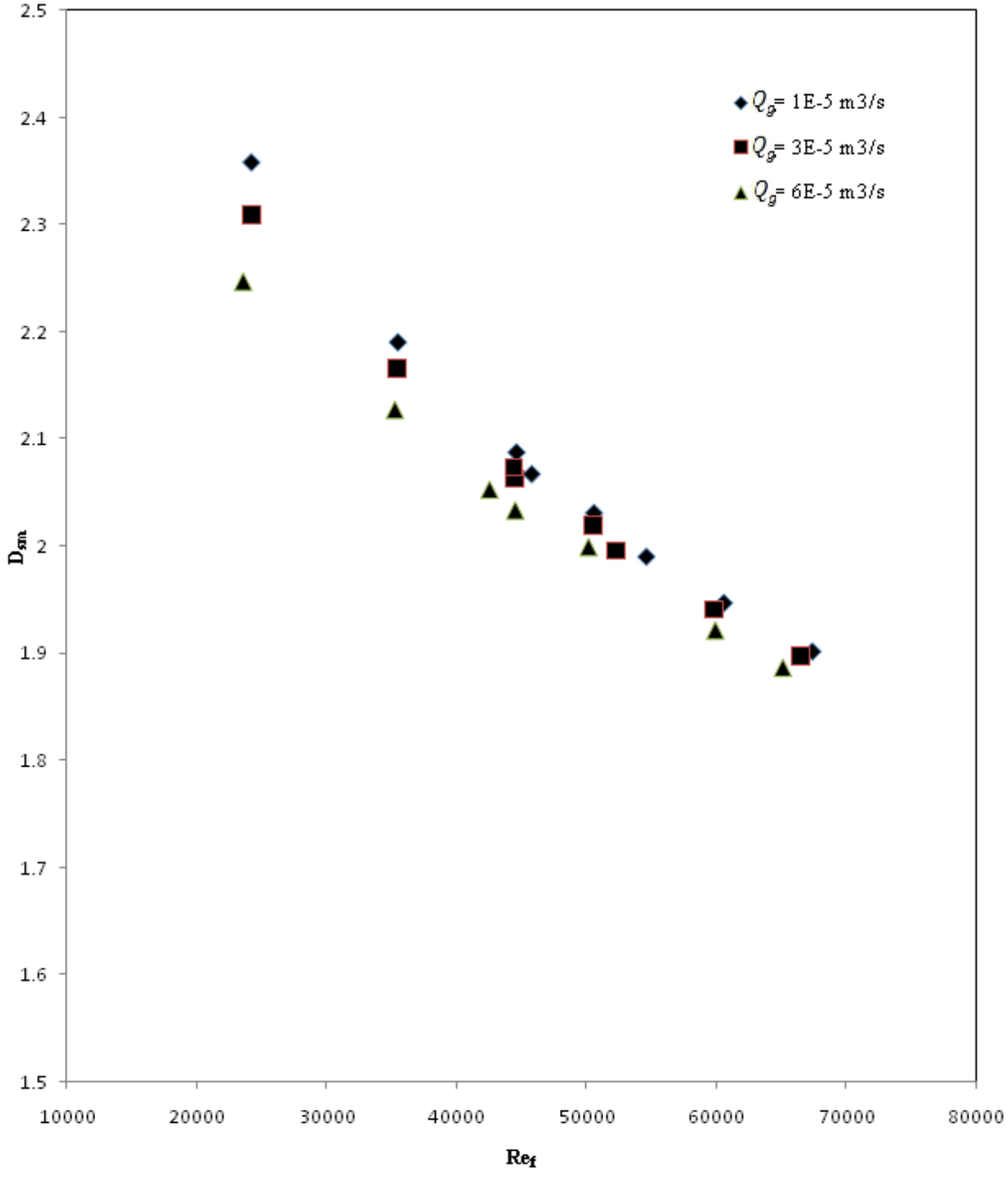

Figure 5.10 Predicted Sauter mean bubbles diameter versus liquid Reynolds number for 3/4 " pipe

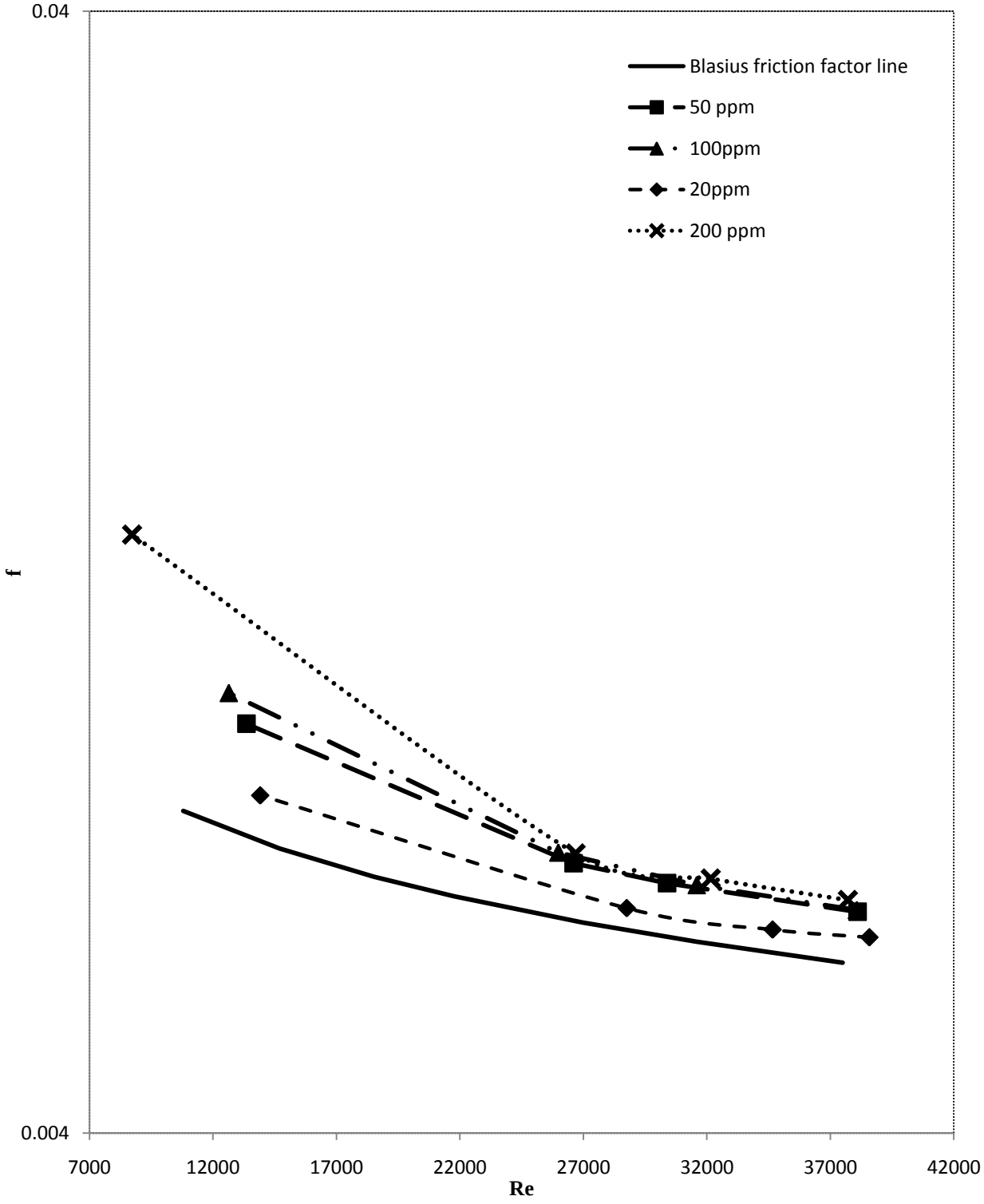

Figure 5.11 Effect of different concentration of frother on friction factor in ½" pipe (air flowrate = 1E-5 m^3/s)

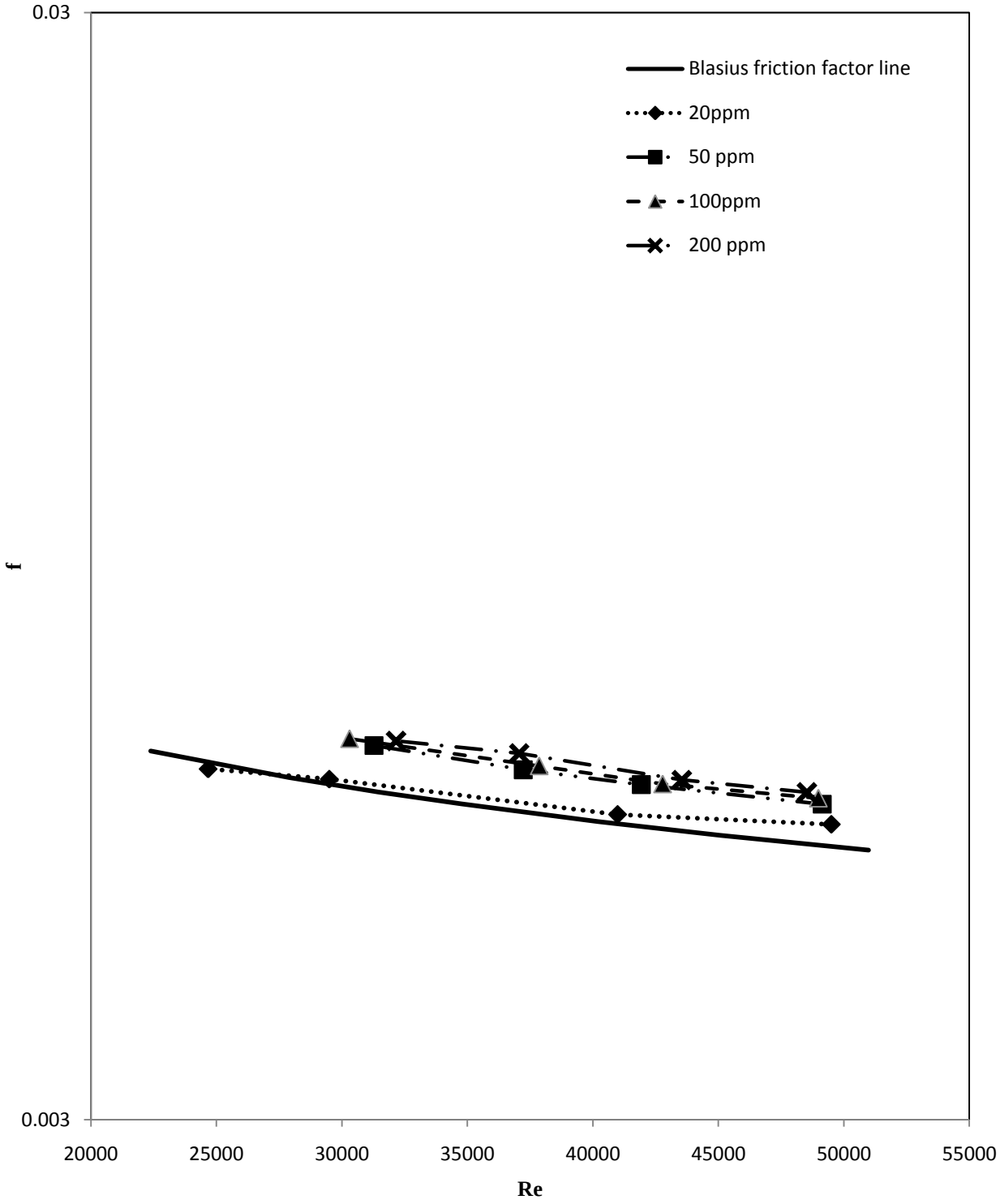

Figure 5.12 Effects of different concentration of frother on friction factor in ¾" pipe (air flow rate=1E-5 m^3/s)

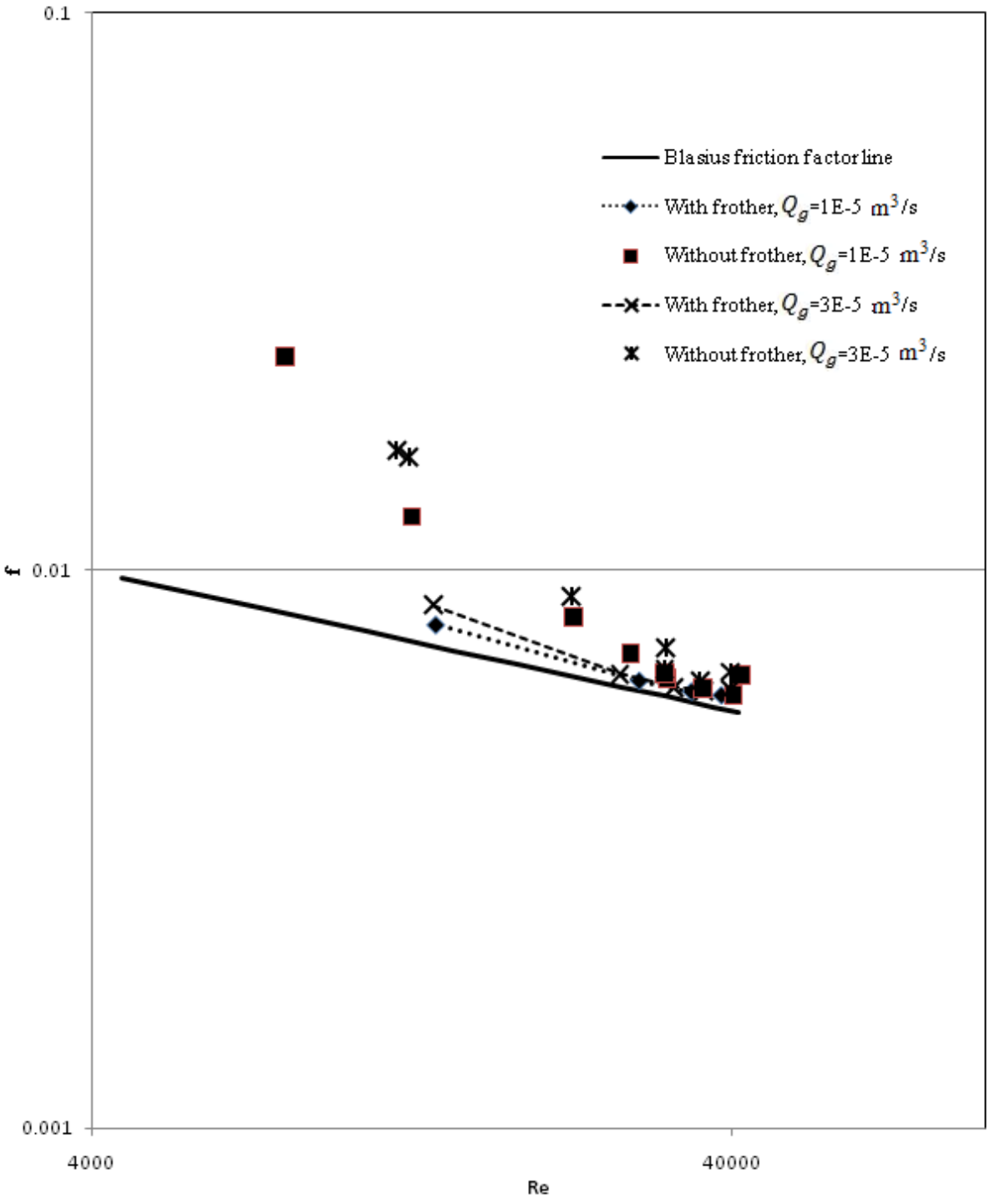

Figure 5.13 Effects of 20ppm frother on friction factor in ½" pipe

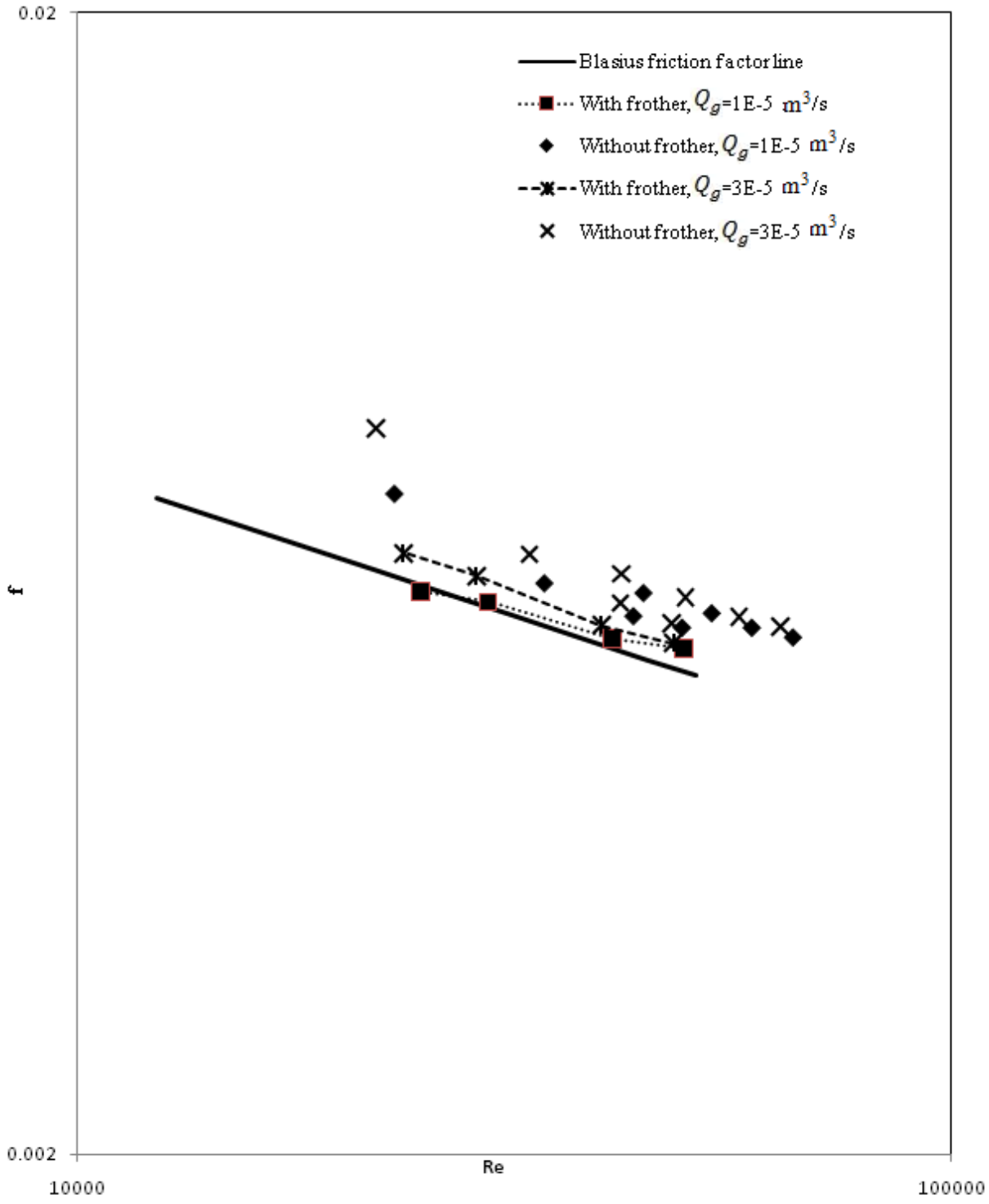

Figure 5.14 Effects of 20ppm frother on friction factor in ¾" pipe

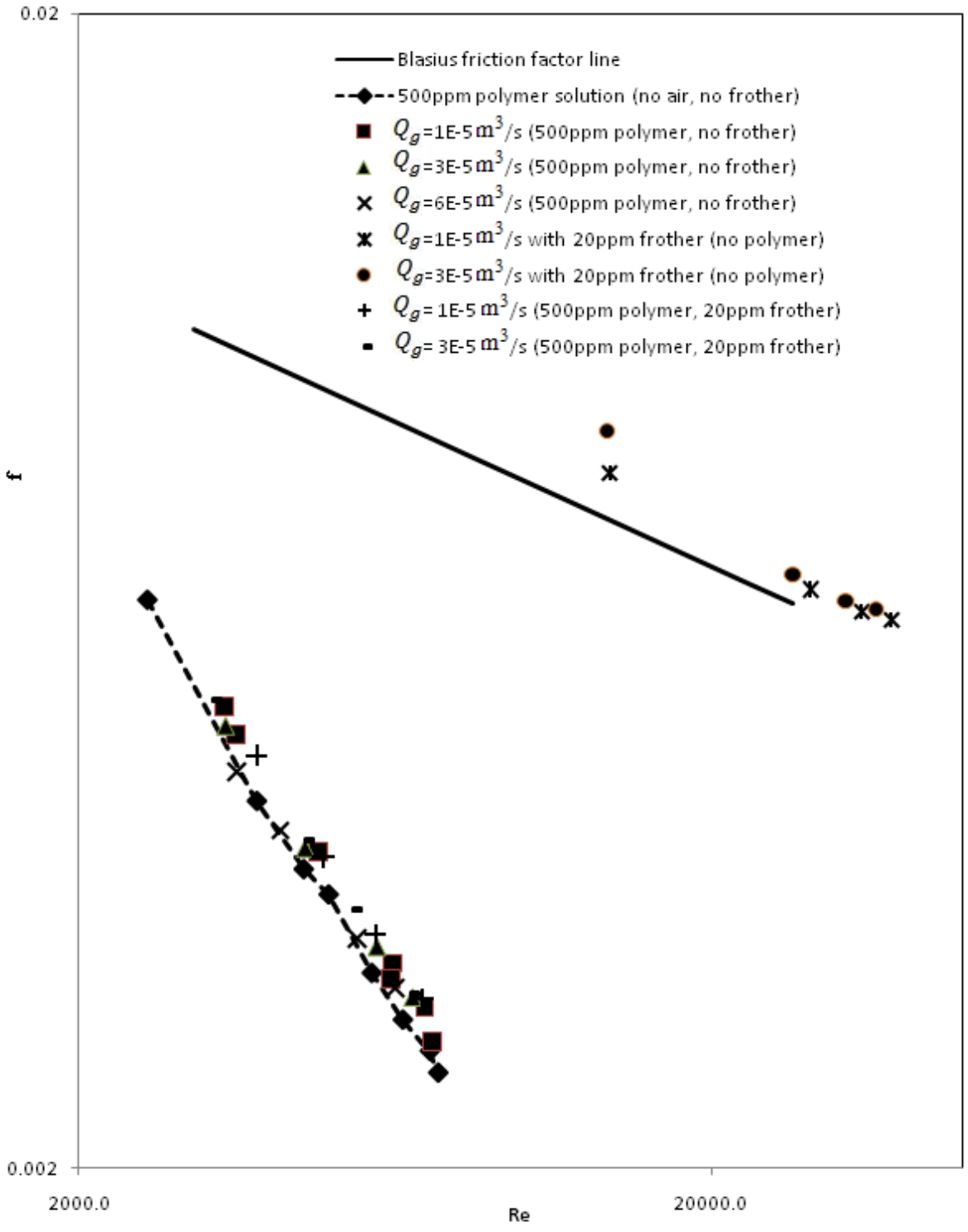

Figure 5.15 Effect of polymer on friction factor (pipe diameter= ½") at different air flow rates (Q_g)

Chapter 6

Conclusions and Recommendations

6.1 Overview

This last chapter of the thesis summarizes the conclusions and gives recommendations for further experimental work. The experiments carried out in this work looked at the effects of air bubbles, polymer, frother, and their combinations on friction in the vertical flow. The initial part of the chapter summarized the conclusions. Recommendations for further experimental work are also presented.

6.2 Conclusions

An experimental study was carried out to investigate the influence of polymer, air bubbles, frother, and their combinations on drag force in the vertical flows. Different flow conditions were investigated and the corresponding experimental data were recorded.

Pressure drops, air flow rates, and liquid flow rates were the raw data obtained from the experimental set-up. The data from each set of experiments and flow condition were used to calculate different parameters, namely wall shear stress, bubble size, and friction factor. Furthermore, the parameters obtained were plotted either as a function of Reynolds number or in some cases, either gas or liquid velocity.

The conclusions based on the experimental results are presented below:

- The aqueous polymeric solution (500 ppm polyacrylamide) exhibited drag reduction up to 70% at high Reynolds numbers in turbulent flow. No polymeric drag reduction occurred in laminar flow regime.
- From the wall shear stress and bubble size data one can conclude that bubbles in the range of 1 mm-3 mm increase the wall shear stress, and hence, no drag-reduction effect is observed in this bubble size range. The air-water two-phase mixture exhibits a significant deviation from the homogeneous model at low Reynolds numbers as a result of larger bubble sizes and lower turbulence intensities
- The reduction of friction factor for air-water mixture at low Reynolds numbers can be achieved by reducing the bubble sizes with the help of a frother. The frother concentration of 20 ppm was enough to make the two-phase mixture homogeneous.
- The combination of polymer and air-water flow system shows a drag reduction of up to 60%. It is also evident from the experiments that the addition of polymer to the bubbly flow system produces fully homogeneous mixture.

6.3 Recommendations for Future Work

Some recommendations for future experiments are presented below:

- The effects of different gases (instead of air) could be investigated to see the effect of gas density on drag force.
- Extend the flow rate range which was not possible in this work due to the system constraints.
- Vary the bubble size to investigate the effect of bubble size on drag force in the pipeline.
- Work with different types of polymers to study the influence of different polymer parameters on drag reduction
- Vary the concentration of polymer in the case of polymer solution-air bubble system.

References

Afacan, A., Sanders, S.R., Razzaque, M.M., Schaan, J., Nandakumar, K., Masliyah, J.H., Liu, S. (2004) "Bubble Size Distribution for Dispersed Air-Water Flows in a 100 mm Horizontal Pipeline" CJCHE. 82: 858-864

Astarita, G. (1965) "Possible Interpretations of the Mechanism of Drag Reduction in Viscoelastic Liquids" Ind Eng Chem Fundam. 4: 354-356

Aziz, K., Govier, G.W., Fogarasi, M. (1972) "Pressure Drop in Wells Producing Oil and Gas" J. Canadian Petro. Tech. 38-48

Banijamali, S.H., Merrill, E.W., Smith, K.A., Peebles, L.H. (1974) "Turbulent Drag Reduction by Polyacrylic Acid" AIChE J .20: 824-826

Beggs, H.D., Brill, J.P. (1973) "Two-Phase Flow in Inclined Pipes" J. Petro. Tech. 607-617

Bewersdorff, H.W. (1982) "Effect of Centrally Injected Polymer Thread on Drag in Pipe Flow" Rheol Acta. 21: 587-589

Blasius, H. (1913) "Das Ahnlichkeitsgesetz bei reibungsvorgangen in flussigkeiten" Ver. Dtsch. Ing. Forschungsh. 131: 6-25

Blatch, N.S. (1906) "Water Filtration at Washington" Trans Am Soc Civ Eng. 57: 400-406

Boggs, F.W., Tompson, J. (1966) "Flow Properties of Dilute Solution of Polymers" Part I: Mechanism of drag reduction U.S. Rubber Co. Research Center Report on Contract No. Nonr. 3123(00)

Clift, R., Grace, J.R., Weber, M. (2005) "Bubble, Particles, and Drops" Dover Publications, Inc., Mineola, New York. 169-202.

Colebrook, C.F. (1938) "Turbulent Flow in Pipes, with Particular Reference to the Transition Region Between the Smooth and Rough Pipe Laws" J. Inst. Civ Eng. Lond. 11: 133-156

Cooper, M., Scott, D., Dahlke, R., Gomez, C.O., Finch, J.A. (2004) "Impact of Air Distribution Profile on Banks in Zn Cleaning Circuit" Proceeding 36th annual meeting of the CMP. 525-540

Descamps, M.N., Oliemans, R.V.A., Ooms, G., Mudde, R.F. (2008) "Air–Water Flow in a Vertical Pipe: Experimental Study of Air Bubbles in the Vicinity of the Wall" Exp Fluids. 45: 357–370

Dodge, D.W., Metzner, A.B. (1959) "Turbulent Flow of Non-Newtonian System" AIChE J. 5: 189-204

EI'perin, I.T., Smol'skii, B.M., Leventhal, L.I. (1967) "Decreasing the Hydrodynamic Resistence of Pipelines" Int Chem Eng. 7: 276-295

Ellis, A.T., Ting, R.Y., Napolink, R.H. (1970) "Some Effects of Storage and Shear History on the Friction Reducing Properties of Dilute Polymer Solutions" Prog Astronaut Aeronaut 70: Viscous flow flow drag reduction (AIAA) 532

Ferrante, A., Elghobashi, S. (2004) "On the Physical Mechanisms of Drag Reduction in a Spatially Developing Turbulent Boundary Layer Laden with Microbubbles" J. Fluid Mech. 503: 345–355

Finch, J.A., Nesset, J.E., Acuña, C. (2008) "Role of Frother on Bubble Production and Behaviour in Flotation" Minerals Eng. 21: 949–957

Gadd, G.E. (1965) "Turbulence Damping and Drag Reduction Produced by Certain Additives in Water" Nature. 206: 463-472

Gadd, G.E. (1966) "Differences in Normal Stress in Aqueous Solutions of Turbulent Drag Reducing Additives" Nature. 212: 1348-1356

Gampert, B,. Wagner, P. (1985) "The Influence of Molecular Weight and Molecular Weight Distribution on Drag Reduction and Mechanical Degradation in Turbulent Flow of Highly Dilute Polymer Solutions" Springer-Verlag, Berlin, New York

Grau, R.A., Laskowski, J.S. (2006) "Role of Frothers in Bubble Generation and Coalescence in a Mechanical Flotation Cell" CJCHE. 84: 170–182

Guet, S., Ooms, G., Oliemans, R., Mudde, R. (2003) "Bubble Injector Effect on the Gaslift Efficiency" AIChE J. 49(9): 2242–2252

Guin, M.M., Kato, H., Maeda, M., Miyanaga, M. (1996) "Reduction of Skin Friction by Microbubbles and Its Relation with Near-Wall Bubble Concentration in a Channel" Journal of Marine Science and Technology. 1 (5): 241-254.

Gyr, A. (1968) "Analogy Between Vortex Stretching by Drag-Reducing Additives and Vortex Stretching by Fine Suspensions" Nature. 219:928-929

Gyr, A., Mueller, A. (1974) "The Effect of Wall Adsorption on the Toms Effect" Chem Eng Sci. 29: 1057-1060

Hershey, H.C., Zakin, J.L. (1967) "Existence of Two Types of Drag Reduction in Pipe Flow of Dilute Polymer Solutions" Ind Eng Chem Fundam. 6: 381-392

Hibiki, T., Ishii, M. (2002) "Interfacial Area Concentration of Bubbly Flow Systems" Chemical Engineering Science. 57: 3967-3977

Hoyt, J.W., Fabula, A.G. (1964) "The Effect of Additives on Fluid Friction" Proc 5th Symp on Naval Hydrodynamics, Bergen, Norway 112: 947-959

Johnson, B., Barchi, R.H. (1968) "Effect of Drag Reducing Additives on Boundary-Layer Turbulence" J Hydronautics. 2: 168-175

Kanai, A., Miyata, H. (2001) "Direct Numerical Simulation of Wall Turbulent Flows with Microbubbles" International Journal for Numerical Methods in Fluids. 35 (5): 593–615

Kodama, Y., Kakugawa, A., Takahashi, T., Kawashina, H. (1999) "Experimental Study on Microbubbles and Their Applicability to Ships for Skin Friction Reduction" 1st Int. Symp. On Turbulent Shear Flow Phenomena, Santa Barbara, U.S.A., 1-6

Kotter, M., Kulicke, W., Grager, H. (1989) "Drag Reduction Phenomenon with Special Emphasis on Homogeneous Polymer Solutions" Adv. Polym. Sci. 89: 1-8

Kulicke, W.M. (1986) "Unusual Instability Effects Observed in Ionic and Non-ionic Water Soluble Polymers" Makromol Chem, Macromol Syrup. 2: 137-139

Legner, H.H. (1984) "A Simple Model for Gas Bubble Drag Reduction" Phys Fluids. 27 (12): 2788–2790

Little, R.C. (1967) "Drag Reduction by Dilute Polymer Solutions in Turbulent Flow" Naval Research Laboratory Report 6542

Lu, J., Fernández, A., Tryggvason, G. (2005) "The Effect of Bubbles on the Wall Drag in a Turbulent Channel Flow" Phys Fluids. 17: 95-102

Madavan, N., Deutsch, S., Merkle, C. (1984) "Reduction of Turbulent Skin Friction by Microbubbles" Phys Fluids. 27(2): 356–363

Madavan, N.K., Merkle, C.L., Deutsch, S. (1985) "Numerical Investigations into the Mechanisms of Microbubble Drag Reduction" Journal of Fluids Eng. 107: 370–377.

Magaud, F., Souhar, M., Wild, G., Boisson, N. (2001) "Experimental Study of Bubble Column Hydrodynamics" Chem Eng Sci. 56:4597–4607

Malysa, K., Krasowska, M., Krzan, M. (2005) "Influence of Surface Active Substances on Bubble Motion and Collision with Various Surfaces" Advances in Colloid and Interface Science. (114/115): 205–225

McComb, W.D., Rabie, L.H. (1982) "Local Drag Reduction Due to Injection of Polymer Solutions into Turbulent Flow in a Pipe" AIChE J. 28:547-557

McCormick, M., Bhattacharyya, R. (1973) "Drag Reduction of a Submersible Hull by Electrolysis" Naval Eng J. 85(2):11–16

Meng, J.C.S., Uhlman, J.S. (1998) "Microbubble Formation and Splitting in a Turbulent Boundary Layer for Turbulence Reduction" Proceedings of the International Symposium on Seawater Drag Reduction. 341–355

Merkle C.L., Madavan, N.K., Deutsch, S. (1985) "Measurements of Local Skin Friction in a Microbubble-Modified Turbulent Boundary Layer" J. Fluid Mech. 156: 237-256.

Merkle, C.L., Deutsch S., Pal, S. (1986) "Microbubble Drag Reduction" 16th Symp. On Naval Hydrodynamics, Berkeley, U.S.A., 199-215

Nesset, J.E., Finch, J.A., Gomez, C.O. (2007) "Operating Variables Affecting the Bubble Size in Forced-Air Mechanical Flotation Machines" Proceedings AusIMM 9th Mill Operators' Conference, Fremantle, Australia. 66–75.

Nesset, J.E., Hernandez-Aguilar, J.R., Acuña, C., Gomez, C.O., Finch, J.A. (2006) "Some Gas Dispersion Characteristics of Mechanical Flotation Machines" Minerals Eng. 19: 807–815

Nikuradse, J. (1932) "Gesetzmassigkeiten der turbulenten stromung in glatten Rohren" Ver. Dtsch. Ing. Forschungsh. 356-362

Orkiszewski, J. (1967) "Predicting Two-Phase Pressure Drop in Vertical Pipe" J. Pet. Tech., 829-838

Peterlin, A. (1970) "Molecular Model of Drag Reduction by Polymer Solutes" Nature. 227:598-609

Pfenninger, W. (1967) "A Hypothesis of the Reduction of the Turbulent Friction Drag in Fluid Flows by Means of Additives" Northrop Corp Norair Division Report BLC-179

Sanders, W.C., Winkel, E.W., Dowling, D.R., Perlin, M., Ceccio, S.L. (2006) "Bubble Friction Drag Reduction in a High Reynolds Number Flat Plate Turbulent Boundary Layer" J Fluid Mech. 552:353–380

Savins, J.G. (1964) "Drag Reduction Characteristics of Solution of Macromolecules in Turbulent Pipe Flow" Soc Petrol Eng J. 4:203-207

Skudarnov, P.V., Lin, C.X. (2006) "Drag Reduction by Gas Injection into Turbulent Boundary Layer: Density Ratio Effect" Int J. of Heat and Fluid Flow. 27: 436–444

Sweet, C., van Hoogstraten, J., Harris, M., Laskowski, J.S. (1997) "The Effect of Frothers on Bubble Size and Frothability of Aqueous Solutions" The Metallurgical Society of CIM. 235–246

Takahashi, T., Kakugawa, A., Kodama, Y. (1997) "Streamwise Distribution of the Skin Friction Reduction by Microbubbles" J. Soc. Naval Architects of Japan. 182: 1-8

Tokunaga, K. (1987) "Reduction of Frictional Resistance of a Flat Plate by Microbubbles" Trans. West-Japan Society of Naval Architects. 73: 79-82

Toms, B.A. (1948) "Some Observations on the Flow of Linear Polymer Solutions Through Straight Tubes at Large Reynolds-numbers" Proc 1st Intern Congr on Rheology North Holland Amsterdam II. 135-139

Tulin, M.P. (1966) "Hydrodynamic Aspects of Macromolecular Solutions" Proceed 6th Symp on Naval Hydrodynamics, Washington, ONR CR-136: 3-8

Walsh, M. (1967) "Theory of Drag Reduction in Dilute High-Polymer Flows" Int Shipbuilding Prog. 14:134-139

Wells, C.S., Spangler, J.G. (1967) "Injection of a Drag Reducing Fluid into Turbulent Pipe Flow of a Newtonian Fluid" Phys Fluids. 10:1880-1890

Xu, J., Maxey, M.R., Karniadakis, G.E. (2002) "Numerical Simulation of Turbulent Drag Reduction Using Microbubbles" J Fluid Mech. 468: 271–281.

Zaruba, A., Lucas, D., Prasser, H., Ho Hne, T. (2007) "Bubble–Wall Interactions in a Vertical Gas–Liquid Flow: Bouncing, Sliding and Bubble Deformations" Chem Eng Sci. 62: 1591–1605

Nomenclature

A	Total cross-sectional flow area
A_g	Cross-sectional flow area occupied by the gas phase
A_l	Cross-sectional flow area occupied by the liquid phase
D	Diameter
D_H	Hydraulic equivalent diameter of flow channe
D_{sm}	Sauter mean diameter of bubble
$\widetilde{D}_{sm}$	Non-dimensional Sauter mean diameter of bubble
$(-\frac{dp}{dz})_F$	Pressure loss per unit length due to friction
f	Friction factor
g	Gravity
G_g	Gas mass flux
G_l	Liquid mass flux
G_{tp}	Two-phase mass flux
j	Mixture volumetric flux
K	Power law constant
L	Length
L_e	Length of fully developed velocity profile
L_0	Laplace length
$\tilde{L}_0$	Non-dimensional Laplace length

$\dot{M}_g$	Gas mass flow rate
$\dot{M}_l$	Liquid mass flux
$\dot{M}_{tp}$	Total mass flow rate
n	Power law constant
P	Pressure
ΔP_f	Frictional pressure drop
ΔP_{meas}	Pressure drop measured by the transducers
Q_g	Volumetric gas flow rates
Q_l	Volumetric liquid flow rates
Q_{tp}	Volumetric total flow rates
Re	Reynolds number
Re_f	Liquid Reynolds number
Re_G	Generalized Reynolds number
$\bar{V}$	The velocity of the conductor
V_{sg}	Gas superficial velocity
V_{sl}	Liquid superficial velocity
$\bar{V}_{tp}$	Average homogenous flow velocity
X	Quality
z	Elevation

Greek Symbols:

α	Void fraction
β	Volumetric flow fraction
ε	Energy dissipation rate per unit mass
$\tilde{\varepsilon}$	Non-dimensional energy dissipation rate per unit mass
ϵ	Roughness
μ_g	Liquid dynamic viscosity
μ_l	Liquid dynamic viscosity
μ_{tp}	Mixture dynamic viscosity
$\Delta\rho$	Density difference
ρ_G	Gas density
ρ_{im}	Density of liquid inside the impulse tubing
ρ_L	Liquid density
ρ_{tp}	Density of mixture
τ_w	Wall shear stress
v_f	Kinematic viscosity of liquid
σ_L	Surface tension

Appendix A

Calibration Data

- Calibration Data for Differential Pressure Transducers
- Calibration Data for Magnetic Flowmeter
- Calibration Data for the Air Rotameter

A.1. Calibration Data for the Pressure Transducers

5 psi Pressure transducer		
pressure (inch Hg)	**Pressure (psi)**	**voltage(V)**
10.2	**5.01**	**5.104668191**
9	**4.42**	**4.644419734**
8	**3.93**	**4.24049949**
7	**3.44**	**3.830189694**
6	**2.95**	**3.437571672**
5	**2.46**	**3.037208386**
4	**1.96**	**2.629949136**
3	**1.47**	**2.2297329**
2	**0.98**	**1.833864496**
1	**0.49**	**1.438409107**
0	**0.00**	**1.024341278**

Regression Equation:

$$\Delta P \text{ (psi)} = 1.2264\ V - 1.2648$$

Table A.1 Calibration data of 5 psi Rosemount transducer

0.5 psi Pressure Transducer		
Pressure (in Hg)	**Pressure (psi)**	**Voltage (v)**
0.101801064	**0.05**	**1.568121353**
0.20563815	**0.101**	**1.988548428**
0.307439215	**0.151**	**2.384166809**
0.529365535	**0.26**	**3.324515966**
0.735003685	**0.361**	**4.185862156**
0.918245601	**0.451**	**4.954588511**

Regression Equation:

$$\Delta P \text{ (psi)} = 0.1181\ V - 0.1333$$

Table A.2 Calibration data of 0.5psi Rosemount pressure transducer

A.2. Calibration Data of Magnetic Flowmeter

Magnetic Flowmeter Calibration Data	
voltage (V)	**Flow rate(LPM)**
0.4	**0**
0.704	**34.018**
0.726	**36.369**
0.798	**44.469**
0.876	**53.402**
0.974	**64.696**
1.02	**69.633**
1.023	**70.108**
1.037	**71.667**
1.042	**72.415**

Regression Equation:

$$Q\ (LPM) = 112.81\ V - 45.338$$

Table A.3 Calibration data of Magnetic flowmeter

A.3. Calibration Data for Air Rotameter

Air Rotameter Calibration Data	
Meter Scale (mm)	**Air flowrate (ml/min)**
0	**0**
10	**995.91**
20	**2295.79**
30	**3502.35**
40	**4661.2**
50	**5803.69**
60	**6888.83**
70	**8057.2**
80	**9204.83**
90	**10290.37**
100	**11269.8**
110	**12435.91**
120	**13515.18**
130	**14657.99**
140	**15761.4**
150	**16736.68**

Regression Equation:

$$Q\ (SMLM) = 0.0002\ S^3 - 0.0804\ S^2 + 120.88\ S - 80.478$$

Table A.4 Calibration data for air rotameter

Appendix B

Experimental Data

- Pressure drop and friction factor coefficient for single-phase flows
- Pressure drop and friction factor coefficient for two-phase flows

B.1. Single-Phase Flow Experimental Data

B.2.1 Experimental Data for Pure Water

Pressure Drop and Friction Factor for Pure Water in 1/2" Pipeline												
Diameter (in)	**Flow voltage**	**Pressure voltage**	**PT range**	**Flow (m^3/s)**	**PD (pa)**	**Actual radius (m)**	**Length (m)**	**Area (m^2)**	**Velocity (m/s)**	**Re**	**Exp. Friction factor**	**theory**
0.5	0.624945	4.319466	5	0.000418	27803.75	0.006604	3.3	0.000137	3.050955	40994.62	0.005995	0.005552
0.5	0.605731	3.817828	5	0.000382	23562.03	0.006604	3.3	0.000137	2.790507	37495.07	0.006073	0.005677
0.5	0.573334	3.087104	5	0.000322	17383.23	0.006604	3.3	0.000137	2.351374	31594.59	0.00631	0.005925
0.5	0.54798	2.600542	5	0.000275	13269	0.006604	3.3	0.000137	2.007704	26976.82	0.006607	0.006164
0.5	0.519314	2.094768	5	0.000222	8992.303	0.006604	3.3	0.000137	1.619128	21755.66	0.006885	0.006505
0.5	0.501588	1.82561	5	0.000189	6716.378	0.006604	3.3	0.000137	1.378859	18527.25	0.00709	0.006771
0.5	0.480555	1.553294	5	0.00015	4413.747	0.006604	3.3	0.000137	1.093754	14696.39	0.007405	0.007175
0.5	0.459131	1.333564	5	0.00011	2555.769	0.006604	3.3	0.000137	0.803353	10794.38	0.007948	0.00775
0.5	0.440319	1.183238	5	7.51E-05	1284.656	0.006604	3.3	0.000137	0.548366	7368.203	0.008575	0.008527
0.5	0.424387	1.086912	5	4.55E-05	470.1486	0.006604	3.3	0.000137	0.332403	4466.383	0.00854	0.009664
0.5	0.638439	8.438699	5	0.000443	28491.63	0.006604	3.3	0.000137	3.233861	43452.27	0.005468	0.005472
0.5	0.634768	8.233386	5	0.000436	27784.12	0.006604	3.3	0.000137	3.184098	42783.61	0.0055	0.005493
0.5	0.621545	7.436885	5	0.000412	25039.38	0.006604	3.3	0.000137	3.00487	40375.4	0.005566	0.005573
0.5	0.615186	7.043754	5	0.0004	23684.65	0.006604	3.3	0.000137	2.918667	39217.11	0.005581	0.005614
0.5	0.605986	6.556883	5	0.000383	22006.89	0.006604	3.3	0.000137	2.79396	37541.47	0.005658	0.005675
0.5	0.59271	5.81035	5	0.000358	19434.34	0.006604	3.3	0.000137	2.614012	35123.57	0.005709	0.005771
0.5	0.581892	5.267541	5	0.000338	17563.82	0.006604	3.3	0.000137	2.467374	33153.24	0.005791	0.005855
0.5	0.565962	4.48308	5	0.000308	14860.57	0.006604	3.3	0.000137	2.251445	30251.88	0.005884	0.00599
0.5	0.546709	3.649704	5	0.000273	11988.76	0.006604	3.3	0.000137	1.990467	26745.21	0.006074	0.006178
0.5	0.52116	2.625817	5	0.000225	8460.443	0.006604	3.3	0.000137	1.644153	22091.91	0.006282	0.00648

Table B.1 Pressure drop and friction factor for 1/2" pipe with pure water

Pressure Drop and Friction Factor for Pure Water in 3/4" Pipeline												
Diameter	**Flow voltage**	**Pressure voltage**	**PT range**	**Flow (m^3/s)**	**PD (pa)**	**Actual radius (m)**	**Length (m)**	**Area (m^2)**	**Velocity (m/s)**	**Re**	**Exp. friction factor**	**theory**
0.75	0.792821	2.355993	5	0.00073	11201.15	0.009271	2.48	0.00027	2.702734	50981.66	0.005749	0.005257
0.75	0.747249	2.103309	5	0.000645	9064.524	0.009271	2.48	0.00027	2.38929	45069.15	0.005953	0.005422
0.75	0.709687	1.898371	5	0.000575	7331.628	0.009271	2.48	0.00027	2.130939	40195.89	0.006054	0.005579
0.75	0.667885	1.703218	5	0.000498	5681.459	0.009271	2.48	0.00027	1.843432	34772.65	0.006268	0.005785
0.75	0.642142	1.589832	5	0.00045	4722.698	0.009271	2.48	0.00027	1.666373	31432.79	0.006377	0.005933
0.75	0.614737	1.486356	5	0.000399	3847.738	0.009271	2.48	0.00027	1.477882	27877.28	0.006605	0.006114
0.75	0.572359	1.338919	5	0.00032	2601.047	0.009271	2.48	0.00027	1.186407	22379.18	0.006928	0.006459
0.75	0.49477	1.138875	5	0.000176	909.5349	0.009271	2.48	0.00027	0.652753	12312.88	0.008003	0.0075
0.75	0.460177	1.078625	5	0.000112	400.0756	0.009271	2.48	0.00027	0.41483	7824.935	0.008717	0.0084
0.75	0.434685	1.047077	5	6.47E-05	133.3155	0.009271	2.48	0.00027	0.239495	4517.595	0.008715	0.009636
0.75	0.806756	3.379473	5	0.000756	11057.54	0.009271	2.48	0.00027	2.798573	52789.46	0.005294	0.005212
0.75	0.795703	3.214994	5	0.000735	10490.74	0.009271	2.48	0.00027	2.722553	51355.49	0.005307	0.005248
0.75	0.783499	3.051979	5	0.000712	9928.997	0.009271	2.48	0.00027	2.638613	49772.14	0.005347	0.005289
0.75	0.772382	2.890596	5	0.000692	9372.871	0.009271	2.48	0.00027	2.562156	48329.93	0.005353	0.005328
0.75	0.758039	2.699928	5	0.000665	8715.829	0.009271	2.48	0.00027	2.463505	46469.08	0.005385	0.005381
0.75	0.72887	2.337123	5	0.000611	7465.602	0.009271	2.48	0.00027	2.262882	42684.73	0.005466	0.005496
0.75	0.702143	2.01407	5	0.000561	6352.361	0.009271	2.48	0.00027	2.079053	39217.15	0.00551	0.005614
0.75	0.67625	1.744465	5	0.000513	5423.302	0.009271	2.48	0.00027	1.900964	35857.86	0.005627	0.005741

Table B.2 Pressure drop and friction factor for 3/4" pipe with pure water

B.2.2 Experimental Data for Single Phase Polymeric Flow

Pressure drop and Friction Factor for single phase polymeric solution in 1/2" pipe													
Water flow voltage	**Pressure Voltage**	**Pressure transducer range**	**Water Mass Flowrate (kg/s)**	**Water flow rate (m^3/s)**	**Pressure Drop (pa)**	**Actual radius (m)**	**Length (m)**	**Area (m^2)**	**Velocity (m/s)**	**n**	**K**	**Re_g**	**Exp. Friction factor**
0.6948056	3.32713	5	0.54911	0.00055	19412.8	0.0066	3.3	0.00014	4.01251	0.827	0.00714	27380.7	0.002415863
0.6594455	3.00462	5	0.48287	0.00048	16685.8	0.0066	3.3	0.00014	3.5285	0.827	0.00714	23548.4	0.00268523
0.6318589	2.75895	5	0.4312	0.00043	14608.4	0.0066	3.3	0.00014	3.15089	0.827	0.00714	20620.6	0.002948167
0.5814101	2.32709	5	0.3367	0.00034	10956.8	0.0066	3.3	0.00014	2.46035	0.827	0.00714	15426.8	0.003626645
0.5532336	2.08709	5	0.28392	0.00028	8927.36	0.0066	3.3	0.00014	2.07467	0.827	0.00714	12630.4	0.004155673
0.5080435	1.72719	5	0.19927	0.0002	5884.17	0.0066	3.3	0.00014	1.4561	0.827	0.00714	8338.02	0.005560522
0.4729349	1.45259	5	0.1335	0.00013	3562.22	0.0066	3.3	0.00014	0.97554	0.827	0.00714	5212.2	0.007499778
0.4422017	1.21634	5	0.07593	7.6E-05	1564.58	0.0066	3.3	0.00014	0.55486	0.827	0.00714	2688.84	0.010182327
0.6859808	3.28653	5	0.53258	0.00053	19069.5	0.0066	3.3	0.00014	3.89171	0.827	0.00714	26416.4	0.002522744
0.6334031	2.80898	5	0.43409	0.00043	15031.5	0.0066	3.3	0.00014	3.17203	0.827	0.00714	20782.9	0.002993244
0.5984895	2.50848	5	0.36869	0.00037	12490.5	0.0066	3.3	0.00014	2.69413	0.827	0.00714	17160.1	0.003447933
0.5607019	2.20752	5	0.29791	0.0003	9945.66	0.0066	3.3	0.00014	2.17689	0.827	0.00714	13363.5	0.004205086
0.5186252	1.85755	5	0.21909	0.00022	6986.45	0.0066	3.3	0.00014	1.60095	0.827	0.00714	9319.06	0.00546158
0.5034521	1.74274	5	0.19067	0.00019	6015.64	0.0066	3.3	0.00014	1.39326	0.827	0.00714	7917.48	0.006209187
0.4757214	1.53562	5	0.13872	0.00014	4264.26	0.0066	3.3	0.00014	1.01368	0.827	0.00714	5452.04	0.008314935
0.4520666	4	0.5	0.09441	9.5E-05	2408.34	0.0066	3.3	0.00014	0.68989	0.827	0.00714	3471.58	0.010138467
0.4382292	2.4	0.5	0.06849	6.9E-05	1107.71	0.0066	3.3	0.00014	0.50048	0.827	0.00714	2382.44	0.008860591
0.4293307	2	0.5	0.05182	5.2E-05	782.555	0.0066	3.3	0.00014	0.37868	0.827	0.00714	1717.72	0.010934138
0.4211775	1.7	0.5	0.03655	3.7E-05	538.687	0.0066	3.3	0.00014	0.26708	0.827	0.00714	1140.48	0.015131185
0.4124998	1.45	0.5	0.02029	2E-05	335.464	0.0066	3.3	0.00014	0.1483	0.827	0.00714	571.982	0.030562395

Pressure drop and Friction Factor for single phase polymeric solution in 1/2" pipe													
Water flow voltage	**Pressure Voltage**	**Pressure transducer range**	**Water Mass Flowrate (kg/s)**	**Water flow rate (m^3/s)**	**Pressure Drop (pa)**	**Actual radius (m)**	**Length (m)**	**Area (m^2)**	**Velocity (m/s)**	**n**	**K**	**Re_g**	**Exp. Friction factor**
0.693517	3.56553	5	0.5467	0.00055	21428.7	0.0066	3.3	0.00014	3.99487	0.827	0.00714	27239.6	0.002690328
0.6500862	3.12252	5	0.46534	0.00047	17682.7	0.0066	3.3	0.00014	3.40039	0.827	0.00714	22548.7	0.003064132
0.6065018	2.68436	5	0.3837	0.00038	13977.7	0.0066	3.3	0.00014	2.8038	0.827	0.00714	17982.3	0.003562515
0.5617533	2.26968	5	0.29988	0.0003	10471.3	0.0066	3.3	0.00014	2.19128	0.827	0.00714	13467.2	0.004369376

Table B.3 Pressure drop and friction factor for single phase polymeric flows in 1/2" pipe

Pressure drop and Friction Factor for single phase polymeric solution in 3/4" pipe													
Water flow voltage	**Pressure Voltage**	**Pressure transducer range**	**Water Mass Flowrate (kg/s)**	**Water flow rate (m^3/s)**	**Pressure Drop (pa)**	**Actual radius (m)**	**Length (m)**	**Area (m^2)**	**Velocity (m/s)**	**n**	**K**	**Re_g**	**Exp. Friction factor**
0.846782226	1.8768926	5	0.8337925	0.0008348	7150.0086	0.009271	2.48	0.00027	3.0915436	0.827	0.00714	26696.083	0.002799962
0.805717865	1.7875208	5	0.7568707	0.0007578	6394.305	0.009271	2.48	0.00027	2.8063324	0.827	0.00714	23830.821	0.003038866
0.76640055	1.7031997	5	0.6832215	0.000684	5681.308	0.009271	2.48	0.00027	2.5332552	0.827	0.00714	21134.269	0.003313499
0.725422811	1.6150657	5	0.606462	0.0006072	4936.0713	0.009271	2.48	0.00027	2.2486456	0.827	0.00714	18377.024	0.003653724
0.682724437	1.5269066	5	0.5264794	0.0005271	4190.6216	0.009271	2.48	0.00027	1.9520854	0.827	0.00714	15567.789	0.004116017
0.608616705	4.8510999	0.5	0.3876608	0.0003881	3100.191	0.009271	2.48	0.00027	1.4373724	0.827	0.00714	10871.779	0.005616247
0.561610966	3.8524282	0.5	0.2996097	0.0003	2288.3788	0.009271	2.48	0.00027	1.1108956	0.827	0.00714	8036.122	0.006940293
0.524448591	3.0992054	0.5	0.2299971	0.0002303	1676.0901	0.009271	2.48	0.00027	0.8527854	0.827	0.00714	5893.1416	0.008626094
0.478072885	2	0.5	0.1431261	0.0001433	782.55495	0.009271	2.48	0.00027	0.5306844	0.827	0.00714	3378.3516	0.010400124
0.449022189	1.35	0.5	0.0887084	8.881E-05	254.17523	0.009271	2.48	0.00027	0.3289137	0.827	0.00714	1927.5648	0.008793578
0.839456108	1.7995517	5	0.8200692	0.0008211	6496.035	0.009271	2.48	0.00027	3.0406603	0.827	0.00714	26181.419	0.002629716
0.788894643	1.6964113	5	0.7253574	0.0007262	5623.9079	0.009271	2.48	0.00027	2.6894872	0.827	0.00714	22671.18	0.002910017
0.74684976	1.6149756	5	0.646599	0.0006474	4935.3092	0.009271	2.48	0.00027	2.3974658	0.827	0.00714	19811.685	0.003213704
0.69526578	1.513363	5	0.5499719	0.0005506	4076.1002	0.009271	2.48	0.00027	2.0391909	0.827	0.00714	16385.735	0.003668812
0.652444688	1.4351465	5	0.4697594	0.0004703	3414.7229	0.009271	2.48	0.00027	1.7417783	0.827	0.00714	13619.353	0.004212754
0.619281653	1.3722149	5	0.4076384	0.0004081	2882.5904	0.009271	2.48	0.00027	1.5114455	0.827	0.00714	11531.856	0.004722743
0.60053176	1.337286	5	0.3725161	0.000373	2587.241	0.009271	2.48	0.00027	1.3812187	0.827	0.00714	10375.277	0.005075845
0.577014449	1.2956143	5	0.3284635	0.0003289	2234.8763	0.009271	2.48	0.00027	1.21788	0.827	0.00714	8951.2953	0.005639504
0.547620885	3.3856066	0.5	0.2734034	0.0002737	1908.9033	0.009271	2.48	0.00027	1.0137279	0.827	0.00714	7218.0122	0.006952444
0.509478435	2.6352876	0.5	0.201955	0.0002022	1298.9751	0.009271	2.48	0.00027	0.7488107	0.827	0.00714	5059.5305	0.008670679
0.470258077	1.8	0.5	0.1284874	0.0001286	619.97657	0.009271	2.48	0.00027	0.4764069	0.827	0.00714	2976.7344	0.010223875
0.453008512	1.4	0.5	0.0961755	9.629E-05	294.81982	0.009271	2.48	0.00027	0.3566006	0.827	0.00714	2119.2461	0.008677386

Table B.4 Pressure drop and friction factor for single phase polymeric flow in 3/4" pipe

B.2. Two-Phase Flow Experimental Data

B.2.1 Pressure Drop and Friction Factor for Air-Water System in 1/2” Pipe

Pressure Drop and Friction Factor for Air-Water System in 1/2" Pipe														
Liquid flow voltage	**Pressure Voltage**	**Liquid flow rate (Kg/s)**	**Gas flow rate (m3/s)**	**ΔPmeas (Pa)**	**Quality of gas phase**	**Mixture density (kg/m3)**	**Mixture Viscosity (Pa.s)**	**Usg (m/s)**	**Wall shear stress (KPa)**	**ΔPF /ΔL (Kpa / m)**	**ΔPH /ΔL (Kpa/ m)**	**ΔPT (Kpa/m)**	**Re**	**Exp. friction factor**
0.625937	4.331699	0.419452	1.31128E-05	27907.19	3.77E-05	968.0297	0.000998	0.095704	0.0289	8.752394	9.486691	18.23909	40436.19	0.00597
0.602407	3.728339	0.375795	1.31128E-05	22805.34	4.2E-05	964.6428	0.000998	0.095704	0.023905	7.239569	9.453499	16.69307	36227.74	0.00613
0.577705	3.16629	0.329966	1.31128E-05	18052.8	4.79E-05	960.1599	0.000998	0.095704	0.019295	5.84334	9.409567	15.25291	31809.93	0.006388
0.555867	2.821376	0.289449	1.31128E-05	15136.3	5.46E-05	955.0654	0.000997	0.095704	0.016541	5.009478	9.359641	14.36912	27904.11	0.007079
0.63219	4.844501	0.431052	1.31128E-05	32243.3	3.67E-05	968.8177	0.000998	0.095704	0.033214	10.05864	9.494414	19.55306	41554.47	0.006502
0.576181	3.175288	0.327139	1.31128E-05	18128.89	4.83E-05	959.8437	0.000998	0.095704	0.019381	5.869494	9.406469	15.27596	31537.35	0.006526
0.526553	2.347449	0.235063	1.31128E-05	11128.91	6.72E-05	945.6119	0.000997	0.095704	0.012837	3.887759	9.266996	13.15476	22661.37	0.008247
0.470663	1.433249	0.131371	1.31128E-05	3398.678	0.00012	907.8645	0.000994	0.095704	0.006324	1.915191	8.897072	10.81226	12665.53	0.012487
0.444636	1.982572	0.083084	1.31128E-05	768.3879	0.00019	862.5081	0.000991	0.095704	0.00516	1.562626	8.452579	10.0152	8010.692	0.024197
0.622388	4.555351	0.412867	2.98183E-05	29798.33	8.7E-05	931.1574	0.000996	0.21763	0.031986	9.686815	9.125342	18.81216	39803.37	0.006559
0.576067	3.386334	0.326927	2.98183E-05	19913.44	0.00011	915.0044	0.000995	0.21763	0.022618	6.849693	8.967043	15.81674	31518.87	0.007268
0.5253	2.327125	0.232739	2.98183E-05	10957.05	0.000154	885.1533	0.000992	0.21763	0.014622	4.428176	8.674502	13.10268	22439.25	0.008968
0.469754	4.481466	0.129684	2.98183E-05	2799.719	0.000277	812.089	0.000986	0.21763	0.008824	2.672287	7.958473	10.63076	12504.88	0.015989
0.466792	3.676988	0.124189	2.98183E-05	2145.765	0.000289	805.4457	0.000986	0.21763	0.008385	2.539224	7.893368	10.43259	11975.13	0.016431
0.62242	4.292724	0.412925	2.98183E-05	27577.63	8.7E-05	931.1662	0.000996	0.21763	0.029764	9.013788	9.125429	18.13922	39809.01	0.006102
0.599452	3.698541	0.370314	2.98183E-05	22553.38	9.7E-05	924.0266	0.000995	0.21763	0.024967	7.561256	9.05546	16.61672	35701.3	0.006315
0.575645	3.144546	0.326144	2.98183E-05	17868.94	0.00011	914.8214	0.000995	0.21763	0.020578	6.231941	8.965249	15.19719	31443.4	0.006643
0.552801	2.761886	0.283762	2.98183E-05	14633.27	0.000127	903.5502	0.000994	0.21763	0.017705	5.361893	8.854792	14.21669	27357.76	0.007457
0.607654	4.303021	0.38553	6.14654E-05	27664.7	0.000192	861.3181	0.000991	0.448607	0.032111	9.724684	8.440917	18.1656	37171.77	0.006984
0.575968	3.426823	0.326744	6.14654E-05	20255.8	0.000227	840.5844	0.000989	0.448607	0.025368	7.682755	8.237727	15.92048	31504.89	0.007496

Pressure Drop and Friction Factor for Air-Water System in 1/2" Pipe														
Liquid flow voltage	**Pressure Voltage**	**Liquid flow rate (Kg/s)**	**Gas flow rate (m3/s)**	**ΔPmeas (Pa)**	**Quality of gas phase**	**Mixture density (kg/m3)**	**Mixture Viscosity (Pa.s)**	**Usg (m/s)**	**Wall shear stress (KPa)**	**ΔPF /ΔL (Kpa / m)**	**ΔPH /ΔL (Kpa/ m)**	**ΔPT (Kpa/m)**	**Re**	**Exp. friction factor**
0.52592	2.299883	0.233889	6.14654E-05	10726.7	0.000317	791.0139	0.000985	0.448607	0.017438	5.28094	7.751936	13.03288	22553.77	0.009461
0.468407	2.270822	0.127186	6.14654E-05	1002.704	0.000582	673.7594	0.000972	0.448607	0.011502	3.483368	6.602842	10.08621	12267.76	0.017966
0.617371	4.280977	0.403558	6.14654E-05	27478.3	0.000183	866.6261	0.000991	0.448607	0.031753	9.616181	8.492936	18.10912	38909.7	0.006342
0.596145	3.668752	0.364178	6.14654E-05	22301.49	0.000203	854.4498	0.00099	0.448607	0.026967	8.166779	8.373608	16.54039	35113.48	0.00652
0.571554	3.073628	0.318555	6.14654E-05	17269.28	0.000232	837.1869	0.000989	0.448607	0.02249	6.811045	8.204432	15.01548	30715.46	0.006963
0.550076	2.691864	0.278707	6.14654E-05	14041.18	0.000266	818.3195	0.000987	0.448607	0.019871	6.017733	8.019531	14.03726	26874.14	0.007855

Table B.5 Pressure drop and friction factor for air-water flow in 1/2" pipe

Pressure Drop and Friction Factor for Air-Water Flow in 3/4" pipe												
Liquid flow voltage	**Pressure Voltage**	**Liquid flow rate (Kg/s)**	**Gas flow rate (m3/s)**	**ΔPmeas (Pa)**	**Quality of gas phase**	**Mixture density (kg/m3)**	**Mixture Viscosity (Pa.s)**	**Wall shear stress (KPa)**	**ΔPF (KPa)**	**ΔPH (KPa)**	**ΔPT (KPa)**	**Re**
0.9281123	3.3903417	0.9800767	1.311E-05	19947.3261	1.612E-05	985.06032	0.0009992	0.0378815	20.266673	23.940906	44.207579	67300.702
0.8748082	2.9682	0.8811817	1.311E-05	16377.8312	1.793E-05	983.60724	0.0009991	0.0312756	16.732494	23.90559	40.638084	60509.812
0.8281182	2.6442257	0.7945577	1.311E-05	13638.3701	1.989E-05	982.0421	0.000999	0.0262262	14.031072	23.867551	37.898623	54561.536
0.7590739	2.1958465	0.6664598	1.311E-05	9846.9966	2.371E-05	978.99627	0.0009988	0.0192779	10.313724	23.793525	34.107249	45765.349
0.7965888	2.3659741	0.7360612	1.311E-05	11285.5502	2.147E-05	980.78043	0.0009989	0.0218858	11.708916	23.836888	35.545803	50544.715
0.7499215	2.0809972	0.6494794	1.311E-05	8875.8624	2.433E-05	978.50411	0.0009988	0.0174851	9.3545513	23.781564	33.136115	44599.343
0.678459	1.7129492	0.516895	1.311E-05	5763.7476	3.057E-05	973.57685	0.0009985	0.0118919	6.3621886	23.661812	30.024	35495.074
0.5902426	1.3546128	0.3532271	1.311E-05	2733.7518	4.473E-05	962.57539	0.0009978	0.0067282	3.5995724	23.394432	26.994005	24256.382
0.9214783	3.3743491	0.9677686	2.982E-05	19812.0967	3.713E-05	968.45143	0.0009982	0.0383833	20.535106	23.537244	44.072349	66456.916
0.8691839	2.9516026	0.8707469	2.982E-05	16237.4667	4.126E-05	965.2463	0.000998	0.0318473	17.038373	23.459346	40.49772	59794.658
0.8097445	2.5281203	0.760469	2.982E-05	12656.6141	4.725E-05	960.64758	0.0009977	0.0253631	13.569288	23.347579	36.916867	52222.129
0.7486735	2.1326505	0.647164	2.982E-05	9312.6281	5.552E-05	954.36202	0.0009973	0.0193982	10.378066	23.194815	33.572881	44441.735
0.7961748	2.3449251	0.7352931	2.982E-05	11107.5652	4.886E-05	959.41184	0.0009976	0.0225238	12.050273	23.317545	35.367818	50493.356
0.7482735	2.0586223	0.6464218	2.982E-05	8686.6660	5.558E-05	954.3139	0.0009973	0.0182304	9.7532738	23.193645	32.946919	44390.769
0.67764	1.692794	0.5153756	2.982E-05	5593.3203	6.971E-05	943.76412	0.0009966	0.0129277	6.9163298	22.937243	29.853573	35392.124
0.589968	1.3153523	0.3527177	2.982E-05	2401.7749	0.0001019	920.61424	0.000995	0.0080138	4.2874193	22.374608	26.662028	24222.783
0.9105226	3.355835	0.9474426	6.147E-05	19655.5468	7.817E-05	937.56306	0.0009962	0.0394938	21.129267	22.786533	43.9158	65063.797
0.8696743	2.9783969	0.8716567	6.147E-05	16464.0316	8.496E-05	932.63769	0.0009958	0.0337522	18.057458	22.666826	40.724284	59859.753
0.7488659	2.130966	0.6475208	6.147E-05	9298.3848	0.0001144	911.90786	0.0009944	0.0213002	11.395629	22.163009	33.558638	44468.855
0.7333114	2.015274	0.6186626	6.147E-05	8320.1245	0.0001197	908.24585	0.0009941	0.019638	10.50637	22.074007	32.580377	42487.229
0.7930979	2.318587	0.7295845	6.147E-05	10884.8571	0.0001015	920.86108	0.000995	0.0238588	12.764502	22.380608	35.14511	50103.98
0.6762198	1.6481152	0.5127407	6.147E-05	5215.5287	0.0001444	891.64909	0.0009929	0.014589	7.805142	21.670639	29.475781	35213.811
0.5845845	1.2222976	0.3427296	6.147E-05	1614.9299	0.0002161	846.81975	0.0009894	0.0098954	5.2940755	20.581107	25.875183	23539.54
0.7924167	2.3066009	0.7283207	7.672E-05	10783.5060	0.0001269	903.33684	0.0009938	0.0244655	13.08906	21.954699	35.043759	50018.457

Pressure Drop and Friction Factor for Air-Water Flow in 3/4" pipe												
Liquid flow voltage	**Pressure Voltage**	**Liquid flow rate (Kg/s)**	**Gas flow rate (m3/s)**	**ΔPmeas (Pa)**	**Quality of gas phase**	**Mixture density (kg/m3)**	**Mixture Viscosity (Pa.s)**	**Wall shear stress (KPa)**	**ΔPF (KPa)**	**ΔPH (KPa)**	**ΔPT (KPa)**	**Re**
0.7470415	2.0075968	0.6441361	7.672E-05	8255.2079	0.0001435	892.25627	0.000993	0.020243	10.830064	21.685396	32.515461	44237.699
0.6761762	1.6290941	0.5126596	7.672E-05	5054.6916	0.0001803	868.61739	0.0009912	0.0153347	8.2040674	21.110877	29.314944	35209.507
0.5847937	1.189741	0.3431178	7.672E-05	1339.6398	0.0002694	816.27173	0.0009869	0.0107686	5.7612246	19.838668	25.599893	23567.457

Table B.6 Pressure drop and friction factor for air-water flow in the 3/4" pipe

Pressure drop and Friction Factor for Air-water flow system in 1/2" pipe in presence of 20ppm Frother												
Liquid flow voltage	**Pressure Voltage**	**Liquid flow rate (Kg/s)**	**Gas flow rate (m3/s)**	**ΔPmeas (Pa)**	**Quality of gas phase**	**Mixture density (kg/m3)**	**Mixture Viscosity (Pa.s)**	**Mixture velocity (m/s)**	**ΔPF /ΔL (Kpa / m)**	**ΔPH /ΔL (Kpa/ m)**	**ΔPT (Kpa/m)**	**Re**
0.624894	4.305189	0.417515	1.31E-05	27683.03103	3.78E-05	934.1862	0.000998	3.262048	9.016132	9.155025	18.17116	40249.53
0.602864	3.715208	0.376643	1.31E-05	22694.30861	4.2E-05	932.5146	0.000998	2.947999	7.52078	9.138643	16.65942	36309.48
0.569617	2.947664	0.314961	1.31E-05	16204.15905	5.02E-05	930.4615	0.000998	2.470674	5.574189	9.118522	14.69271	30363.43
0.485439	1.429636	0.158786	1.31E-05	3368.130649	9.95E-05	866.2898	0.000995	1.33791	2.313365	8.48964	10.80301	15308.3
0.622306	4.285286	0.412714	2.98E-05	27514.7316	8.71E-05	912.8949	0.000996	3.299905	9.173787	8.94637	18.12016	39788.66
0.600661	3.676476	0.372556	2.98E-05	22366.7995	9.64E-05	890.9838	0.000995	3.052096	7.828536	8.731642	16.56018	35917.41
0.568056	2.897117	0.312064	2.98E-05	15776.7521	0.000115	867.3993	0.000994	2.626087	6.062681	8.500513	14.56319	30086.05
0.490638	1.373358	0.168431	2.98E-05	2892.2567	0.000213	768.8197	0.00099	1.599285	3.124368	7.534433	10.6588	16240.05
0.616579	4.22734	0.40209	6.15E-05	27024.7618	0.000184	836.1698	0.000991	3.510292	9.777217	8.194464	17.97168	38768.13
0.596954	3.642913	0.365679	6.15E-05	22083.0035	0.000203	808.743	0.00099	3.300749	8.548498	7.925682	16.47418	35258.19
0.565566	2.808223	0.307445	6.15E-05	15025.0913	0.000241	765.1751	0.000988	2.933233	6.836702	7.498716	14.33542	29644.52
0.501685	1.422015	0.188927	6.15E-05	3303.6845	0.000392	659.9582	0.000981	2.090175	4.315886	6.46759	10.78348	18219.48
0.615377	4.227934	0.39986	7.67E-05	27029.7786	0.000231	831.2129	0.000989	3.511807	9.827316	8.145886	17.9732	38554.94
0.594848	3.60989	0.361771	7.67E-05	21803.7694	0.000255	806.8823	0.000988	3.273176	8.482117	7.907446	16.38956	34883.23
0.56356	2.786356	0.303724	7.67E-05	14840.1896	0.000304	754.9192	0.000985	2.937279	6.881179	7.398208	14.27939	29287.53
0.500224	1.389273	0.186215	7.67E-05	3026.8257	0.000496	550.9085	0.000976	2.468228	5.300677	5.398903	10.69958	17959.82

Table B.7 Pressure drop and friction factor for air-water flow in the 1/2" pipe in presence of 20ppm frother

Pressure Drop and Friction Factor for Air-Water Flow in the 3/4" Pipe in Presence of 20ppm Frother												
Liquid flow voltage	**Pressure Voltage**	**Liquid flow rate (Kg/s)**	**Gas flow rate (m3/s)**	**ΔPmeas (Pa)**	**Quality of gas phase**	**Mixture density (kg/m3)**	**Mixture Viscosity (Pa.s)**	**Wall shear stress (KPa)**	**ΔPF (KPa)**	**ΔPH (KPa)**	**ΔPT (KPa)**	**Re**
0.798229	2.32137	0.739104	1.31E-05	10908.3877	2.14E-05	956.398	0.000999	0.022288	11.92434	23.2443	35.16864	50753.66
0.731249	1.9215	0.614835	1.31E-05	7526.9268	2.57E-05	951.6298	0.000999	0.016185	8.658768	23.12841	31.78718	42220.42
0.640789	1.494432	0.447005	1.31E-05	3916.0272	3.53E-05	948.8732	0.000998	0.00956	5.114866	23.06141	28.17628	30695.9
0.602706	1.331499	0.376351	1.31E-05	2538.3101	4.2E-05	941.3194	0.000998	0.007328	3.920735	22.87783	26.79856	25844.25
0.797298	2.298674	0.737377	2.98E-05	10716.4807	4.87E-05	922.9498	0.000998	0.023449	12.54536	22.43137	34.97673	50636.45
0.731638	1.903352	0.615558	2.98E-05	7373.7410	5.84E-05	922.1727	0.000997	0.017236	9.221508	22.41249	31.63399	42271.4
0.643175	1.460185	0.451432	2.98E-05	3626.4391	7.96E-05	909.9927	0.000996	0.010785	5.77023	22.11646	27.88669	31001.28
0.603303	1.271107	0.377457	2.98E-05	2027.6453	9.52E-05	892.3563	0.000995	0.008598	4.600071	21.68783	26.2879	25921.6
0.795524	2.280995	0.734086	6.15E-05	10566.9880	0.000101	879.6416	0.000995	0.025137	13.44843	21.37881	34.82724	50413.09
0.729182	1.852611	0.611002	6.15E-05	6944.6899	0.000121	868.9089	0.000994	0.018854	10.08698	21.11796	31.20494	41961.19
0.645191	1.363967	0.455172	6.15E-05	2812.8466	0.000163	830.4038	0.000992	0.01288	6.890966	20.18213	27.0731	31260.73
0.607926	1.178124	0.386034	6.15E-05	1241.4121	0.000192	808.4868	0.000991	0.010939	5.852203	19.64946	25.50166	26513.17
0.794115	2.261671	0.731471	7.67E-05	10403.5948	0.000126	885.4307	0.000994	0.024569	13.14434	21.51951	34.66385	50234.82
0.728766	1.829524	0.610229	7.67E-05	6749.4708	0.000151	859.6881	0.000993	0.018908	10.11586	20.89386	31.00972	41909.37
0.646324	1.338241	0.457274	7.67E-05	2595.3124	0.000202	807.2264	0.00099	0.013527	7.236735	19.61883	26.85557	31406.33
0.609267	1.137926	0.388523	7.67E-05	901.5056	0.000238	776.7028	0.000988	0.011747	6.284775	18.87698	25.16176	26685.36

Table B.8 Pressure drop and friction factor for air-water flow in the 3/4" pipe in presence of 20 ppm frother

Pressure Drop and Friction Factor For Polymeric Air-water Solution in the 1/2" Pipe													
Liquid flow voltage	**Pressure Voltage**	**Liquid flow rate (Kg/s)**	**Gas flow rate (m^3/s)**	**ΔP_{meas} (Pa)**	**Mixture density (kg/m^3)**	**Mixture Viscosity (Pa.s)**	**Mixture velocity (m/s)**	**Wall shear stress (KPa)**	**$\Delta P_F/\Delta L$ (Kpa / m)**	**$\Delta P_H/\Delta L$ (Kpa/ m)**	**$\Delta P_T/\Delta L$ (Kpa/m)**	**Re**	**Exp. friction factor**
0.6909014	3.5407042	0.5399793	1.311E-05	21218.7508	974.60459	0.0070658	4.04	0.0219951	6.6611595	9.551125	16.212284	26962.5	0.0027602
0.6595924	3.1938975	0.4818917	1.311E-05	18286.2466	971.83559	0.0070569	3.62	0.0191505	5.799658	9.5239888	15.323647	23604.7	0.0030089
0.6003764	2.5983651	0.3720283	1.311E-05	13250.5855	964.31456	0.0070328	2.82	0.0143551	4.3474063	9.4502826	13.797689	17449.1	0.0037549
0.5443322	2.0471377	0.2680494	1.311E-05	8589.5553	951.78205	0.006992	2.06	0.0100968	3.0577914	9.3274641	12.385256	11906.2	0.0050211
0.6989709	3.501069	0.5549506	1.311E-05	20883.6063	975.22647	0.0070677	4.15	0.0216397	6.5535061	9.5572194	16.110726	27838.4	0.0025727
0.6579663	3.0954466	0.4788749	1.311E-05	17453.7731	971.67392	0.0070564	3.60	0.0183227	5.5489777	9.5224044	15.071382	23432.1	0.0029147
0.5503277	2.0823218	0.279173	1.311E-05	8887.0627	953.54873	0.0069978	2.14	0.0103373	3.1306318	9.3447775	12.475409	12483.8	0.0047481
0.51477	1.7636542	0.2132028	1.311E-05	6192.4954	940.53168	0.0069549	1.65	0.0080624	2.4416632	9.2172105	11.658874	9121.2	0.0062625
0.4499368	1.2	0.0929178	1.311E-05	132.2414	875.09604	0.0067292	0.78	0.0041159	1.246492	8.5759412	9.8224332	3486.8	0.015658
0.694508	3.4679768	0.5466707	2.982E-05	20603.7878	946.71949	0.0069754	4.21	0.0222822	6.7480811	9.277851	16.025932	27493.8	0.0026499
0.6336984	2.8309922	0.4338506	2.982E-05	15217.6174	934.19179	0.0069338	3.39	0.0172981	5.2386797	9.1550795	14.393759	21013.2	0.0032229
0.5475944	1.9664351	0.2741019	2.982E-05	7907.1560	900.54138	0.0068191	2.22	0.0110721	3.3531624	8.8253055	12.178468	12340.8	0.0049815
0.5031318	1.5558087	0.1916105	2.982E-05	4435.0100	864.15066	0.0066897	1.62	0.0087755	2.657626	8.4686765	11.126302	8167.3	0.0077521
0.4561846	1.1	0.1045093	2.982E-05	50.9523	777.19517	0.0063557	0.98	0.0072026	2.1812874	7.6165127	9.7978001	4086.2	0.0192297
0.6883181	3.5061664	0.5351865	2.982E-05	20926.7089	945.673	0.0069719	4.13	0.0226391	6.8561915	9.2675954	16.123787	26822.7	0.002806
0.6550525	3.139982	0.4734689	2.982E-05	17830.3518	939.23098	0.0069506	3.68	0.0197494	5.9810333	9.2044637	15.185497	23259.5	0.0031063
0.5997267	2.5209059	0.370823	2.982E-05	12595.6112	924.12086	0.0069	2.93	0.0150004	4.5428274	9.0563845	13.599212	17512.4	0.0037842
0.5526697	2.0231822	0.2835181	2.982E-05	8386.9944	903.47667	0.0068293	2.29	0.0114573	3.4698021	8.8540713	12.323873	12832.3	0.0048338
0.6901988	3.4402128	0.5386758	6.147E-05	20369.0226	896.25454	0.0068041	4.39	0.0236803	7.1714966	8.7832945	15.954791	27282.3	0.0027454
0.6528515	3.0239973	0.4693853	6.147E-05	16849.6166	882.94511	0.0067572	3.88	0.0205894	6.2354424	8.652862	14.888304	23274.1	0.003097
0.5611583	1.9750013	0.299267	6.147E-05	7979.5896	828.57521	0.0065574	2.64	0.0134734	4.0803804	8.120037	12.200417	13880.5	0.0046778
0.5195273	1.5217915	0.222029	6.147E-05	4147.3694	782.34289	0.0063765	2.07	0.0111349	3.3721782	7.6669604	11.039139	9878.4	0.0066303

Pressure Drop and Friction Factor For Polymeric Air-water Solution in the 1/2" Pipe													
Liquid flow voltage	**Pressure Voltage**	**Liquid flow rate (Kg/s)**	**Gas flow rate (m^3/s)**	**ΔP_{meas} (Pa)**	**Mixture density (kg/m^3)**	**Mixture Viscosity (Pa.s)**	**Mixture velocity (m/s)**	**Wall shear stress (KPa)**	**$\Delta P_F/\Delta L$ (Kpa / m)**	**$\Delta P_H/\Delta L$ (Kpa/ m)**	**$\Delta P_T/\Delta L$ (Kpa/m)**	**Re**	**Exp. friction factor**
0.472637	1.1	0.1350335	6.147E-05	50.9523	686.72321	0.0059657	1.44	0.0101302	3.0679127	6.7298874	9.7978001	5639.7	0.0143088
0.6854033	3.4595256	0.5297787	6.147E-05	20532.3268	894.72017	0.0067988	4.32	0.0238933	7.2360196	8.7682577	16.004277	26762.5	0.002859
0.6507679	3.0288734	0.4655196	6.147E-05	16890.8478	882.09948	0.0067542	3.85	0.0206581	6.2562238	8.6445749	14.900799	23053.3	0.0031561
0.5939437	2.35203	0.3600938	6.147E-05	11167.6421	853.05681	0.006649	3.08	0.0158712	4.8065372	8.3599568	13.166494	17157.6	0.0039187
0.5671895	2.0080093	0.3104566	6.147E-05	8258.6964	833.68003	0.0065768	2.72	0.0135875	4.1149309	8.1700643	12.284995	14475.7	0.0044105

Table B.9 Pressure drop and friction factor for polymeric air-water solution in the 1/2" pipe

Pressure Drop and Friction Factor for Polymeric Air-Water Solution in the 3/4" Pipe

Liquid flow voltage	Pressure Voltage	Liquid flow rate (Kg/s)	Gas flow rate (m^3/s)	ΔP_{meas} (Pa)	Mixture density (kg/m^3)	Mixture Viscosity (Pa.s)	Mixture velocity (m/s)	Wall shear stress (KPa)	$\Delta P_F/\Delta L$ (Kpa / m)	$\Delta P_H/\Delta L$ (Kpa/ m)	$\Delta P_T/\Delta L$ (Kpa/m)	Re	Exp. friction factor
0.8447843	1.8694776	0.8254783	1.311E-05	7087.3095	982.63789	0.0070913	3.11	0.0139542	3.0102947	9.6298513	12.640146	26459.3	0.0029343
0.8024876	1.7659096	0.7470053	1.311E-05	6211.5660	981.03124	0.0070862	2.82	0.0123903	2.6729176	9.6141062	12.287024	23540.4	0.0031764
0.7304237	1.6019608	0.6133051	1.311E-05	4825.2597	977.36667	0.0070746	2.32	0.0099656	2.1498359	9.5781934	11.728029	18691.1	0.0037759
0.6233329	4.6729849	0.4146195	1.311E-05	2955.4027	967.68886	0.0070436	1.59	0.0069102	1.4907038	9.4833508	10.974055	11829.0	0.0056719
0.586666	3.9341238	0.3465915	1.311E-05	2354.7885	961.91816	0.007025	1.33	0.0060497	1.3050735	9.4267979	10.731871	9596.3	0.0070637
0.5307333	2.7080542	0.2428196	1.311E-05	1358.1264	947.20574	0.006977	0.95	0.0048551	1.0473754	9.2826162	10.329992	6338.7	0.0113725
0.8370171	1.9028152	0.8110677	1.311E-05	7369.2029	982.36578	0.0070904	3.06	0.0144935	3.1266281	9.6271847	12.753813	25919.5	0.0031561
0.7606442	1.7135085	0.6693732	1.311E-05	5768.4765	979.07824	0.00708	2.53	0.0116508	2.5133918	9.5949668	12.108359	20704.6	0.0037124
0.716537	1.6044181	0.5875411	1.311E-05	4846.0380	976.47302	0.0070717	2.23	0.010045	2.1669719	9.5694356	11.736408	17776.3	0.0041433
0.6397606	1.4259319	0.4450978	1.311E-05	3336.8069	969.71844	0.0070501	1.70	0.0075309	1.6246059	9.5032407	11.127847	12850.6	0.0053751
0.8492021	1.8499761	0.8336747	2.982E-05	6922.4102	963.83142	0.0070312	3.20	0.0145003	3.1281065	9.4455479	12.573654	26858.1	0.0029322
0.7535169	1.6174909	0.65615	2.982E-05	4956.5781	954.93633	0.0070023	2.54	0.01123	2.4226042	9.358376	11.78098	20313.9	0.0036319
0.6540763	4.8687762	0.4716578	2.982E-05	3114.5598	939.018	0.0069499	1.86	0.0085101	1.8358545	9.2023764	11.038231	13832.1	0.0052375
0.5546162	2.5493267	0.2871295	2.982E-05	1229.0982	904.55615	0.006833	1.18	0.0065514	1.4133138	8.8646503	10.277964	7778.3	0.0104796
0.5169879	1.5019831	0.2173176	2.982E-05	377.7211	878.09752	0.0067399	0.92	0.006162	1.3293112	8.6053557	9.9346669	5639.2	0.0167021
0.8360336	1.8801487	0.8092432	2.982E-05	7177.5413	962.83062	0.007028	3.11	0.0150227	3.2407898	9.4357401	12.67653	25941.9	0.0032206
0.7442174	1.6439259	0.6388966	2.982E-05	5180.1054	953.82	0.0069987	2.48	0.0116985	2.5236762	9.347436	11.871112	19692.8	0.0039859
0.7088232	1.5543886	0.5732297	2.982E-05	4423.0014	948.98696	0.0069828	2.24	0.0105029	2.2657561	9.3000722	11.565828	17355.7	0.0044228
0.6477146	1.3898643	0.4598549	2.982E-05	3031.8291	937.59133	0.0069452	1.82	0.0084203	1.8164767	9.1883951	11.004872	13430.5	0.0054434
0.834896	1.8443563	0.8071325	6.147E-05	6874.8903	927.76674	0.0069123	3.22	0.0160499	3.4623791	9.092114	12.554493	26030.5	0.0033326
0.7552874	1.6228938	0.6594347	6.147E-05	5002.2637	913.33418	0.0068632	2.67	0.0132053	2.8487268	8.950675	11.799402	20592.7	0.0040437
0.6893099	1.4277082	0.5370266	6.147E-05	3351.8269	895.97357	0.0068031	2.22	0.010909	2.3533621	8.780541	11.133903	16239.2	0.0049409
0.6348254	1.268782	0.4359416	6.147E-05	2007.9893	875.19408	0.0067295	1.84	0.0093411	2.0151311	8.576902	10.592033	12767.6	0.006271
0.8521565	1.8234833	0.8391559	6.147E-05	6698.3943	930.27144	0.0069207	3.34	0.0156062	3.3666653	9.1166602	12.483325	27233.2	0.003006

Pressure Drop and Friction Factor for Polymeric Air-Water Solution in the 3/4" Pipe													
Liquid flow voltage	**Pressure Voltage**	**Liquid flow rate (Kg/s)**	**Gas flow rate (m^3/s)**	**ΔP_{meas} (Pa)**	**Mixture density (kg/m^3)**	**Mixture Viscosity (Pa.s)**	**Mixture velocity (m/s)**	**Wall shear stress (KPa)**	**$\Delta P_F/\Delta L$ (Kpa / m)**	**$\Delta P_H/\Delta L$ (Kpa/ m)**	**$\Delta P_T/\Delta L$ (Kpa/m)**	**Re**	**Exp. friction factor**
0.7578359	1.5750996	0.6641629	6.147E-05	4598.1281	913.88725	0.0068651	2.69	0.0124248	2.6803488	8.9560951	11.636444	20763.8	0.0037529
0.6568247	4.0249988	0.4767568	6.147E-05	2428.6600	884.52396	0.0067628	2.00	0.0097036	2.0933236	8.6683348	10.761658	14154.6	0.0055049
0.5607221	1.4573137	0.2984578	6.147E-05	341.4097	828.19373	0.006556	1.33	0.0083612	1.8037266	8.1162986	9.9200252	8265.8	0.0113307

Table B.10 Pressure drop and friction factor for polymeric air-water solution flow in the 3/4" pipe

Pressure Drop and Friction Factor For 500ppm Polymeric Air-water Solution with 20ppm Frother in the 1/2" Pipe													
Liquid flow voltage	**Pressure Voltage**	**Liquid flow rate (Kg/s)**	**Gas flow rate (m^3/s)**	**ΔP_{meas} (Pa)**	**Mixture density (kg/m^3)**	**Mixture Viscosity (Pa.s)**	**Mixture velocity (m/s)**	**Wall shear stress (KPa)**	**$\Delta P_F / \Delta L$ (Kpa / m)**	**$\Delta P_H / \Delta L$ (Kpa/ m)**	**$\Delta P_T / \Delta L$ (Kpa/m)**	**Re**	**Exp. friction factor**
0.6891641	3.5474005	0.5367562	1.311E-05	21275.3731	974.46628	0.0073848	4.02	0.0220563	6.6796733	9.5497695	16.229443	7006.8	0.0028008
0.6447331	3.0576939	0.4543233	1.311E-05	17134.5463	970.28059	0.0074259	3.42	0.0180484	5.4658969	9.5087498	14.974647	5898.0	0.0031852
0.6039295	2.6452097	0.3786203	1.311E-05	13646.6905	964.88481	0.0074779	2.86	0.014733	4.4618497	9.4558711	13.917721	4881.0	0.0037229
0.5617113	2.2240988	0.300293	1.311E-05	10085.8910	956.55795	0.0075562	2.29	0.0114395	3.4644227	9.3742679	12.838691	3831.2	0.0045556
0.6876846	3.5133904	0.5340112	2.982E-05	20987.7929	945.56351	0.0076557	4.12	0.0227038	6.8757749	9.2665224	16.142297	6724.6	0.0028261
0.6354589	2.9391594	0.4371168	2.982E-05	16132.2501	934.63957	0.0077502	3.41	0.0181988	5.5114528	9.1594678	14.670921	5437.4	0.0033418
0.5997979	2.5465448	0.3709551	2.982E-05	12812.4070	924.14528	0.007837	2.93	0.0152166	4.6082838	9.0566237	13.664908	4563.3	0.0038361
0.5460575	1.9628289	0.2712504	2.982E-05	7876.6629	899.61628	0.0080245	2.20	0.0110716	3.352988	8.8162395	12.169228	3259.0	0.0050812
0.6850466	3.4456338	0.529117	6.147E-05	20414.8614	894.6042	0.0080601	4.32	0.0237796	7.2015605	8.7671212	15.968682	6329.1	0.0028521
0.6456399	2.9797193	0.4560057	6.147E-05	16475.2134	879.96445	0.0081591	3.78	0.0203113	6.1511973	8.6236516	14.774849	5388.5	0.0032261
0.6029433	2.47205	0.3767907	6.147E-05	12182.4994	858.58792	0.0082897	3.20	0.0167077	5.0598648	8.4141617	13.474026	4382.5	0.0037922
0.5531075	1.8606818	0.2843304	6.147E-05	7012.9349	821.24594	0.0084786	2.53	0.0127433	3.8592816	8.0482102	11.907492	3233.6	0.0048578

Table B.11 Pressure drop and friction factor for system with 500ppm polymer, 20ppm frother, and airbubbles in ½" pipe

Appendix C

Materials and Equipment

- Aerofroth Information
- Polymer Information
- Computer Interface
- Viscometer Information

C.1. Materials

C.1.1. Aerofroth

CYTEC

MSDS: 0005214
Print Date: 03/03/2008
Revision Date: 03/03/2008

MATERIAL SAFETY DATA SHEET

1. CHEMICAL PRODUCT AND COMPANY IDENTIFICATION

Product Name: AEROFROTH® 68 Frother
Synonyms: None
Product Description: Mineral processing reagent
Intended/Recommended Use: Frother for flotation
Supplied By: CYTEC CANADA INC., 9061 GARNER ROAD
NIAGARA FALLS, ONTARIO, CANADA L2E 6S5 1-905/356-9000
EMERGENCY PHONE: In CANADA: 905/356-8310 In USA: 1-800/424-9300 or 1-703/527-3887.
Manufactured By: CYTEC INDUSTRIES INC., FIVE GARRET MOUNTAIN PLAZA,
WEST PATERSON, NEW JERSEY 07424, USA - 973/357-3100
® indicates trademark registered in the U.S. Outside the U.S., mark may be registered, pending or a trademark. Mark is
or may be used under license.

2. COMPOSITION/INFORMATION ON INGREDIENTS

WHMIS REGULATED COMPONENTS
Component / CAS No. % (w/w) OSHA (PEL): ACGIH (TLV) Carcinogen
Potassium hydroxide
1310-58-3
0 - 2.0 2 mg/m3 (ceiling) 2 mg/m3 (Ceiling) -
Dipropylene glycol methyl
ether
34590-94-8
0 - 40 600 mg/m3; 100 ppm
(PEL)
(skin)
600 mg/m3; 100 ppm
(TWA)
900 mg/m3 150 ppm
(STEL)
100 ppm (TWA)
150 ppm (STEL)
(skin)
-
2-Ethyl hexanoic Acid
149-57-5
0 - 1.6 Not established 5 mg/m3 (TWA) -
No Permissible Exposure Limits (PEL/TLV) have been established by OSHA or ACGIH.

3. HAZARDS IDENTIFICATION

EMERGENCY OVERVIEW

APPEARANCE AND ODOR:

Appearance: liquid
Odor: low

STATEMENTS OF HAZARD:

AEROFROTH® 68 Frother MSDS: 0005214 Print Date: 03/03/2008 Page 2 of 6

POTENTIAL HEALTH EFFECTS

EFFECTS OF EXPOSURE:
The acute oral (rat) LD50 and dermal (rabbit) LD50 values are estimated to be > 3,700 mg/kg and > 2,000 mg/kg, respectively. Direct contact with this material may cause moderate eye and skin irritation. Refer to Section 11 for toxicology information on the regulated components of this product.

4. FIRST AID MEASURES

Ingestion:

If swallowed, call a physician immediately. Only induce vomiting at the instruction of a physician. Never give anything by
mouth to an unconscious person.

Skin Contact:

Remove contaminated clothing and shoes without delay. Wash immediately with plenty of water. Do not reuse contaminated clothing without laundering. Get medical attention if pain or irritation persists after washing or if signs and
symptoms of overexposure appear.

Eye Contact:

Rinse immediately with plenty of water for at least 15 minutes. Obtain medical advice if there are persistent symptoms.

Inhalation:

Remove to fresh air. If breathing is difficult, give oxygen. Obtain medical advice if there are persistent symptoms.

5. FIRE-FIGHTING MEASURES

Suitable Extinguishing Media:

Use water spray or fog, carbon dioxide or dry chemical.

Protective Equipment:

Firefighters, and others exposed, wear self-contained breathing apparatus. Wear full firefighting protective clothing. See
MSDS Section 8 (Exposure Controls/Personal Protection).

Special Hazards:

Keep containers cool by spraying with water if exposed to fire.

6. ACCIDENTAL RELEASE MEASURES

Personal precautions:

Where exposure level is not known, wear approved, positive pressure, self-contained respirator. Where exposure level is
known, wear approved respirator suitable for level of exposure. In addition to the protective clothing/equipment in Section
8 (Exposure Controls/Personal Protection), wear impermeable boots.

Methods For Cleaning Up:

Cover spills with some inert absorbent material; sweep up and place in a waste disposal container. Flush spill area with
water.

7. HANDLING AND STORAGE

HANDLING
Precautionary Measures: Avoid contact with eyes, skin and clothing. Wash thoroughly after handling.
WARNING! CAUSES EYE AND SKIN IRRITATION

Special Handling Statements: None
STORAGE
None
Storage Temperature: Room temperature
Reason: Safety.

8. EXPOSURE CONTROLS/PERSONAL PROTECTION

Engineering Measures:
Where this material is not used in a closed system, good enclosure and local exhaust ventilation should be provided to
control exposure.
Respiratory Protection:
Where exposures are below the established exposure limit, no respiratory protection is required. Where exposures exceed the established exposure limit, use respiratory protection recommended for the material and level of exposure.
Eye Protection:
Wear eye/face protection such as chemical splash proof goggles or face shield.
Skin Protection:
Avoid skin contact. Wear impermeable gloves and suitable protective clothing.
Additional Advice:
Food, beverages, and tobacco products should not be carried, stored, or consumed where this material is in use. Before
eating, drinking, or smoking, wash face and hands thoroughly with soap and water.

9. PHYSICAL AND CHEMICAL PROPERTIES

Appearance: liquid
Odor: low
Boiling Point: Not available
Melting Point: Not available
Vapor Pressure: Not available
Specific Gravity/Density: 0.95 - 1.0
Vapor Density: Not available
Percent Volatile (% by wt.): Not available
pH: Not applicable
Saturation In Air (% By Vol.): Not available
Evaporation Rate: Not available
Solubility In Water: Not available
Volatile Organic Content: Not available
Flash Point: >95 °C 203 °F Pensky-Martens Closed Cup
Flammable Limits (% By Vol): Not available
Autoignition Temperature: Not available
Decomposition Temperature: Not available
Partition coefficient (noctanol/ water):
Not available
Odor Threshold: Not available

10. STABILITY AND REACTIVITY

Stability: Stable
Conditions To Avoid: Avoid contact with acids and oxidizing agents. Avoid exposure to heat.

Polymerization: Will not occur

Conditions To Avoid: None known
Materials To Avoid: aluminum
Acids and oxidizers
moisture
copper
Hazardous Decomposition
Products:
Carbon dioxide
Carbon monoxide (CO)
water
hydrocarbons

11. TOXICOLOGICAL INFORMATION

Toxicological information for the product is found under Section 3. HAZARDS IDENTIFICATION.
Toxicological information on the regulated components of this product is as follows:

12. ECOLOGICAL INFORMATION

This material is not classified as dangerous for the environment.
The ecological assessment for this material is based on an evaluation of its components.

13. DISPOSAL CONSIDERATIONS

The Company encourages the recycle, recovery and reuse of materials, where permitted, as an alternative to disposal as
a waste. The Company recommends that organic materials classified as hazardous waste according to the relevant local
or national regulations be disposed of by thermal treatment or incineration at approved facilities. All local and national
regulations should be followed.

14. TRANSPORT INFORMATION

Dipropylene glycol methyl ether has acute oral (rat) and dermal (rabbit) LD50 values of 5135 mg/kg and 9500 mg/kg,
respectively. Direct contact can cause mild eye and skin irritation.
2-Ethyl hexanoic acid has an oral LD50 (rat) of 1600 mg - 3000 mg/kg. Inhalation of vapor is irritating to upper respiratory
tract, eyes, skin and mucose membranes. Liquid is absorbed through the skin. Liquid will cause skin and eye burns.
Potassium hydroxide has an acute oral (rat) LD50 value of 273 mg/kg. Acute overexposure to potassium hydroxide or
dusts causes severe respiratory irritation. Potassium hydroxide is severely irritating to the eyes and skin.

14. TRANSPORT INFORMATION

This section provides basic shipping classification information. Refer to appropriate transportation regulations for specific
requirements.
US DOT
Proper Shipping Name: Environmentally hazardous substance, liquid, n.o.s.
Hazard Class: 9
Packing Group: III
UN/ID Number: UN3082
Transport Label Required: Miscellaneous
Technical Name (N.O.S.): Potassium hydroxide

Hazardous Substances:
Component / CAS No. Reportable Quantity of Product (lbs)
Potassium hydroxide 50000
Comments: Hazardous Substances/Reportable Quantities - DOT requirements specific to Hazardous Substances only apply if the quantity in one package equals or exceeds the product reportable quantity.

TRANSPORT CANADA
Proper Shipping Name: Not applicable/Not regulated

ICAO / IATA
Proper Shipping Name: Not applicable/Not regulated
Packing Instructions/Maximum Net Quantity Per Package:
Passenger Aircraft: -
Cargo Aircraft: -

IMO
Proper Shipping Name: Not applicable/Not regulated

15. REGULATORY INFORMATION

This product has been classified in accordance with the hazard criteria of the Controlled products Regulations and this
Material Safety Data Sheet contains all the information required by the Controlled Products Regulations.

WHMIS CLASSIFICATION:
Class D2B Toxic

INVENTORY INFORMATION

United States (USA): All components of this product are included on the TSCA Chemical Inventory or are not required to be listed on the TSCA Chemical Inventory. This product contains a chemical substance that is subject to export notification under Section 12 (b) of the Toxic Substances Control Act, 15 U. S. C. 2601 et. seq. (This requirement applies to exports from the United States only.)

Canada: All components of this product are included on the Domestic Substances List (DSL) or are not required to be listed on the DSL.

European Union (EU): All components of this product are included on the European Inventory of Existing Chemical Substances (EINECS) or are not required to be listed on EINECS.

Australia: All components of this product are included in the Australian Inventory of Chemical Substances (AICS).

China: All components of this product are included on the Chinese inventory or are not required to be listed on the Chinese inventory.

Japan: All components of this product are included on the Japanese (ENCS) inventory or are not required to be listed on the Japanese inventory.

Korea: All components of this product are included on the Korean (ECL) inventory or are not required to be listed on the Korean inventory.

Philippines: All components of this product are included on the Philippine (PICCS) inventory or are not required to be listed on the Philippine inventory.

16. OTHER INFORMATION

NFPA Hazard Rating (National Fire Protection Association)
Health: 2 - Materials that, under emergency conditions, can cause temporary incapacitation or residual injury.
Fire: 1 - Materials that must be preheated before ignition can occur.
Reactivity: 0 - Materials that in themselves are normally stable, even under fire exposure conditions.

Reasons For Issue: New Format

Prepared By: Randy Deskin, Ph.D., DABT +1-973-357-3100
03/03/2008

C.1.2. Polymer

hyperdrill®

AF 207

ANIONIC DRY SHALE INHIBITOR

DESCRIPTION

HYPERDRILL® AF 207 is a high molecular weight, medium charge, polyacrylamide supplied as a dry granular powder. It has excellent handling characteristics, mixes easily and dissolves quickly when added to water-based fluid systems.

TYPICAL PROPERTIES

Appearance:	White Granular Powder
Ionic Character:	Anionic
Bulk Density:	0.8 gr/cc (50 lbs./cu. ft.)
pH of 0.5% Soln. @ 25°C:	6.0 - 8.0

APPLICATIONS

HYPERDRILL® AF 207 is a very versatile polymer which can be used for oil, gas, water well and mineral drilling. It can be added to fresh, KCL or sea water based drilling fluid systems. **HYPERDRILL® AF 207** functions primarily as a:

- **SHALE INHIBITOR**
- **VISCOSIFIER**
- **FLOW LINE FLOCCULANT**
- **FRICTION REDUCER/LUBRICANT**
- **FOAM STABILIZER**

PRINCIPAL FUNCTIONS

Shale Inhibitor

HYPERDRILL® AF 207 can be used alone or in conjunction with KCL to stabilize active shales by decreasing the shale's tendency to absorb water, swell and slough-off. As an additional benefit, fluid loss is often reduced when using this product. The recommended dosage rate is 0.25 - 1.0 ppb as supplied.

Viscosifier

The addition of 0.5 - 1.0 ppb of **HYPERDRILL® AF 207** is a cost effective way to generate viscosity in fresh or low salinity drilling fluids. It's shear thinning capacity assures maximum power at the bit under high shear while retaining excellent carrying capacity under low shear conditions.

Flow Line Flocculant

HYPERDRILL® AF 207 can also be utilized for clear water or low solids drilling. The addition of a 0.5% solution of **HYPERDRILL® AF 207** into the flow line or just prior to any mechanical separation equipment will greatly enhance the removal of drill solids.

Friction Reducer

The addition of **HYPERDRILL® AF 207** into a drilling fluid will help reduce turbulent flow, friction and power losses at points of high shear. Lowering turbulent flow also helps reduce erosion and washouts of fragile geologic structures.

Foam Stabilizer

HYPERDRILL® AF 207 assists in foam drilling by creating a very stable foam, thereby increasing foam life. This results in enhanced cuttings removal and reduced water requirements. The product is compatible with most commonly used foamers.

PACKAGING

HYPERDRILL® AF 207 is supplied in 50 lb. (net), multi-walled, polyethylene-lined, paper bags, packed 30 to a shrink-wrapped pallet or in 1500 lb. (net) bulk bags.

STORAGE

HYPERDRILL® AF 207 should be stored inside under cool dry conditions. When stored under these conditions, the product has a shelf life of at least one year.

HEALTH AND SAFETY

HYPERDRILL® AF 207 exhibits a low order of toxicity. However, precautions should be taken to avoid inhalation, ingestion or contact with skin or eyes. For additional information, see the relevant MSDS.

SPILLS: Polymer spills are extremely slippery and therefore hazardous. They should be addressed immediately. Dry polymer spills should be left dry, swept up and disposed of according to local, state or federal regulations. If the polymer becomes wet, an absorbent material should be applied to the spill, then swept up and discarded. **Do not add water to a spill.**

TDS/207/V2/1-97

C.2. Equipments

C.2.1. Computer Interface

Specifications

Typical for 25 °C unless otherwise specified.
Specifications in *italic text* are guaranteed by design.

Analog input section

Table 1. Analog input specifications

Parameter	Conditions	Specification
A/D converter type		16-bit successive Approximation type
Number of channels		8 single-ended
Input configuration		Individual A/D per channel
Sampling method		Simultaneous
Absolute maximum input voltage	*CHx IN to GND.*	*±15 V max*
Input impedance		100 MOhm, min
Input ranges	Software selectable	±10 V, ±5 V, ±2 V, ±1 V
Sampling rate	Scan to PC memory	0.6 S/s to 50 kS/s, software programmable
	Burst scan to 32 k sample FIFO	20 S/s to 50 kS/s, software programmable
Throughput	Software paced	500 S/s all channels
	Scan to PC memory (Note 1)	= (100 kS/s) / (# of channels), max of 50 kS/s for any channel
	Burst scan to 32 k sample FIFO	= (200 kS/s) / (# of channels), max of 50 kS/s for any channel
Gain queue		Software configurable. Eight elements, one gain element per channel.
Resolution		16 bits
No missing codes		*15 bits*
Crosstalk	Signal DC-25 KHz	-80 dB
CAL output	User calibration source	0.625 V, 1.25 V, 2.5 V, 5.0 V, software selectable
CAL output accuracy (Note 2)		±0.5% typ, ±1.0% max
CAL current		±5 mA max
Trigger source	Software selectable	External digital: TRIG_IN

Note 1: Maximum throughput scanning to PC memory is machine dependent. While the majority of XP equipped PC's we tested allowed acquisition at the maximum rates, a few would not. The lowest maximum rate we observed on an XP equipped PC during multi-channel testing was 95 kS/s, aggregate. The rates specified are for Windows XP only. Maximum rates on operating systems that predate XP may be less and must be determined through testing on your machine.

Note 2: Actual values used for calibration are measured and stored in EEPROM.

Table 2. Calibrated absolute accuracy

Range	Accuracy (mV)
±10 V	5.66
±5 V	2.98
±2 V	1.31
±1 V	0.68

Table 3. Accuracy components - All values are (±)

Range	% of Reading	Gain error at FS (mV)	Offset (mV)
±10 V	0.04	4.00	1.66
±5 V	0.04	2.00	0.98
±2 V	0.04	0.80	0.51
±1 V	0.04	0.40	0.28

Table 4 summarizes the noise performance for the USB-1608FS. Noise distribution is determined by gathering 50 K samples with inputs tied to ground at the user connector. Samples are gathered at the maximum specified sampling rate of 50 kS/s.

Table 4. Noise performance

Range	Typical counts	LSBrms
±10 V	10	1.52
±5 V	10	1.52
±2 V	11	1.67
±1 V	14	2.12

Digital input/output

Table 5. Digital I/O specifications

Digital type	CMOS
Number of I/O	8 (DIO0 through DIO7)
Configuration	Independently configured for input or output
Pull-up/pull-down configuration	All pins pulled up to Vs via 47 K resistors (default). Positions available for pull down to ground. Hardware selectable via zero ohm resistors as a factory option.
Input high voltage	2.0 V min, 5.5 V absolute max
Input low voltage	0.8 V max, –0.5 V absolute min
Output high voltage (IOH = –2.5 mA)	3.8 V min
Output low voltage (IOL = 2.5 mA)	0.7 V max
Power on and reset state	Input

External trigger

Table 6. External trigger specifications

Parameter	Conditions	Specification
Trigger source (Note 3)	External digital	TRIG_IN
Trigger mode	Software selectable	Edge sensitive: user configurable for CMOS compatible rising or falling edge.
Trigger latency		10 µs max
Trigger pulse width		1µs min
Input high voltage		4.0 V min, 5.5 V absolute max
Input low voltage		1.0 V max, –0.5 V absolute min
Input leakage current		*±1.0µA*

Note 3: TRIG_IN is a Schmitt trigger input protected with a 1.5K Ohm series resistor.

External clock input/output

Table 7. External clock I/O specifications

Parameter	Conditions	Specification
Pin name		SYNC
Pin type		Bidirectional
Software selectable direction	Output	Outputs internal A/D pacer clock.
	Input	Receives A/D pacer clock from external source.
Input clock rate		50 kHz, maximum
Clock pulse width	Input	1µs min
	Output	5µs min
Input leakage current		*±1.0µA*
Input high voltage		4.0 V min, 5.5 V absolute max
Input low voltage		1.0 V max, –0.5 V absolute min
Output high voltage (Note 4)	IOH = –2.5 mA	3.3 V min
	No load	3.8 V min
Output low voltage (Note 4)	IOL = 2.5 mA	1.1 V max
	No Load	0.6 V max

Note 4: SYNC is a Schmitt trigger input and is over-current protected with a 200 Ohm series resistor.

Counter section

Table 8. Counter specifications

Pin name (Note 5)	CTR
Counter type	Event counter
Number of channels	1
Input type	TTL, rising edge triggered
Input source	CTR screw terminal
Resolution	32 bits
Schmidt trigger hysteresis	*20 mV to 100 mV*
Input leakage current	*±1µA*
Maximum input frequency	1 MHz
High pulse width	*500 ns min*
Low pulse width	*500 ns min*
Input high voltage	4.0 V min, 5.5 V absolute max
Input low voltage	1.0 V max, –0.5 V absolute min

Note 5: CTR is a Schmitt trigger input protected with a 1.5K Ohm series resistor.

Memory

Table 9. Memory specifications

Data FIFO	32,768 samples, 65,536 bytes		
EEPROM	1,024 bytes		
EEPROM configuration	**Address range**	**Access**	**Description**
	0x000-0x07F	Reserved	128 bytes system data
	0x080-0x1FF	Read/write	384 bytes cal data
	0x200-0x3FF	Read/write	512 bytes user area

Microcontroller

Table 10. Microcontroller specifications

Type	*High performance 8-bit RISC microcontroller*
Program memory	*16,384 words*
Data memory	*2,048 bytes*

Power

Parameter	Conditions	Specification
Supply current	USB enumeration	< 100 mA
Supply current (Note 6)	Continuous mode	150 mA
+5 V USB power available (Note 7)	▪ Connected to self-powered hub ▪ Connected to externally-powered root port hub	4.5 V min, 5.25 V max
Output current (Note 8)		350 mA max

Note 6: This is the total current requirement for the USB-1608FS which includes up to 10 mA for the status LED.

Note 7: "Self-powered hub" refers to a USB hub with an external power supply. Self-powered hubs allow a connected USB device to draw up to 500 mA. "Root port hubs" reside in the PC's USB host Controller. The USB port(s) on your PC are root port hubs. All externally-powered root port hubs (desktop PC's) provide up to 500 mA of current for a USB device. Battery-powered root port hubs provide 100 mA or 500 mA, depending upon the manufacturer. A laptop PC that is not connected to an external power adapter is an example of a battery-powered root port hub. If your laptop PC is constrained to the 100 mA maximum, you need to purchase a self-powered hub.

Note 8: This refers to the total amount of current that can be sourced from the USB +5 V and digital outputs.

General

Device type	USB 2.0 (full-speed)
Device compatibility	USB 1.1, USB 2.0

Environmental

Operating temperature range	0 to 70 °C
Storage temperature range	-40 to 70 °C
Humidity	0 to 90% non-condensing

Mechanical

Dimensions	79 mm (L) x 82 mm (W) x 25 mm (H)
USB cable length	*3 meters max*
User connection length	*3 meters max*

Main connector and pin out

Connector type	Screw terminal
Wire gauge range	16 AWG to 30 AWG

Pin	Signal Name	Pin	Signal Name
1	CH0 IN	21	DIO0
2	AGND	22	GND
3	CH1 IN	23	DIO1
4	AGND	24	GND
5	CH2 IN	25	DIO2
6	AGND	26	GND
7	CH3 IN	27	DIO3
8	AGND	28	GND
9	CH4 IN	29	DIO4
10	AGND	30	GND
11	CH5 IN	31	DIO5
12	AGND	32	GND
13	CH6 IN	33	DIO6
14	AGND	34	GND
15	CH7 IN	35	DIO7
16	AGND	36	SYNC
17	CAL	37	TRIG_IN
18	AGND	38	CTR
19	AGND	39	PC +5V
20	AGND	40	GND

CE Declaration of Conformity

Manufacturer: Measurement Computing Corporation
Address: 10 Commerce Way
Suite 1008
Norton, MA 02766
USA

Category: Electrical equipment for measurement, control and laboratory use.

Measurement Computing Corporation declares under sole responsibility that the product

USB-1608FS

to which this declaration relates is in conformity with the relevant provisions of the following standards or other documents:

EU EMC Directive 89/336/EEC: Electromagnetic Compatibility, EN 61326 (1997) Amendment 1 (1998)

Emissions: Group 1, Class A

- EN 55011 (1990)/CISPR 11: Radiated and Conducted emissions.

Immunity: EN61326, Annex A

- IEC 1000-4-2 (1995): Electrostatic Discharge immunity, Criteria A.
- IEC 1000-4-3 (1995): Radiated Electromagnetic Field immunity Criteria A.
- IEC 1000-4-8 (1994): Power Frequency Magnetic Field immunity Criteria A.

Declaration of Conformity based on tests conducted by Chomerics Test Services, Woburn, MA 01801, USA in May, 2004. Test records are outlined in Chomerics Test Report #EMI3876.04.

We hereby declare that the equipment specified conforms to the above Directives and Standards.

Carl Haapaoja, Director of Quality Assurance

C.2.2. Cylindrical Viscometer

Viscosity of polymeric solution was measured by coaxial cylindrical viscometer. The measuring device is consisted of two concentric cylinders; the outer cylinder (rotor) which is rotates around the inner cylinder (bob) that is stationary. The rotation of rotor around the bob produces shear stress on the solution between two cylinders. The produced shear stress has been expressed as a function of dial numbers that are given by the viscometer. The shear stress equation that has been obtained by calibration of viscometer for this experiment is given by

$$\tau = 0.0881\ (Dial\ reading) - \ 0.3694 \tag{C.1}$$

The next necessary parameter that needs to be calculate in order to measure viscosity of solution by this type of viscometer is shear rate which is calculated by

For Newtonian fluids:

$$\dot{\gamma} = \frac{2S^2}{S^2 - 1}\ \Omega \tag{C.2}$$

And for power-law fluids:

$$\dot{\gamma} = \frac{2N\Omega}{1 - S^{-2N}} \tag{C.3}$$

Where

S	Ratio of rotor radius to bob radius
N	Constant
Ω	Rotation speed (rad/s)

The constant N is the slope of ln Ω versus ln ŋ (torque) which can be expressed by:

$$\eta = 2\pi L_b {R_b}^2 \tau \quad \text{(C.5)}$$

Where L and R are bob length and radius.

By knowing these values, the solution viscosity can be calculated by:

For Newtonian fluid:

$$\tau = \mu\dot{\gamma} \quad \text{(C.6)}$$

For non-Newtonian fluid:

$$\tau = K\,\dot{\gamma}^n \quad \text{(C.7)}$$